ANALYSIS OF THE FUNGAL VIRULENCE OF *CRYPTOCOCCUS* AND EXPLORATION OF NOVEL ANTIFUNGALS AGAINST CRYPTOCOCCOSIS

A Dissertation

by

BING ZHAI

Submitted to the Office of Graduate and Professional Studies of
Texas A&M University
in partial fulfillment of the requirements for the degree of

DOCTOR OF PHILOSOPHY

Chair of Committee,	Xiaorong Lin
Committee Members,	Matthew S. Sachs
	L. Rene Garcia
	Jeffrey D. Cirillo
Head of Department,	Thomas D. McKnight

August 2014

Major Subject: Biology

ABSTRACT

Cryptococcosis is one of the leading causes of the deaths among AIDS patients. The high mortality rates of cryptococcosis are mainly due to inadequate information of its major causative agent *Cryptococcus neoformans* and the limitations of current therapies.

Cryptococcus neoformans is an unconventional dimorphic fungus that can grow either as a yeast or in a filamentous form. To study this dimorphism that is critical to the pathogenicity of many fungi, we constructed the congenic **a** and α strains for XL280(α), a strain with robust ability to undergo the yeast-hyphal transition. We compared the congenic strains in different *in vivo* models and found they are equivalent in virulence. Furthermore, deletion or overexpression of a known transcription factor Znf2 in XL280 abolished or enhanced filamentation and biofilm formation, consistent with its established role. Therefore, the congenic strains provide a new resource for the study of morphogenesis and the related virulence of *Cryptococcus*.

Meanwhile, we searched for novel antifungals by screening of a clinical compound library. Two hits from the screen, the antibiotic polymyxin B and the antidepressant sertraline are all potently fungicidal against *Cryptococcus*. Polymyxin B works synergistically with the azoles both *in vitro* and *in vivo*, thus it may serve as an adjunctive therapy with fluconazole in clinic. Our investigation on sertraline has implicated its unique advantage in treating cryptococcal infections since it is able to traverse the blood brain barrier and reduce the fungal burden in brains. We further

examined the fungal target of sertraline and found that this compound inhibits the fungal protein synthesis.

Taken together, the studies in this thesis facilitate further research on the pathogenesis of *Cryptococcus* and provide new antifungal drug candidates with clinical value.

ACKNOWLEDGEMENTS

I would like to express my greatest gratitude towards my advisor, Dr. Xiaorong Lin, for her invaluable advices that inspire me, for her constant enthusiasm on research that encourage me, for granting me most freedom to study projects of my interests. I am particularly grateful to her understanding and patience in my nadir period.

Special thanks go to my committee members, Dr. L. Rene Garcia and Dr. Jeffrey D. Cirillo, for their insights and suggestions. I would express my deep honor to Dr. Matthew S. Sachs for the informative discussions and continuous support of my research.

My sincere thanks to the Lin Lab family: Dr. Linqi Wang, Dr. Xiuyun Tian, Dr. Xinping Xu, Dr. Nadia Chacko, Dr. Youbao Zhao, Srijana Upadhyay, Rachana Gyawali, Yunfang Meng, and the former lab members Dylon Foyle, for their kind assistance in my study and precious friendships. With all of you, I had a joyful experience here.

I am greatly indebted to Dr. Alexander Idnurm, Dr. Aaron P. Mitchell, and Dr. Joseph Heitman for their generous help and support to my Ph.D. study. Many Thanks go to Dr. Xin Xiang, Dr. Pinkuan Zhu and Dr. Cheng Wu for their help with my research projects. I would like to thank Ms. Suat Cirillo for teaching me helpful research skills.

Finally, I would like to thank my dear mother, for her continuous love, understanding, and support during my entire study.

NOMENCLATURE

AIDS	Acquired Immune Deficiency Syndrome
AMB	Amphotericin B
BBB	Blood Brain Barrier
CFU	Colony Forming Unit
CNS	Central Nervous System
DMEM	Dulbecco's Modified Eagle Medium
DPI	Days Post Infection
FFCI	Fractional Fungicidal Concentration Index
FLC	Fluconazole
GalXM	Galactoxylomannan
GPI	Glycosylphosphatidylinositol
GO	Gene Ontology
GXM	Glucuronoxylomannan
HIV	Human Immunodeficiency Virus
IFN-γ	Interferon-γ
IRZ	Itracazole
MAT	Mating Type
MFC	Minimum Fungicidal Concentration
MIC	Minimum Inhibitory Concentration
MOPS	morpholinepropanesulfonic acid

mTOR	mammalian Target Of Rapamycin
PDCD4	Programmed Cell Death 4
PMB	Polymyxin B
PMDD	PreMenstrual Dysphoric Disorder
REDD1	Regulated in Development and DNA damage response 1
SRT	Sertraline
VVC	VulvoVaginal Candidiasis
YPD	Yeast Peptone Dextrose

TABLE OF CONTENTS

Page

LIST OF FIGURES

Page

LIST OF TABLES

Page

CHAPTER I

INTRODUCTION AND LITERATURE REVIEW

As a result of the expansion of the immunocompromised population, invasive infections caused by opportunistic pathogenic fungi have become a severe threat to public health since the 1980s. The three primary invasive mycoses, aspergillosis, candidiasis, and cryptococcosis caused by fungal species of *Aspergillus*, *Candida*, and *Cryptococcus* respectively, have mortality rates ranging from 10 to 90% (1-4). The basidiomycetous yeast *Cryptococcus neoformans* is the major causative agents of cryptococcal meningoencephalitis, one of the leading causes of deaths among the AIDS patients (4). According to the estimation from the Centers for Disease Control, over one million new cases of cryptococcosis are documented annually, and more than 0.6 million deaths are related to *Cryptococcus* infection worldwide (4).

In contrast to many pathogenic microbes that are always associated with the host, *Cryptococcus* is a free living organism in the environment. It is ubiquitous and people are exposed to this microbe since childhood. Therefore it is unlikely to control the disease by preventing human exposure to this pathogen. Therefore, a comprehensive understanding of mechanisms of fungal pathogenesis would provide a powerful platform to develop effective strategies for the prevention or the treatment of the disease. *Cryptococcus* has a defined sexual cycle, and several congenic pair strains with different genetic backgrounds had been developed (5-7), which enable the various genetic analyses on this organism. The genome of several *Cryptococcus* strains with different

genetic background have been sequenced (8); and the partial genome deletion set in H99 background with ~1100 genes disrupted is now available (9). With these useful genetic tools, researchers have gained some substantial insight into its physiology and related pathogenicity. The first section of this chapter reviews the life cycle, the infectious route and the virulence related factors of *Cryptococcus*.

Cryptococcus tends to cross the blood brain barrier (BBB) and invade the central nervous system (CNS) during systemic infections, leading to the fatal meningitis (10). As the BBB dramatically blocks a vast number of compounds that can approach the brain, this neurotropic trait grants *Cryptococcus* a natural protection against most of the antifungals, which are already extremely limited in number. Moreover, few immunomodulation methods such as application of IFN-γ as adjunctive therapy have showen positive therapeutic effect in preclinical or clinical trials (11). Furthermore, there is still no vaccination to protect people from *Cryptococcus* infection. Thus there is urgent need of new therapeutic methods to treat the disease. The second part of this chapter reviewed current immunotherapy and chemotherapy methods against systemic cryptococcosis, as well as the progress in the development of novel antifungal compounds.

1.1. The mechanisms of fungal virulence in *Cryptococcus*

After first isolation from patients in 1894 (10), *Cryptococcus* has been studied for over a century. Up to date, the *Cryptococcus* genus contains 37 recognized species, among which only two sibling species, *Cryptococcus neoformans* and *Cryptococcus*

gattii, are the main causative agents of invasive mycosis. According to the result of serological test and DNA fingerprint patterns, *C. neoformans* can be further classified into two subspecies including four serotypes: *C. neoformans* (further classified as serotype A *var. grubii* and serotype D *var. neoformans*) and *C. gattii* (further classified as serotype B and C) (12, 13). *C. gattii* was reported to be closely associated with gum and eucalyptus trees and the infections caused by *C. gattii* were primarily found in immunocompetent people in Australia where eucalyptus trees are native (14). However, most of the isolates from the recent epidemic outbreak of cryptococcosis in Vancouver Island and the Pacific Northwest of the United States among immunocompetent people also belong to this species (15), suggesting the expansion of geographical range for *C. gattii*. *C. neoformans*, on the other hand, is frequently isolated from soil contaminated with pigeon guano (16). *C. neoformans* is responsible for the vast majority of the clinical cryptococcosis cases worldwide, specifically areas where AIDS is prevalent, such as sub-Saharan African (4). Although serotype A of *C. neoformans* is predominantly sampled from patients and responsible for over 90% of the cryptococcosis worldwide (17-20), the two serotypes in general share similar life cycles and virulence factors, which will be discussed in the following sections.

1.1.1. Life cycle and sexual reproduction

Before 1960s, *Cryptococcus neoformans* was considered strictly locked in the yeast form with only asexual reproduction (21). Later studies have demonstrated that *Cryptococcus* has a defined bipolar mating system that is controlled by a single mating

type locus with two opposite alleles, **a** and α; and *Cryptococcus* is capable of undergoing a morphotype transition from the yeast to the filamentous form during mating (21).

The mating event in *Cryptococcus* is usually triggered by nutritional limitation and other environmental stimuli, such as desiccation or inositol from plants (16, 22). As the upper panel of Fig. 1 shown, the haploid **a** and α cells recognize each other by sensing the presence of α and **a** peptide pheromones, respectively, and fuse to form heterokaryon cells (23, 24). This further leads to the development of dikaryon hyphae, where the two parental nuclei remain separate and migrate coordinately via the clamp connections between adjacent hyphal compartments during filamentous elongation (23, 24). The tips of aerial hyphae will enlarge and form basidia, where the two nuclei fuse and further undergo a single meiotic event to generate four haploid nuclei followed by multiple rounds of mitosis to form four chains of basidiospores (23, 25). The basidiospores are more tolerant to the harsh conditions and will geminate under suitable environment (26). Spores are also considered the infectious particles of *Cryptococcus*. The size of spores (1 ~ 2 μm) is smaller than normal yeast cells (3 ~ 5 μm), which renders them easier to disperse and lodge at the alveoli of the lungs (26, 27).

The **a**-α mating process results in an equal proportion of **a** and α spores. However, both clinical and environmental isolates of *Cryptococcus* tend to highly tilt towards the α (>99%), despite the fact that there is no advantage of α mating type stains in either germination or stress resistance (10). This conundrum is at least partially attributed to the complexity of its mating behavior: besides the traditional bisexual

mating, some haploid *Cryptococcus* strains are also able to undergo monokaryotic fruiting, a self-filamentation event followed by sporulation (28-30).

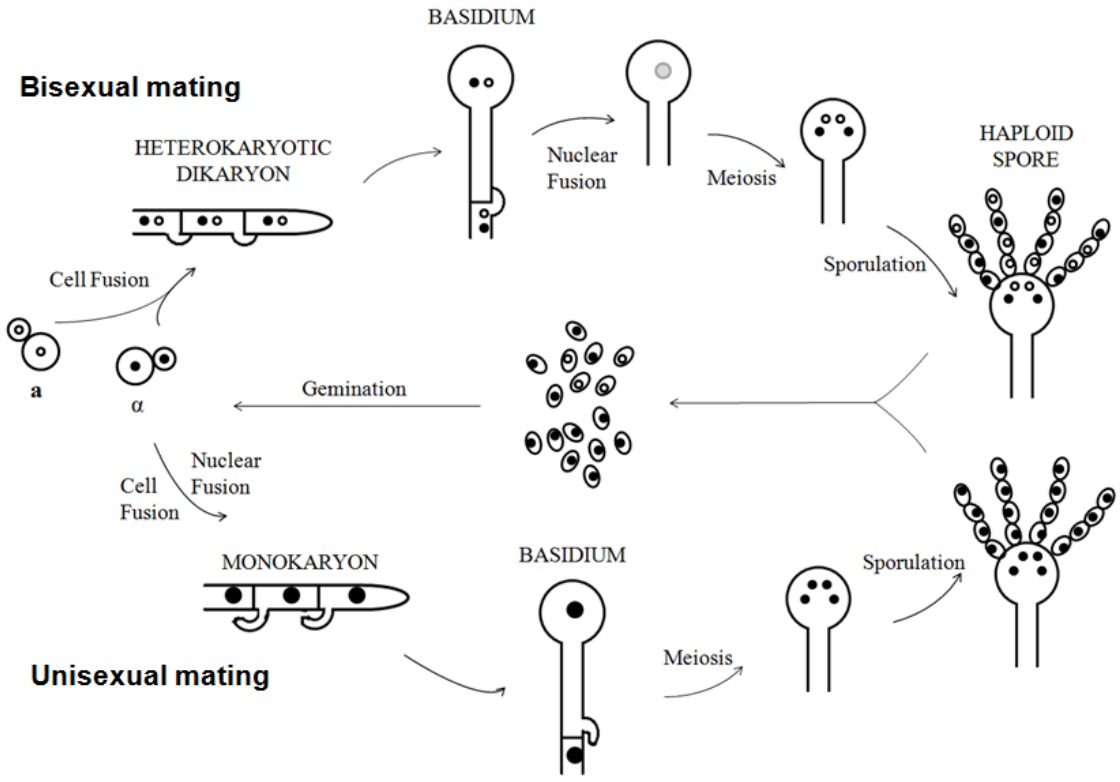

Figure 1 The life cycle of *Cryptococcus*
The upper part describes the process of bisexual mating that involves partners of the opposite mating types (a and α), and the lower part shows the process of unisexual mating that occurs with itself or involves partners of the same mating type.

Monokaryotic fruiting was considered as an asexual event due to the lack of the opposite mating partner in the process. Therefore, it is striking that high frequency of genetic recombination and ploidy change during fruiting was observed (30). In addition,

mutation of the meiosis-specific factor Dmc1 or Spo11 severely hampers sporulation and the germination rate of spores (30). Taken together, the evidence suggests that monokaryotic fruiting is a novel form of sexual reproduction – unisexual mating – in *Cryptococcus*.

In contrast to the bisexual mating, which requires the opposite mating partners, unisexual mating only involves cells of one mating type (Fig. 1 lower part). In response to similar environmental stimuli for bisexual mating, haploid cells undergo diploidization by either endoduplication or nuclear fusion after cell fusion of two cells with same mating type (24). The single nucleus will not be transferred during the development of hyphae, which will remain monokaryotic until the formation of the basidium. The diploid nucleus undergoes meiosis in basidium to form four recombinant haploid basidiospores (23). The benefit of unisexual mating is obvious: it provides *Cryptococcus* an alternative resource to create genetic diversity, which grants the species advantage in survival in changing environment.

Notably, the efficiency of both bisexual and unisexual mating varies a lot among different subspecies of *Cryptococcus*. For bisexual mating, although observed in all serotypes of *Cryptococcus*, Serotype D in general is robust in mating (31); and most *C. gattii* isolates (serotype B & C) from diverse sources are sterile under laboratory conditions (32). Unisexual mating has only been observed under laboratory conditions among some serotype D strains, and the frequency of unisexual mating among **a** isolates is much less than that of α isolates (29, 30). However, homozygous of mating type locus has been detected among natural isolates of *Cryptococcus* (33), which could potentially

serve as intermediate during unisexual mating; and genetic recombination has been equally detected in the **a**-α mixed and solo α populations (34). Population genetic studies also suggest that some of the natural diploid serotype A strains are derived from the fusion of two distinct α mating type strains (35). Such evidence strongly implicates the presence of unisexual mating of *Cryptococcus* in nature. Moreover, although *C. gattii* strains were thought to be sterile in general, the highly virulent isolates from the cryptococcosis outbreak on Vancouver Island can mate robustly; and a diploid α mating type strain was identified, suggesting the origin of the hypervirulent strain might be derived from unisexual mating (15).

It is necessary to point out that there is no evidence of either bisexual or unisexual mating behavior during cryptococcal infection. In fact, *in vivo* conditions of a mammalian host (e.g. the high body temperature), are prohibitory to the yeast-hyphae transition that is associated with mating. Thus mating is less likely to occur directly in response to the selective pressures from the host. Since this free-living organism infects humans by accident, it is plausible that mating provides an essential platform for generating diverse traits to combat with environmental pressures, which may include one(s) that is/are also crucial to the development of infection in host. This speculation has been supported by a similar regulon of gene expression profile when *Cryptococcus* interacts with *Acanthamoeba castellanii* or macrophage from a recent comparative transcriptome analysis (36). In addition, some classic virulence factors of *Cryptococcus*, such as capsule or melanin, play a protective role against multiple stresses in environment, which will be reviewed in the next section.

1.1.2. Infection cycles and virulence factors

1.1.2.1. Infection cycles

In natural conditions, *Cryptococcus* is usually associated with soil contaminated by bird excreta (*C. neoformans*) or with some tree species (*C. gattii*) (37). The infection of *Cryptococcus* can occur in human and other domestic or wild animals such as cats, dogs, koalas, mice, *etc* (10). Spores and desiccated yeast cells of *Cryptococcus* may serve as air-borne infectious particles and be inhaled by the host, leading to the primary pulmonary infection. There is no evidence indicating the transmission of this pathogen from human to human (10). This facultative pathogen can be engulfed by alveolar macrophage or other local phagocytes. Most immunocompetent individuals are able to clear the infection via efficient phagocytosis or suppress fungal growth to maintain it in a latent status (10). Serologic studies suggest that the majority of people in areas where *Cryptococcus* is endemic have been exposed to this fungus since childhood; and the fungal cells are able to remain latent in lungs for decades (38). However, under certain conditions, especially when the host immune system is compromised by HIV infection or certain chemotherapy, newly inhaled or latent fungal cells can replicate either extracellularly or even within the phagocytes and eventually escape the local sequestration. The dissemination of cryptococcal cells via blood circulation further results in the infections in other organs, which usually includes the central nervous system and leads to fatal meningoencephalitis.

The high rate of CNS invasion associated with *Cryptococcus* infection makes it distinct from other fungal pathogens. This remarkable neurotropism of *Cryptococcus*

could be related to the enrichment of inositol in the brain, given that this fungus has developed a complicated inositol acquisition system and is capable to utilize inositol as the sole nutrition source (39). The favor of inositol by *Cryptococcus* can also be observed in environment since *Cryptococcus* is frequently isolated from plants with high inositol levels (22). Meanwhile, the highly selective permeability formed by the tight junctions around the capillaries of BBB may play a dual role during infection: on the one hand, BBB prevents CNS from the damage by most neurotoxic molecules or infectious microbes; on the other hand, BBB also blocks the vast majority of antimicrobial compounds from reaching to the established infections in CNS.

Investigators have speculated that *Cryptococcus* traverses across BBB by different mechanisms: direct invasion, the "Trojan Horse" strategy by which the yeast migrates into CNS within host macrophages, or both (40). Some factors of *Cryptococcus*, including phospholipase B1, urease, and a recently identified metalloprotease, have been suggested to help this fungus penetrate BBB (41-43). A bioimaging study shows that a urease-dependent crossing of BBB is always followed by a sudden stop of the fungal cells at the brain capillaries, which indicates the preparation of penetration (44). Meanwhile, the "Trojan Horse" theory is supported by some indirect evidences that when infected by macrophages containing *Cryptococcus* cells intravenously, the murine host would develop meningitis faster, and that in the meningeal vasculature the fungal cells are found always associated with phagocytes (45, 46). A very recent study also suggests that a high rate of engulfment of *Cryptococcus* by macrophage *in vitro* is correlated with high brain fungal burden (47). This study

indicates the positive role of macrophage in promoting the CNS invasion of fungal cells. In this thesis, we discovered a reduction of brain fungal burden due to the transcription factor Znf2 controlled morphological transition in *Cryptococcus*. Our data suggest a new mechanism related to the fungal cell invasion to CNS.

A primary question during the study of the pathogenesis of *Cryptococcus* is, how could an environmental organism become a major human pathogen (40)? Although *Cryptococcus* is not naturally associated with human or other mammalian hosts, some of its endogenous traits may also have facilitated the establishment of infection in mammals. For instance, the polysaccharides capsule and the dark melanin pigment are the two representative virulence factors which are critical in combating with both environmental stress and host defense.

1.1.2.2. Capsule

Cryptococcus is the only encapsulated fungal pathogen. The polysaccharides, which are mainly composed of glucuronoxylomannan (GXM) and (GalXM), attach to the α-glucan of the fungal cell wall and form a highly negatively charged layer around the cell surface (10). Capsule is produced constitutively, yet the production is drastically induced during infection (10). A series of studies have revealed that capsule protects fungal cells from desiccation or natural predators, such as amoebae or nematodes (48-50). Moreover, high temperature, high level of CO_2, serum, and other *in vivo* cues such as neutral to alkaline pH induces the formation of a much more robust layer of capsule. Mutants with defective capsule are always of low virulence (51-53). Both the intact capsule coat and the shed capsule components promote the virulence of *Cryptococcus*.

The increase in the capsule size confers resistance to phagocytosis (54). Furthermore, capsule is able to quench the cytotoxic free radicals and protect the fungal cells from lysosome digestion (55). This extra layer on cell surface also conceals the antigenic components of *Cryptococcus* and prevents the recognition by the immune system. In addition, the polysaccharides component, either within the intact capsule or on shedding, actively suppress the host immune response by inducing the production of IL-10, which has a broad suppressive effect on the immune system (56). Changes of the structure of capsule alter the ability of *Cryptococcus* to penetrate CNS (57). Therefore, capsule promotes the virulence of *Cryptococcus* via protection from host stress and immunomodulation effect. Interestingly, we found that capsule renders the fungal cells more susceptible to a potential antifungal candidate, polymyxin B, and this part will be discussed in Chapter III.

1.1.2.3. Melanin

Melanin is another well-characterized virulence factor of *Cryptococcus*. This cell wall-associated dark pigment protects fungal cells from environmental damages, such as ultraviolet (UV) light, oxidizing agents and ionizing radiation (10). Melanin contributes to the virulence of many pathogenic fungi (e.g. *Aspergillus fumigatus*, *Paracoccidioides brasiliensis*, and *Cryptococcus*) (58). Cryptococcal melanin modulates the immune function by decreasing the rate of phagocytosis and/or altering the level of inflammatory cytokine production (59, 60). Melanin is associated with the dissemination of *Cryptococcus* as the deletion of *LAC1*, a laccase gene in the biosynthesis pathway of melanin, restricts the fungal cells in the lungs in a murine

inhalation model of cryptococcosis (61). In addition, melanin may contribute to the antifungal drug resistance by binding the compound, consequently reducing the drug concentration and decreasing the cell wall permeability (62).

1.1.2.4. Mating type locus

Besides the classical virulence factors discussed above, α mating type locus is also considered to be related to the pathogenesis of *Cryptococcus*. This point of view up for debate since it is difficult to specify the contribution of virulence from an individual gene in the mating type locus. Analyses of genomic sequence show an unusual complicated mating type locus (>100kb) of *Cryptococcus*. The mating type locus contains around 20 genes encoding pheromones and some components of pheromone sensing pathway (63). A few of the genes in mating type locus such as the p21-activated kinase Ste20 and transcription factor Ste12 have some impact on virulence (64). However, most of these genes are dispensable for virulence (65, 66). In addition, there is a uniformly increased expression pattern of genes in mating type locus during the early stage of phagocytosis (67).

Meanwhile, mating type locus has been proved to be a quantitative trait locus and the α allele significantly promotes unisexual mating (68). It is proposed that the enhanced ability of unisexual mating and the production of spores among α isolates contributes to the predominance of the α mating type in both the environmental and the clinical isolates. Meanwhile, higher frequencies of genetic recombination among α strains than **a** strains also increase the possibility to generate more α progeny with

infectious potential. Therefore, this enhanced level of unisexual mating associated with the α mating type locus may indirectly contribute to the virulence of *Cryptococcus*.

In addition, whether the mating type locus has an allelic affect on the virulence is still under debating. This question will be further studied via a newly developed congenic pair strains of *Cryptococcus* in Chapter II.

1.1.3. Morphogenesis and virulence

The morphological switch between yeast and hyphae is commonly observed among pathogenic fungi and closely related to virulence. For instance, the classic dimorphic fungi *Histoplasma capsulatum* and *Blastomyces dermatitidis* undergo morphological transition in response to the environmental temperature changes: The filamentous form is found in nature where the temperature is low, while the yeast form is always associated with infection in the host where the temperature is high(69, 70). By contrast, the hyphal formation of *Candida albicans* is always related to infection and tissue tropism *in vivo* (71). These morphological changes have crucial impacts on the fungal virulence in many steps of host-pathogen interactions such as adherence, tissue tropism, dissemination, and resistance to antimicrobial immune response (72-74). It is worth to note that in addition to the physical aspects of morphogenesis, alterations in cell surface molecules during morphogenesis could change the interaction between the pathogen and the host, and consequently shape the outcome of fungal infections.

Although comparisons of cryptococcal strains indicate a wide range in their capabilities to undergo filamentation, intensive research in the past four decades on the pathogenesis of *Cryptococcus* has been focused on the yeast isolates and without much

consideration of other morphotypes because yeast form is predominantly observed *in vivo*. Recently, a series of studies have demonstrated that *Cryptococcus* species could undergo different types of morphological transition. These morphotypes include giant cells that are strongly anti-phagocytic (75-77) and filamentous cells (pseudohyphae or hyphae) (28, 78-80), both of which impact virulence. Interestingly, the pseudohypha or the hypha form of *Cryptococcus* attributes negatively on disease development and induces a protective response from the host (81-83). This is consistent with earlier studies in 1960s and 1970s that purified filaments inoculated via various routes (e.g., intraperitoneally, intravenously, or intracranially) were found to be either avirulent or significantly attenuated in virulence compared to yeast cells purified from the same strains (28, 79, 82, 84-86). Moreover, animals inoculated with filaments develop immunity against cryptococcosis (83, 87). It was proposed that the reduced virulence associated with pseudohyphae or hyphae of *Cryptococcus* is due to stronger host immune responses elicited by this morphotype. Thus, understanding the molecular mechanism of morphotype transition and virulence will help identify novel antifungal targets or means to modulate host immune response against cryptococcosis.

The most common occurrence associated with hypha formation in *Cryptococcus* is during mating, either bisexual or unisexual mating. However, the key components in the mating signaling pathway have no or minimal direct influence on virulence. This is not unexpected since the host relevant conditions (aqueous environment, high temperatures, and high levels of CO_2) are drastically contrary to mating-inducing conditions (desiccation, low temperature, and low levels of CO_2). A key regulator of

morphogenesis in *Cryptococcus*, the transcription factor Znf2, has been identified recently (66, 81). Deletion of *ZNF2* locks cryptococcal cells in the yeast phase and the constitutive expression of *ZNF2* strongly promotes filamentation even in mating-suppressive conditions, indicating that the regulation of filamentation is independent of the mating signaling pathway (81). Moreover, the constitutive expression of *ZNF2* abolishes the fatality caused by cryptococcal infection in murine models (81). Therefore, Znf2 bridges the sex-independent morphotype transition and fungal pathogenicity. Further microarray study suggests that the 23% of genes differentially expressed in the *znf2*Δ mutant encode secretory proteins. Consistently, overexpression of *ZNF2* strongly promotes cell aggregation, suggesting that the alteration of cell surface could potentially change the interaction between the host and the pathogen. Cfl1, one of the secretory proteins regulated by Znf2, not only influences the virulence of *Cryptococcus* but also serves as a paracrinal signal promoting filamentation and biofilm formation (81, 88). Notably, the deletion of *CFL1* cannot abolish hyphal formation or cell aggregation elicited by Znf2 (88). These studies revealed the complexity of regulation of morphogenesis and morphotype transition-related virulence in *Cryptococcus.*

1.1.4. Summary and thesis research

In this section, the life cycle, infection cycle and virulence related factors of *Cryptococcus* have been reviewed. The *Cryptococcus* species are free living organisms that ubiquitously exist in the environment. Given this nature, the environmental cues, rather than host relevant factors are likely to be the main selective pressure that drives the evolution of this organism. The major virulence factors such as capsule and melanin

all possess significant values in combating with harsh environmental conditions or natural predators. The sophisticated mating system of *Cryptococcus* suggests that the impact of genetic diversities created by mating, particularly the unique unisexual mating, on fungal virulence is more profound. The yeast-hyphal transition of *Cryptococcus* also possesses its own value during the infection. The morphotype transition associated cell surface modification has uncovered a set of adhesive proteins as well as other factors that potentially could serve as a new reservoir for vaccine or adjuvant candidates.

Both unisexual mating and morphology associated pathogenicity are primarily deciphered recently. Their significance elicits research interests on further characterization of the molecular mechanisms. However, several classic reference strains of *Cryptococcus* like B3501/JEC21 (serotype D) or H99 (serotype A), are not capable of undergoing unisexual mating and are restricted in the yeast morphology. Therefore, genetics sources related to these strains, such as congenic strains or knock-out mutant collections, are not suitable for the study on unisexual mating or morphotype transition, which impedes the investigation on these fields.

Congenic pair strains are genetically identical in genome except the opposite mating type locus. They are essential source for genetic analysis of the molecular mechanism of fungal virulence of *Cryptococcus*. Previously a sibling strain of JEC21, XL280, was generated and found to be able to undergo self filamentation and unisexual mating (30). This strain could serve as another standard stain for the study on the mechanism of unisexual mating as well as morphotype transition. In order to fully utilize this strain in the future research, in Chapter II we generated the congenic strains

of XL280 by backcrossing. This chapter also includes virulence analyses of mating type locus and the impact of Znf2 on XL280 background.

1.2. Current therapeutic options against systemic cryptococcosis

As reviewed in the first section, cryptococcosis is one of leading cause of death among AIDS patients in Africa. The emergence of highly virulent isolates in the outbreak of cryptococcosis in Northwest Pacific area sets another alert to the public health. The high mortality rate of cryptococcal meningitis ranges from 10% to 70% even with antifungal therapy (4). This unsatisfied outcome is largely due to the inadequate source of either immunotherapy or chemotherapy. The following content will review current immunotherapy and chemotherapy of cryptococcal infections, as well as the progress on the exploration of new antifungals.

1.2.1. Immunotherapy of cryptococcosis

Research on most of immunomodulation strategies against cryptococcal infection could not provide promising evidence to support clinical application. Due to the lack of understanding on the host-pathogen interactions, especially the dominant antigens of *Cryptococcus,* there is no vaccine commercially available or even in clinical trial (89). Preclinical and clinical studies suggest an ambiguous role of passive immunization with monoclonal antibody against capsule component: depending on the different dosage of antibody or host parameters, the antibody mediated effect may be protective, non-protective, or even disease exacerbation (90-92). A series of studies described the benefit of a radioimmunotherapy treatment for cryptococcosis, which is to use

radiolabelled monoclonal antibody to locate and deliver cytotoxic radiation to the infectious site (93). This method has been shown to result in a prolonged survival as well as fungal burden reduction on a murine model of cryptococcosis (93). Although further study suggests a relative mild side effect of this method (94), the influence of radioactive agent *in vivo* requires further examination. The most promising clinical trial of immunotherapy is from a clinical phase II study where adjuvant recombinant IFN-γ1b is applied on HIV-associated cryptococcal meningitis patients, and yields a higher rate of negative cerebrospinal fluid culture comparing with the control group (11). Taken together, the immunotherapies against cryptococcal infections require further investigation with better understanding of host-pathogen interactions.

1.2.2. Antifungal compounds for treating systemic fungal infection

Chemotherapy is the most widely-used treatment for cryptococcal infections in clinic. Sadly, the arsenal of current antifungal compounds is extremely limited in number, especially comparing with that of compounds available to bacterial infections. Only three classes of compounds – polyenes (amphotericin B), azoles (triazoles, particularly fluconazole), and echinocandins (caspofungin) - are applied in the treatment of systemic fungal infections. The emergence of drug resistance with the wide-spread use of antifungals further exacerbates the problem. Currently, the standard regimen for AIDS-related cryptococcal meningitis starts with a two-week induction treatment of amphotericin B, either alone or in combination with flucytosine, followed by a consolidation and a lifelong maintenance antifungal therapy with fluconazole (95).

1.2.2.1. Amphotericin B

Amphotericin B was discovered in 1950s as the first classified antifungal compound for treatment of systemic fungal infection (96). It is natural product derivative from the actinomycetes *Streptomyces nodosus* (97). The compound directly binds to ergosterol, the primary sterol on fungal membrane (analogous to cholesterol in mammalian cells) (97). The integrity of fungal membrane is disrupted, leading to the leakage of ions such as potassium and sodium and eventually cell death (98). Amphotericin B is applied as the primary treatment for invasive mycoses for over 50 years mostly due to its potent fungicidal effect toward a broad spectrum of pathogenic fungi such as *Cryptococcus* and *Candida* species. Resistance to amphotericin B is rarely observed among *Cryptococcus* isolates. However, the application of amphotericin B is hampered by its limitations. Firstly, amphotericin B is still able to bind cholesterol with lower affinity in mammalian cell membrane. It cause strong nephrotoxicity that may lead to renal insufficiency and other acute toxicity including nausea, vomiting, rigors, and fever (99). Although a liposomal form of amphotericin B would partly reduce the side effects (100), this compound is still preferred only as the induction treatment. Secondly, the poor aqueous solubility of amphotericin B sharply limits the delivering methods. Trials with methods other than intravenous administration all failed to achieve equivalent efficacy (101). Therefore amphotericin B is not suitable for outpatient treatment and is restricted to hospital setting. Thirdly, amphotericin B is non-permissive to CNS where cryptococcal cells tend to infect. Due to this poor penetration of BBB, negative brain culture after the induction therapy often cannot be achieved in many

patients (95, 102), and 20-60% of AIDS patients experience relapse without maintenance therapy (103). These deficiencies of amphotericin B restrict it only in induction therapy to treat cryptococcal meningitis.

1.2.2.2. Fluconazole

Fluconazole, as well as other triazoles, targets the cytochrome P450 enzyme 14α-demethylase in the ergosterol synthesis pathway (104, 105). There are four triazole antifungal compounds that are clinically available: fluconazole, itraconazole, voriconazole, and posaconazole, among which fluconazole is the first and most widely-used one. Fluconazole is introduced to clinic in the early 1990s and is mostly favored in prophylactic, therapeutic, and maintenance application to treat cryptococcal meningitis (3, 95, 106, 107). It is well-tolerant in patients and efficiently penetrates CNS. In fact, fluconazole and voriconazole (another triazole compound) are the only two clinical available agents that can penetrate BBB and be solely used to treat the CNS cryptococcal infection (108, 109). However, the fungistatic nature of fluconazole significantly compromises its application. In the study of this thesis, we find some environmental and clinical isolates of *Cryptococcus* is intrinsically resistant to fluconazole; and the long-term fluconazole therapy on AIDS patients creates selective pressure for the pathogen to develop resistance (110-113). According to a recent report, fluconazole resistance occurs to around 30 percent of cryptococcosis patients who have never been exposed to this compound before treatment (114). Several molecular mechanisms attribute to the fluconazole resistance in various fungal species, including enhanced expression of the multidrug transporters (115, 116), point mutations and the related high expression level

of the 14α-demethylase encoding gene (117), and increased drug efflux by positive regulation of efflux pump genes (118, 119). Some non-genetic factors such as biofilm formation also promote the drug resistance against azoles (120, 121). Among these diverse mechanisms, the intrinsic heteroresistance is most commonly observed in *Cryptococcus* (122). Heteroresistance describes the emergence of a fluconazole resistant minor subpopulation. It results from a transient duplication of whole chromosomes harboring the fluconazole resistance relevant genes (123, 124). Although several newly commercialized triazoles such as voriconazole and posaconazole display dramatic enhanced potency against many fungal species (125), they still have the same fungal target and maintain the fungistatic nature.

1.2.2.3. Echinocandins

Echinocandins are a class of newest developed antifungals. They targets the fungal cell wall integrity by inhibition of the β-glucan (major cell wall component) synthase Fks1 (126). Caspofungin is the first commercialized compound in this class of antifungals (126). Although potent against candidiasis and aspergillosis, echinocandins demonstrate no clinical activity against cryptococcosis (126-128). Interestingly, the *FKS1* homolog gene in *Cryptococcus* is essential and the enzymatic activity of the encoding product is inhibited by echinocandins *in vitro* (129, 130). Therefore, the resistance of *Cryptococcus* against echinocandins is less likely due to the altered sensitivity of β-glucan synthase. It is possible that other factors of *Cryptococcus*, such as capsule or melanin, may restrict the access of the compound to the intact cryptococcal cells.

1.2.2.4. The combination of antifungals during therapy

As the variety of compounds for the treatment of invasive mycoses is extremely limited, people seek different drug combinations to increase the potency as well as the diversity of antifungal treatment. One successful example of this strategy is the combination of amphotericin B and flucytosine as the induction treatment for cryptococcal meningitis. Either amphotericin B or 5-flucytosine has its own advantage and severe deficiency: amphotericin B is highly potent against *Cryptococcus* but poor at CNS penetration (131); 5-flucytosine inhibits the fungal DNA or RNA synthesis and frequently induces drug resistance in fungi when used as monotherapy, yet it penetrates well in most body sites including CNS (132). Therefore, amphotericin B and flucytosine complements each other when combined. Notably, antagonistic effect has also been observed among commonly prescribed antifungals. For instance, fluconazole and caspofungin are the two most widely used compounds in treating infections caused by *Candida albicans*, however, the combination of them tends to be antagonistic especially to the *Candida albicans* biofilms (133). This antagonism could happen at either simultaneous or sequential administration of the two compounds (134), which further compound the outcome of clinical treatment. Therefore, for a novel antifungal candidate, it is necessary to test the drug combination effect with current frequently used antifungal compounds.

In the Chapter III and Chapter IV of this thesis, beside the evaluation of the efficacy of the two antifungal candidates by themselves, we further discussed the effect of their combination with fluconazole, which is the most frequently and long-term used

antifungal. Our data indicate different scenarios of the two compounds working together with fluconazole.

1.2.3. Novel antifungal development

As the limitation of clinically available antifungals greatly hampers the efficacy of current treatment against cryptococcosis as well as other invasive mycoses, there is critical need of developing new antifungals with various drug targets and higher potency.

Investigation on the *de novo* synthesis of novel antifungal drug as well as screen of new natural product derivatives has made much progress: An arylamidine derivative T2307 that causes the fungal mitochondria membrane collapse shows high efficacy *in vitro* and *in vivo* on *Candida spp.* and is now on clinical trial (135-138); E1210, an isoxazole derivative that targets the biosynthesis of the Glycosylphosphatidylinositol (GPI)-anchored protein on fungal cell wall, displays a broad antifungal activity *in vitro* as well as in animal models via oral delivery (139, 140); Occidiofungin, a natural derivative from *Burkholderia contaminans*, is also broadly fungicidal by induction of strong apoptosis of cells with no obvious toxicity in an animal model (141-143).

These preclinical results are encouraging in that these compounds are broadly potent against many fungal species. More important, they suggest a diverged new set of fungal drug targets that are different from the current ones. Thus the value of the research on these compounds is not simply restricted in the development of antifungal candidates. They also provide new perspectives in future screening of chemical compound or natural product libraries. However, the final clinical application of them remains questionable. Because of the uncertainty of many features such as the body

tolerance or potential side effects, these novel compounds have to pass through strict tests and clinical trials to be final distributed, the process of which could select off most of the candidates and also take long period of time. For instance, it took around 30 years for caspofungin to progress from bench to bedside (144).

By contrast, drug repositioning, which is to discover the antifungal activity of drugs with other known functions, represents another strategy of searching new antifungals. This strategy has unique advantages in acceleration of the application of new drug candidates, since there are well-established pharmaceutical and safety information of these compounds from previous studies. Many successful examples of drug repositioning have been documented in various medical areas, such as to apply the antifungal itraconazole on therapy for non-small-cell lung cancer (145) and to use the antihypertensive compound minoxidil to prevent hair loss (146). Several reports of antifungal drug repositioning have drawn research attention. Cyclosporin A and FK-506 are calcineurin inhibitors and serve as immunosuppressant in clinical use. They also have been demonstrated to possess antifungal activity especially together with fluconazole (147). Another example is the estrogen receptor antagonist tamoxifen that is for the breast cancer therapy. In a murine model of candidiasis tamoxifen reduces the fungal burden in kidney and its antifungal activity has been attributed to the inhibition of calmodulin (148). Recently, several *in vitro* and *in vivo* screens on alternative animal models have suggested the potential antifungal activity of over one hundred off-patent medication drugs (149, 150). These discoveries of drug repositioning greatly facilitate the search of new antifungals.

1.2.4. Summary and thesis research

Due to the lack of effective immunotherapy, the control of cryptococcosis purely relies on only a few unsatisfied antifungals: amphotericin B is used strictly during induction treatment due to its high toxicity and poor CNS penetration; fluconazole is able to access CNS but its potency is hampered by its fungistatic nature; and the newest antifungal echinocandins are not effective to *Cryptococcus*. The emergence of drug resistance in clinic further compromises the efficacy of antifungals. The limitations of current therapies against systemic cryptococcal infections have greatly undermined the outcome of treatment.

Trials on novel antifungal compound development, including *de novo* synthesis, screen of natural products, and the drug repositioning all have made encouraging progress. In order to find new compounds that can be used in clinical application, we employed the drug repositioning strategy and screened the Johns Hopkins Clinical Compound Library, which contains 1,514 FDA or foreign governmental agencies approved drugs. In the screen, we have identified two repositioning candidates: the antibacterial polymyxin B and the antidepressant sertraline. In Chapter III and IV, the antifungal activities of the two drugs have been evaluated both *in vitro* and *in vivo*. Our data support their potential clinical value as antifungals. Further studies also suggested new mechanisms of the antifungal activity of these compounds.

CHAPTER II

CONGENIC STRAINS OF THE FILAMENTOUS FORM OF *CRYPTOCOCCUS NEOFORMANS* FOR THE STUDY OF VIRULENCE TRAITS[*]

2.1. Introduction

To analyze the molecular mechanism of the virulence of *Cryptococcus*, researchers have developed a series of genetic tools including several congenic strains, which are genetically identical except the mating type locus (*MAT*). The first and widely used *Cryptococcus* congenic strains, JEC21α/JEC20**a**, were constructed in the 1990s and sequenced in the early 2000s (5, 8). They were derived from two serotype D progenitor strains, NIH433 (**a**) and NIH12 (α) (151) (Fig. 2). Both can cause fatalities in mice, with NIH12 displaying a higher level of virulence (10). However, JEC21α/JEC20**a** often fails to cause mortality in infected mice, even with a high infection dose ($1x10^7$ cells/animal) and a long study period (152, 153). Two other related serotype D congenic pairs, KN3501α/**a** and KN433α/**a** (Fig. 2), also exhibit low levels of virulence in an intravenous infection model of murine cryptococcosis (6). Studying cryptococcal virulence with these serotype D congenic pairs often requires long study periods (40 ~ >100 days), the unnatural intravenous inoculation, and relatively high infection doses ($1x10^6$ ~$1x10^7$ cells/mouse) (5, 6, 153, 154).

---

[*] This material has been published in this or similar form in *Infection and Immunity* and is used here with permission of American Society for Microbiology.
Zhai B, Zhu P, Foyle D, Upadhyay S, Idnurm A, and Lin X. (2013) Congenic strains of the filamentous form of *Cryptococcus neoformans* for studies of fungal morphogenesis and virulence. *Infect Immun* 81(7): 2626-2637.

The construction of the H99 congenic pair strains (KN99α/**a**) facilitated genetic analyses in the serotype A background. Examination of cryptococcal virulence with H99-derived strains permits lower inocula ($1x10^3$ ~$1x10^5$), shorter study periods (≤ 40 days), and the more natural inhalation route of infection (7, 153, 155). However, rapid progression of the disease in H99-infected mice may present a challenge to detect a potential protective effect on animal survival of some drugs, including the commonly used antifungal fluconazole. Thus it would be valuable to have a well-characterized strain with a modestly lower virulence than H99.

One general deficiency of current available congenic pair strains is that they are lack of the ability to develop hyphae in most culture conditions and undergo unisexual mating. Although NIH12 is highly self-filamentous, none of the derived congenic pair strains undergo fruiting except stochastic fruiting observed in JEC21α (Fig. 2). Nonetheless, B3502**a** derived from a cross between NIH433 and NIH12 is self-filamentous, and so are many progeny derived from a cross between B3501α and B3502**a** (68). However, a congenic pair in a self-filamentous genetic background has not been constructed because of the technical challenges of dissecting spores generated from the bisexual mating rather than from fruiting (151).

The congenic pair strains also facilitate the study on the direct influence of mating type locus on the virulence of *Cryptococcus*. The results are varied by strain backgrounds: in serotype D strains, JEC21α is more virulent than its congenic pair strain JEC20**a** (5, 153), and KN433α is also more virulent than KN433**a** (6), while there was no difference in virulence levels between the congenic KN3501α and KN3501**a** strains

(6); in serotype A strain, KN99α and KN99**a** exhibit no difference in virulence when they infect mice individually via inhalation route, but KN99α appears to be more efficient in colonizing the brain during coinfection with a mixture of **a**-α cells (6, 7, 156); in a recent study on the congenic strains of *C. gattii*, AIR265α and AIR265**a** are similarly virulent in mouse models, and neither of the mating types confers any competitive advantages during *in vitro* coculture or during a-α coinfection in mice, regardless of the route of inoculation (intranasal or intravenous) (157). One plausible reason to account for the observed differences between strains is that various genetic background of strains may contain factors located outside the mating type locus involved in controlling both virulence and mating behavior.

In this chapter, we used a series of backcrosses to generate a pair of congenic α and **a** strains in the highly self-filamentous XL280 background. We characterized the behaviors of the congenic strains *in vitro* and in two mouse models of cryptococcosis, and further examined the impact of mating type on virulence and tissue tropism during **a**-α co-infection. Furthermore, we tested the function of a known regulator, Znf2, in the XL280 background in cellular and colony development and the impact on fungal virulence. This new strain set fills a missing resource for exploring morphology and pathogenesis in *C. neoformans*.

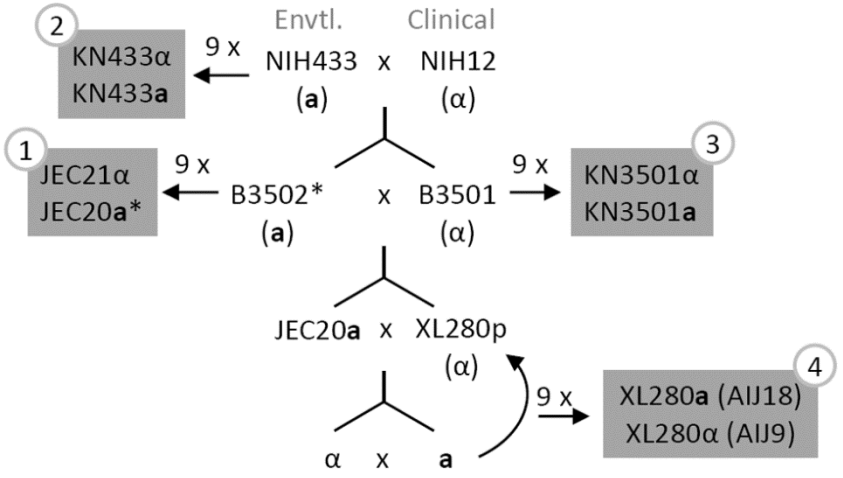

Figure 2 Crossing strategies used to generate the congenic strains XL280a and XL280α in this study and their relationship with other *C. neoformans* congenic pairs

NIH12 is a clinical isolate and NIH433 is an environmental isolate (5, 151). B3501 and B3502 were generated from a cross between NIH12 and NIH433 and they were used to generate the first congenic pair JEC21 and JEC20 in 1992 (5, 151). Two other congenic pairs in the genetic background of NIH433 and B3501 were generated in 2005 (6). XL280p was generated previously by crossing B3501 and B3502 and was found to be hyper-filamentous under a variety of nutrient limiting solid media (68). Based on Next Generation Sequencing analysis, the genome sequence of XL280 is 81% identical with JEC21 (158). *: B3502 is near isogenic with JEC20 based on two previous studies (6, 159).

2.2. Material and methods

2.2.1. Strains, crossing, and isolation of meiotic progeny

Strains XL280p (α) and JEC20 (**a**) were used as the starting parental strains for crosses made in this study. XL280p was generated previously from a cross between two serotype D strains B3501 (α) and B3502 (**a**) (68). JEC20**a** is congenic with the sequenced strain JEC21α (151). Strains were maintained on yeast extract-peptone-

dextrose (YPD) medium. For long-term storage, strains were saved in 15% glycerol stock at −80°C. Crosses were set up by mixing yeast cells of α and a mating partners together on V8 agar plates (5% V8 juice, 0.5 g/liter KH_2PO_4, 4% agar, with pH adjusted to 7 with KOH). Because self-filamentation during the fruiting process on V8 media initiates later than the dikaryotic filamentation during a-α bisexual mating and because sporulation during fruiting is much less efficient, we chose to dissect the spores generated within 3 to 7 days to avoid complications due to sporulation generated from fruiting. Filaments formed on the edges and tops of the mated yeast colonies, and basidiospores were transferred to YPD plates. Spores were micromanipulated with a dissecting microscope, and their mating type was determined by successful mating of their derived colonies with either JEC20**a** or JEC21α. The mating type of a few randomly selected progeny was also tested by the presence or absence of the mating type-specific genes *STE20*α and *STE20***a** as previously described (35). The results obtained by both approaches were consistent.

2.2.2. Molecular markers

The PCR-restriction fragment length polymorphism (RFLP) molecular markers used in this study were originally designed based on single nucleotide polymorphisms (SNPs) identified between B3501α and B3502**a** (nearly isogenic with JEC20**a**) (68, 159). Thirteen pairs of primers selected to include one on most chromosomes of *C. neoformans* were tested on strains JEC20**a** and XL280p (Table 1). Eight of the combinations were different between these two parental strains, while five were identical, consistent with the close relationship between these two strains. These eight markers

were also used to test the final congenic pair, XL280α and XL280**a**. The PCR amplicons were digested with the appropriate restriction enzymes, and fragments were resolved on 1.4% agarose–1× Tris-acetate-EDTA gels.

Table 1 RFLP markers used in comparing the parental strains XL280p and JEC20a

Marker name	Chromosome	Primer sequences (5'-3')	Polymorphic
Hind28	1	GGTGTGCTACATCTCTTGGTTG TCATCATGTCTCATGCAGCTTAC	No
Eco23	2	TATTTAGGTATGGCCGATTGTG TGCCCAACTCTCTTCCTATTTC	No
Pst19	3	AACCTCGTGGAGTCTTTGTCC CTGGATCATGGCTAGATGATTG	Yes
Hind8	3	CTTGATGCTCTTTATGGGGAAG TGTGCCAAGGTTATGGAGATG	Yes
Hind33	4	AGTCACTCTGACACCTCAGTCG CTTACTTGAAGACTCCCGTTCG	Yes
Hind10	4	CGGTATGTCAATGCTCTCAATC TTTCTCCACCTCTGGAAACAAC	No
Hind34	5	AGTCCTCCTCTCCGGGTATTC AGAGCAATGACCCTGTCCAC	Yes
Hind13	6	GTGATCATGCAGAACTTGGTGT CCGAGATGTCGAAGAAGAAGAT	Yes
Hind19	7 or 8	GCCACTCTTCATTCTTCCTCTG TCAACGCCTTCTTCTTCTTCTC	Yes
Hind25	7 or 11	TCATAGTCTCGGCGTATGTCTC ATGGGTTGGCTCTGTTTGTC	No
Hind11	10	ATACGACATACAAGGAGGGTCTG TGATTGACCTGCACAGAGAAAC	Yes
Hind9	12	GGATTCGGCGTTCTATACAGTC TTGCTGATTCAAGTTGTTGCTC	Yes
Hind15	13	GCTATGTGCCTACTGCTACTGG CCGACTCTGCTTCTCATACTTG	No

2.2.3. Pulsed-field gel electrophoresis

Chromosomal DNA was profiled by contour-clamped homogeneous electrical field (CHEF) electrophoresis. The conditions for preparation of chromosomal DNA and its resolution followed methods described previously (159). DNA was separated in a CHEF-DR III system (Bio-Rad) using the following conditions: block 1 was 75 to 150 s of switching with 4 V/cm at 12°C for 24 h, followed by block 2, which was 200 to 400 s of switching with 4 V/cm at 12°C for 24 h.

2.2.4. *In vitro* phenotypic assays of the congenic and the parental strains

Yeast cells were grown on YPD medium overnight and washed three times with water. Cells were suspended in distilled water, and the cell density was determined by measuring the optical density at 600 nm. Then cells were 10× serially diluted. To characterize capsule production, equal numbers of *C. neoformans* cells were transferred to Dulbecco's modified Eagle's medium (DMEM) (Invitrogen, CA) and grown for 3 days at 37°C under 5% CO_2. The appearance of a mucoid colony indicates capsule production. The capsule was visualized under light microscopy as a white halo surrounding the yeast cell in India ink due to the exclusion of ink particles. To examine melanin production, cells were spotted onto melanin-inducing medium containing L-dihydroxyphenylalanine (L-DOPA) (100 mg/liter) and incubated at 22°C in the dark for 6 days. Melanization was observed as the colonies developed a brown color. To analyze growth on a minimal medium, cells were spotted onto yeast nitrogen base (YNB) medium. To analyze resistance to osmotic and oxidative stresses, cells were grown on YNB medium supplemented with 1 M of NaCl or 1 mM H_2O_2, respectively.

2.2.5. The segregation of *znf2* mutations in the XL280 strain background

The *ZNF2* gene, encoding a zinc finger transcription factor that controls filamentation and biofilm formation, was replaced by the nourseothricin acetyltransferase (NAT) marker gene (66). The *ZNF2*^{oe} strain was generated by expressing *ZNF2* under the control of the promoter of the GPD1 gene linked with the G418 resistance marker gene in the *znf2Δ* mutant background. These mutants in the XL280p (α) background were crossed with XL280**a** to isolate the mutations in the MAT**a** background. Dissected progeny were examined for their mating type by crossing with JEC21α or JEC20**a** on V8 medium: their resistance to the drug NAT and/or G418 by growing them on plates containing YPD plus NAT plus G418 (YPD+NAT/G418 plates), their ability to undergo self-filamentation on V8 medium, and their ability to form a complex colony morphology on YNB medium (81). The ratios of these phenotypes in the progeny indicated Mendelian segregation of the mating type and each drug resistance marker. It also indicated the linkage between Znf2 mutations and their corresponding phenotypes.

2.2.6. Virulence assays in two mouse models of cryptococcosis

The animal models of systemic cryptococcosis were induced by two routes: intravenous and intranasal infection. In each infection model, 9 or 10 8- to 10-week-old female A/J mice (Jackson Laboratory) were infected by each *Cryptococcus* strain and were considered one group. All animals per group were used for the survival study, and five or six animals per group were used to examine the fungal burden. For the intravenous infection, each mouse was challenged with 1.0×10^6 fungal cells suspended

in 50 µl of saline. For the intranasal infection, animals were first sedated with ketamine and xylazine, and then 1.0×10^6 fungal cells (or 5×10^5 and 5×10^6 cells for the pilot experiment) suspended in 50 µl of saline were slowly inoculated into the left nostril of sedated animals. After infection, animals were weighed daily and monitored twice a day for disease progression, including weight loss, gait changes, labored breathing, or fur ruffling. Moribund mice were sacrificed, and their organs were dissected. For the intranasal infection model, the lungs, brain, spleen, and the left kidney from terminated mice were harvested. For the intravenous infection model, the brain, spleen, and the left kidney were harvested. The dissected organs were homogenized in 2 ml of cold phosphate-buffered saline (PBS) buffer using an IKA* Ultra-Turrax T18 homogenizer with the same setting for each type of organ. The tissue suspensions were serially diluted (10×), plated onto YNB agar medium, and incubated at 30°C for 2 days such that the colonies became visible to count CFU.

For the examination of the impact of *znf2* mutation in the XL280 background on cryptococcal virulence, animals were infected by the wild type, the *znf2Δ* mutant, and the $ZNF2^{oe}$ strain intranasally with the inoculum of 1.0×10^6 fungal cells per animal as described above. Because the P_{GPD1}-*ZNF2* strain exhibits heterogeneity in cell morphology and its population is a mixture of yeast cells and filamentous cells, only cells in the yeast form were used for animal inoculation to obtain an accurate inoculation and to avoid potential problems caused by differences in cell types at initial infection. The P_{GPD1}-*ZNF2* strain culture with a mixed morphotype was centrifuged briefly at a

low speed to allow the enrichment of yeast cells on the top. The top layer was then centrifuged again at a higher speed, and yeast cells were collected for infection.

2.2.7. Examination of cellular morphology *in vitro* and during infection

To examine cell morphology under culture conditions that are relevant to host physiology, strains XL280α, XL280**a**, and the mixture of equal numbers of XL280α and XL280**a** cells were inoculated into fetal bovine serum and RPMI liquid medium with a final cell density of 1×10^5 cells/ml. Cells cultured in rich YPD liquid medium under the same condition were used as controls. The cells were incubated at 37°C under 5% CO_2. Photographs of the cells were taken after 3 days of incubation.

To examine cellular morphology of XL280 during infection, animals were infected with XL280 at the dose of 5×10^5 cells per mouse intranasally as described above. Moribund mice were sacrificed, and lungs, brains, and kidneys dissected from the sacrificed animals were fixed in 10% formalin, embedded in paraffin, sectioned at a thickness of 5 μm, and stained with Gomori methenamine silver (GMS). Fungal cell morphology was then examined microscopically.

2.2.8. *In vitro* growth competition assay between the congenic **a** and α strains

The congenic strains XL280**a** and XL280α were grown in YPD liquid medium at 30°C overnight and then washed three times with sterile water. The cell density of the suspension of each strain was determined based on hemocytometer counting. XL280**a** and XL280α cells of equal numbers were then mixed and inoculated into liquid DMEM to the final concentration of 1×10^5 cells/ml. The initial inocula were confirmed by plating the XL280**a** and XL280α cell suspension prior to the mixing onto YNB medium,

and their CFU were counted after colonies became visible. The a-α coculture in liquid DMEM was incubated at 37°C under 5% CO_2. Aliquots of the *in vitro* coculture were removed at days 3 and 9 of incubation and plated onto YNB plates with serial dilutions. Single colonies were randomly picked and examined for their mating type through crossing with reference strains JEC20**a** and JEC21α separately on V8 juice agar medium at 22°C in the dark. These single colonies by themselves were included as the negative control. The crosses were examined after 2 to 3 days. Crosses with abundant hyphal formation and sporulation compared to the tested colony alone were scored as successfully mating with the reference strain.

2.2.9. Congenic **a** and α coinfection in two mouse models of cryptococcosis

Mice were challenged with a 1:1 ratio of XL280**a** and XL280α cells (1×10^6 total fungal cells per animal) intranasally or intravenously. The **a** and α cell numbers of the initial mixed inocula were confirmed by measuring the CFU of serial dilutions. The ratio of **a** to α cells in the original inocula was confirmed based on the CFU of a and α cell suspensions prior to the mixing. The organs of sacrificed mice were dissected and processed as described earlier. To determine the ratio of the **a** to α cells in various organs, single colonies recovered from each organ dissected from terminated animals were scored for their mating type by crossing with the reference strains JEC20**a** and JEC21α as described above. In total, more than 9,000 matings were performed and screened to examine the mating type distribution in different organs.

2.2.10. Statistical analysis

Statistical significance of the survival data between different groups was assessed by the Gehan-Breslow Wilcoxon test. The one-way analysis of variance (ANOVA) tests were used in the fungal burden studies. Fisher's exact test was used to analyze the distribution of the **a** and α isolates during the *in vitro* coculture competition. All statistical analyses were performed using the Graphpad Prism 5 program, with P values lower than 0.05 considered statistically significant.

2.3. Results

2.3.1. Generation of a congenic pair of strains in a *C. neoformans* filamentous background by a series of backcrossing

We chose to use XL280 as the genetic background to generate a pair of congenic α and **a** strains that can undergo self-filamentation and unisexual mating for the following three reasons. (**i**) XL280 was an α progeny isolated from a cross between the non-filamentous B3501 and a filamentous B3502 strain (30, 68) (Fig. 2). It is one of the most robust fruiting strains examined and it can self-filament on a variety of nutrient-poor media (68). (**ii**) A genetic map and the genome sequences for XL280's parental strains B3501 and B3502 (near isogenic with JEC20**a**) are available (8, 151). The genome of XL280 itself has been sequenced (158). (**iii**) In the past few years since its creation, XL280 has already been used by several laboratories in a variety of studies (30, 66, 68, 81, 160, 161). Here we refer to this strain as XL280p to distinguish it from the congenic pair strains that will be described later.

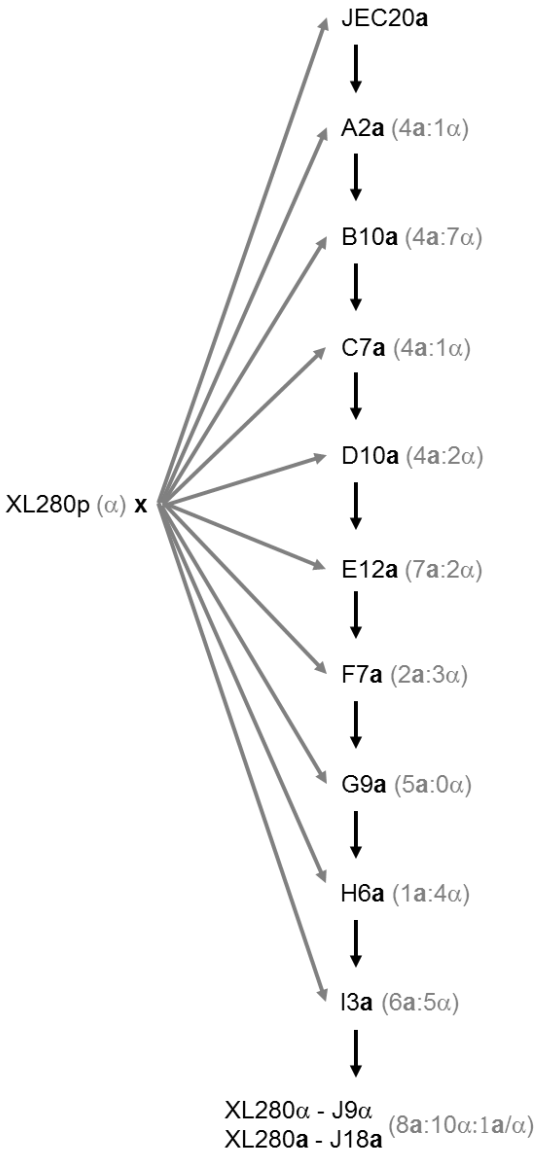

Figure 3 The pedigree of the congenic pair strains XL280α and XL280a
The progeny with the **a** mating type from a cross was selected at random and used for the next backcross with XL280p. The series of backcrosses gave rise to the congenic pair strains XL280α and XL280**a**.

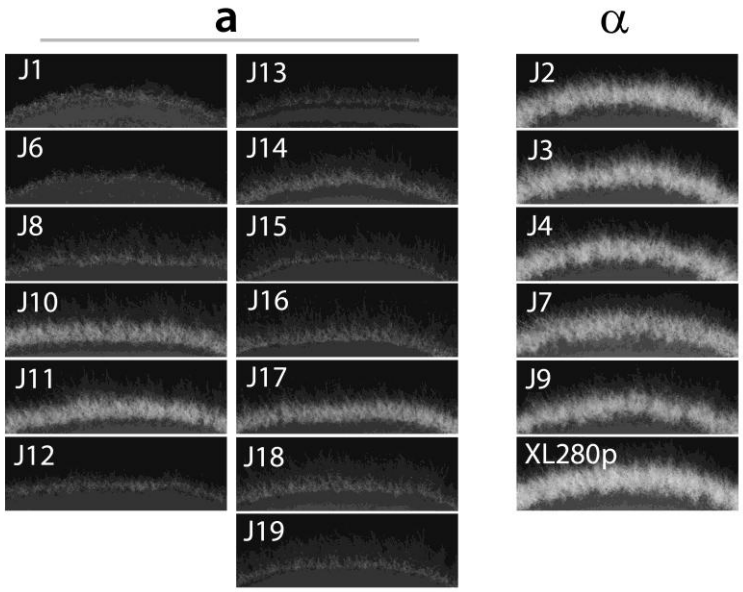

Figure 4 Enhanced self-filemantation is associated with the α mating type locus
All progeny generated in the ten backcrosses (generation J) were examined for self-filamentation on V8 juice agar medium at 22°C in the dark. The parental XL280p strain was also cultured under the same condition for comparison. All the α isolates examined produced filaments as robustly as the parental XL280p strain. By comparison, all the **a** isolates filamented relatively poorly, with strain to strain variations.

We selected JEC20**a** as the donor for the **a** mating type locus for the congenic **a** strain because sequences of its mating type locus are available. Furthermore, JEC20**a** is closely related to XL280p and the contribution of this particularly mating type allele in virulence has been tested in three other strain backgrounds (Fig. 2). A progeny with an **a** mating type from a cross between XL280p and JEC20**a** was selected at random and then backcrossed to XL280p. After additional 9 rounds of backcrosses between a randomly selected **a** progeny with XL280p, we obtained the strain pair XL280**a** (AIJ18) and XL280α (AIJ9) (Fig. 2; Fig. 3). During backcrossing, we noticed that in multiple

generations α progeny in general underwent relatively more robust fruiting than **a** progeny (Fig. 4). This observation is consistent with the previous study showing that the α mating type allele is one of the most significant quantitative trait loci associated with enhanced self-filamentation (68).

XL280p and JEC20**a** are siblings from crosses between B3501 and B3502. Hence, XL280p and JEC20**a** already share a large proportion of their genetic material based on their pedigrees (5, 151). A comparison of the genome sequences of XL280p and JEC21α indicates that their genomes are 81% identical (158). Thus after the cross between XL280p and JEC20**a** and 9 backcrosses to XL280p, in theory both XL280**a** and XL280α should be 99.98% identical to the parental strain XL280p, with the exception of mating type locus difference in XL280**a**. Consistently, when the 8 polymorphic markers between XL280p and JEC20**a** were tested on XL280α and XL280**a**, all their alleles were identical with XL280p (Fig. 5A), indicating that the genetic material from XL280p has been successfully incorporated into the congenic pair strains during the bisexual **a**-α backcrosses (**a** x XL280p). A comparison of the chromosomal profiles of these strains using CHEF gel analysis indicates identical chromosomal profiles between XL280p and the congenic pair of strains (Fig. 5B). These results suggest no gross chromosomal re-arrangement or insertions or deletions of large regions during the backcrosses. The results are consistent with the stable phenotypes and genotypes observed in the related serotype D strains previously generated (Fig. 2). Thus XL280α and XL280**a** are considered congenic, differing at the mating type locus.

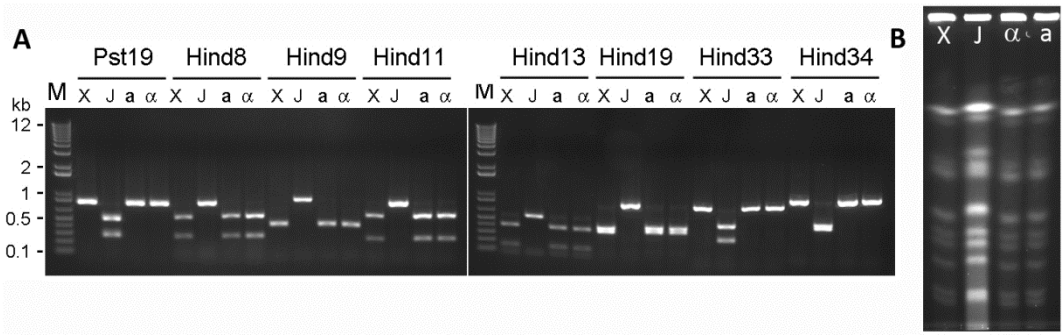

Figure 5 Genetic typing of the XL280 congenic pair strains
(A) After ten backcrosses, both congenic strains XL280α (α) and XL280**a** (**a**) contain all the alleles from XL280p (X) rather than JEC20**a** (J). The molecular marker segregation indicates that genetic materials from XL280p were transferred to the congenic pairs during backcrosses. DNA regions of the four strains were amplified by PCR, the products digested with the diagnostic restriction enzyme, and fragments resolved on agarose gels. M = the Invitrogen 1 Kb+ markers, with a subset of sizes indicated in kilobase pairs. (B) CHEF analyses of chromosomal DNA from the congenic pair strains XL280α (α) and XL280**a** (**a**), XL280p (X), and JEC20**a** (J) indicate identical chromosomal profiles between the congenic pair and XL280p. The *MAT***a** donor JEC20**a** shows a different chromosomal profile.

We further examined the phenotypes of the congenic pair strains XL280α and XL280**a** *in vitro*. As shown in Fig. 6, the congenic pair strains and their parental strains XL280p and JEC20**a** are all prototrophic, capable of growing on minimum YNB media. All the strains grew well and produced capsule visible under light microscope when incubated on DME medium at 37°C under 5% CO_2, a condition that is relevant to the host physiology. All strains produced melanin on L-DOPA medium and showed a similar level of resistance towards NaCl and H_2O_2. Thus, no drastic difference was detected among the strains in respect to these *in vitro* phenotypes. One apparent exception is their ability to undergo morphological switch. JEC20**a** is non-filamentous;

XL280**a** produces filaments profusely; and XL280α and XL280p are much more robust in self-filamentation (Fig. 6).

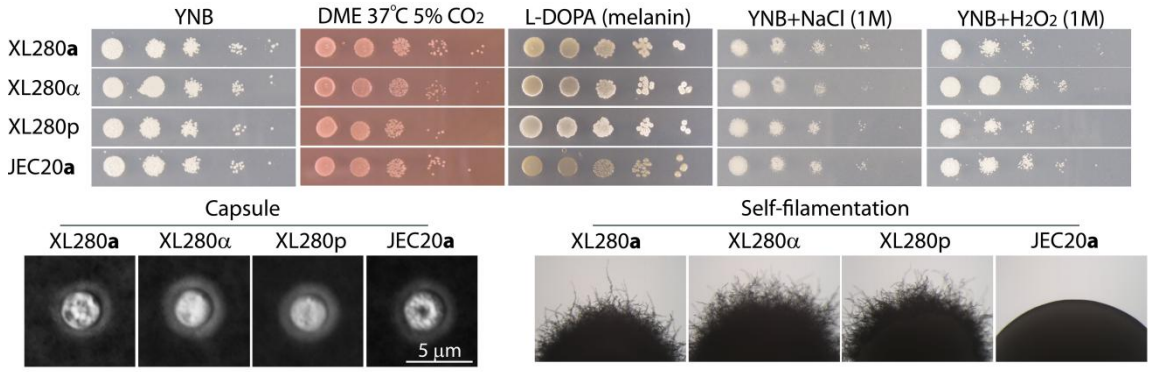

Figure 6 ***In vitro*** **phenotypic assays of the parental strains XL280p and JEC20a, and the two congenic strains XL280α and XL280a**
Yeast cells of each strain were grown in liquid YPD medium overnight and serial dilutions (10-fold) of cells were spotted onto different media. Cells were grown on minimal YNB medium at 22°C for 3 days as a control for growth (first column from the left); cells were grown on DME medium at 37°C under 5% CO_2 to assay growth under host-relevant conditions (2nd column) and capsule production (images below); cells were grown on the L-DOPA medium at 22°C for 6 days (3rd column) to assay melanin production (brown pigment); cells were grown on YNB supplemented with 1 M NaCl or with 1 mM H_2O_2 to assay resistance to osmotic stress (4th column) or oxidative stress (last column). Self-filamentation of these strains on the L-DOPA medium is shown below.

2.3.2. XL280p is virulent to mice and it grows as yeast during infection

We performed pilot experiments to determine if XL280p is virulent to mice. We tested XL280p in the inhalation model with two infection doses ($5x10^5$ and $5x10^6$ CFUs per animal) in two independent experiments and monitored animal survival for 40 days after the infections. As shown in the Fig. 7A, most animals succumbed to XL280p

infection within 40 days post infection in both pilot experiments and the 10x difference in inoculum did not appear to have any drastic effect on animal survival. This is similar to what has been observed in the serotype A strain H99, where lowering the infection inoculum by 100 fold results in only a short delay in causing mortality in mice both in the inhalation infection model and in the intravenous infection model .

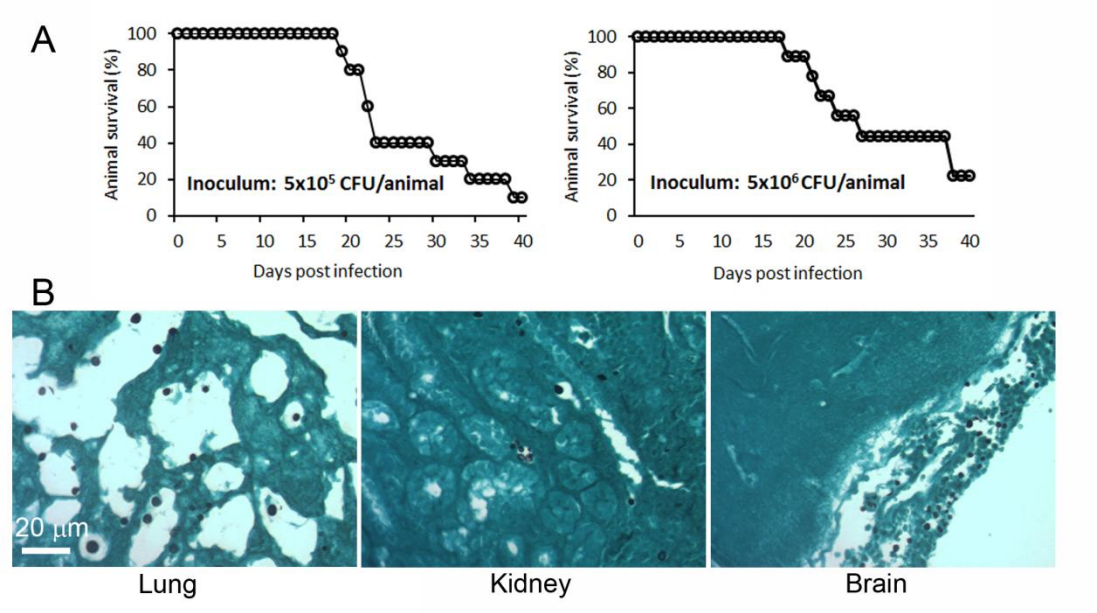

Figure 7 XL280p is virulent in the inhalation infection model of murine cryptococcosis and it grows as yeasts during infection
(A) Each mouse was inoculated intranasally with $5x10^5$ or $5x10^6$ fungal cells of XL280p, and animal survival was monitored for 40 days. (B) Mice were inoculated with $5x10^5$ fungal cells intranasally. Lungs, brains, and kidneys were dissected from sacrificed moribund mice, fixed, and processed for GMS staining to reveal fungal cell morphology in the organs (shown in black).

Although XL280p and its congenic pair strains have been observed to grow as yeast in various liquid media and in rich solid media (Fig. 6 and Fig. 8), these strains can grow in the filamentous form on solid substrates *in vitro* under a variety of nutrient-limiting conditions (Fig. 6) (68). To ascertain the cell morphology of XL280p during infection, we performed histological examination of the lungs (the initial site of infection), kidneys (a dissemination site), and brains (the site of fatal infection) of the XL280p-infected mice. As shown in Fig. 7B, XL280p was in the yeast form in all the organs examined. Thus, like most clinical isolates, XL280p does not generate hyphae *in vivo*, where it grows as yeast.

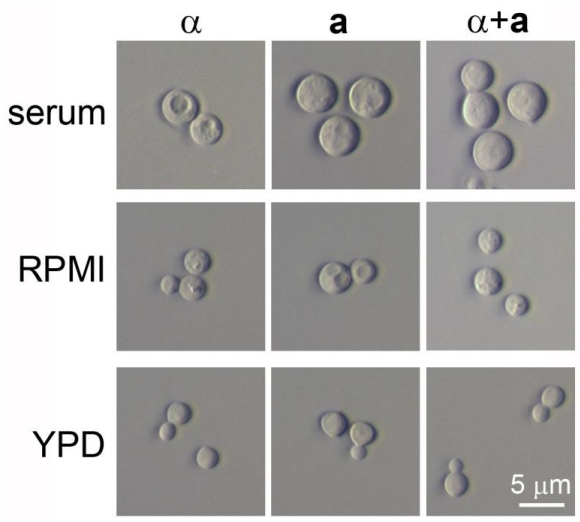

Figure 8 The congenic strains maintained yeast growth when cultured under *in vitro* conditions that are relevant to host physiology
Strains XL280α, XL280**a**, and the mixture of equal number of XL280α and XL280**a** were inoculated into fetal bovine serum, RPMI medium, or YPD medium with the final cell density of 1×10^5 cells/ml. The cells were incubated at 37°C with 5% CO_2. Photographs were taken after 3 days of incubation. All cells were in the yeast form and no filaments were observed.

2.3.3. The congenic pair strains show similar levels of virulence in two mouse models of cryptococcosis

To examine the virulence of the congenic strains, we used the well-established inhalation and intravenous infection models of murine cryptococcosis. We chose to use the intermediate inoculum of $1x10^6$ fungal cells per animal for both models and included XL280p in the comparative virulence assays to determine if the virulence potential of the congenic pair differs from their background parental strain. The congenic pair strains and XL280p caused 100% fatalities in infected mice within 6 days after being introduced into animals intravenously (Fig. 9B), and ~90-100% animal mortality rates within 40 days post infection after being introduced into animals via the respiratory route (Fig. 9B). The XL280 congenic strains are thus much more virulent compared to other serotype D reference strains, which typically require 30-100 days at a similar or higher dose to cause significant mortality in mice even when these strains are introduced to animals intravenously (5, 6, 153).

At the inoculum used in these experiments, we did not observe any difference in animal mortality caused by the parental strain XL280p and the congenic strains XL280α and XL280**a** in either the inhalation infection model (Fig. 9A) or the intravenous infection model (Fig. 9B). The comparable virulence exhibited by the congenic XL280α and XL280**a** strains in these two animal models excludes the mating type locus as one major factor influencing cryptococcal overall virulence in this genetic background under the tested conditions. The high similarity between XL280p and XL280α both *in vitro* and *in vivo* is consistent with the predicted isogenicity between these two strains.

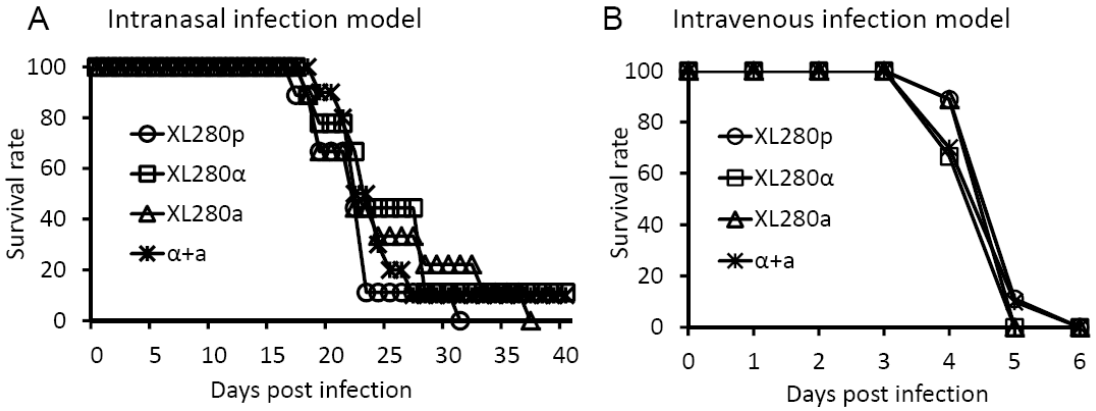

Figure 9 The congenic strains XL280α and XL280a have equal virulence with each other and the parental XL280p strain individually or co-infected together
(A) Mice were inoculated with $1x10^6$ fungal cells intranasally and their survival was monitored for 40 days. There was no difference observed in survival among the strains. The *p* values were 0.833 (XL280p/XL280α), 0.252 (XL280p/XL280**a**), 0.984 (XL280p/**a**+α), 0.075 (XL280α/XL280**a**), 0.754 (XL280α/**a**+α), and 0.053 (XL280**a**/**a**+α). (B) Mice were inoculated with $1x10^6$ fungal cells intravenously and there was no difference among these strains. The *p* values were 0.317 (XL280p/XL280α), 0.317 (XL280p/XL280**a**), 1 (XL280p/**a**+α), 1 (XL280α/XL280**a**), 0.317 (XL280α/**a**+α), and 0.317 (XL280**a**/**a**+α).

2.3.4. The a-α co-infection in the inhalation infection model of murine cryptococcosis

One interesting phenomenon of the *C. neoformans* serotype A congenic pair strains KN99**a** and KN99α is that the α strain tends to dominate in brain during mixed **a**-α co-infection in the inhalation infection model, even though KN99**a** and KN99α are equivalent in virulence when used in infection individually (7, 156). No **a**-α co-infection experiment has been performed for other congenic pairs, except the recently constructed *C. gattii* AIR265α and AIR265**a** strains. AIR265α and AIR265**a** are similar in virulence when tested individually in both the inhalation and the intravenous infection models of murine cryptococcosis (157). Further, neither the α nor the **a** mating type allele confer

any apparent advantages in terms of mortality or neurotropism in the AIR265 background during **a**-α co-infection in either model of murine cryptococcosis (157).

Here, we tested the impact of potential interactions between **a** and α cells on virulence in the inhalation infection model using the co-infection of the congenic pair strains. As shown in Fig. 9A, the XL280**a** and XL280α co-infection exhibited similar dynamics in causing animal fatality as either the **a** or the α strain infection alone in the inhalation infection model. Next, we examined the distribution of the **a** and α mating type in various organs during **a**-α mixed co-infection. We chose the unmarked XL280**a** and XL280α strains for this experiment to preclude the addition of any potential variation by the introduction of genetic markers to the mating type locus, as was employed in the previous study (156). We performed an *in vitro* control to determine if there is any proliferation advantage conferred by one mating type when the **a** and α cells are co-cultured together under a condition that is host physiologically relevant. We inoculated a mixture of **a** and α cells into the mammalian cell culture medium DME at 37°C under 5% CO_2 with the 1:1 ratio (51.5% **a** versus 48.5% α, n=822). The **a**/α ratio in the co-culture was measured again after 3 days and 9 days of incubation. At day 3 post inoculation, there was 44.2% **a** and 55.8% α (n=95); at day 9 post inoculation, there was 46.5% **a** and 53.5% α (n=127). Thus the **a**/α ratio maintained a 1:1 level in the co-culture and there was no statistically significant difference among the time points examined ($p = 0.273$). Therefore, neither the **a** nor the α mating type allele appears to confer any apparent growth advantage in the co-culture under this *in vitro* condition.

We then examined the mating type distribution in eight terminated animals infected by the **a**-α mixture (Fig. 10A). We randomly picked ~ 96 colonies from each of the 32 organs (lungs, brains, kidneys, and spleens of the 8 animals) and determined their mating type. We could not perform as many tests for some spleens due to the low numbers of fungal cells recovered (Fig. 10B). As shown in Fig. 10A, there were uniformly more α cells than **a** cells recovered from lungs of all eight animals examined. The median percentile for α cells in the lungs was ~76% and for **a** cells 24%. This uniform over-representation of α cells in the lungs during **a**-α co-infection likely reflects the better proliferation of α cells in the lungs, as there was higher lung fungal burden in animals infected by α cells alone than those infected by **a** cells alone at the time of termination (Fig. 10B). In contrast to the uniform over-representation of α cells in the lungs during the co-infection, there was no consistent pattern of mating type distribution in other organs. In the brain, **a** and α were roughly equal in 3 out of 8 mice, while **a** dominating in 4 mice and α dominating in 1 mouse. In the kidney, there was an even split between α and **a**, with the **a** dominating in 4 mice and α dominating in the remaining 4 mice. A similar even split between **a** and α was also observed in the spleen. The different pattern of the **a** and α distribution in these organs during **a**-α co-infection is consistent with the organ fungal burden. Here, animals infected by the α strain showed a higher fungal burden in the lungs, but their fungal burdens in the brain, kidney, and spleen showed no statistically significant difference from those infected by **a** or the **a**-α mixture (Fig. 10B). It is not clear why higher proliferation of α in the lungs did not cause higher fungal burden in other organs and why over-representation of the α mating

type in the lungs during the co-infection did not generate any obvious ripple effect in other organs since these organs were infected after extrapulmonary dissemination.

A

	Lung			Brain			Kidney			Spleen		
	α	**a**	n	α	**a**	n	α	**a**	n	α	**a**	n
Mouse #1	71.2%	28.8%	80	100.0%	0%	96	8.3%	91.7%	96	100.0%	0%	96
Mouse #2	81.9%	18.1%	94	46.9%	53.1%	96	71.2%	28.8%	73	33.3%	66.7%	9
Mouse #3	83.3%	16.7%	96	44.9%	55.1%	89	80.2%	19.8%	96	44.1%	55.9%	59
Mouse #4	57.4%	42.6%	94	3.1%	96.9%	96	78.2%	21.8%	87	0%	100%	96
Mouse #5	85.3%	14.7%	95	54.8%	45.2%	93	4.2%	95.8%	96	57.1%	42.9%	7
Mouse #6	65.5%	34.4%	87	29.2%	70.8%	89	33.0%	67.0%	88	77.2%	22.8%	92
Mouse #7	74.5%	25.5%	94	18.8%	81.3%	80	75%	25%	92	55.3%	44.7%	38
Mouse #8	77.2%	22.8%	127	9.1%	90.9%	88	30.5%	69.5%	95	36.7%	63.3%	30
Median	75.9%	24.1%		37.1%	62.9%		52.1%	47.9%		49.7%	50.3%	

Initial inoculation	α	**a**	n
	48.50%	51.50%	822

B

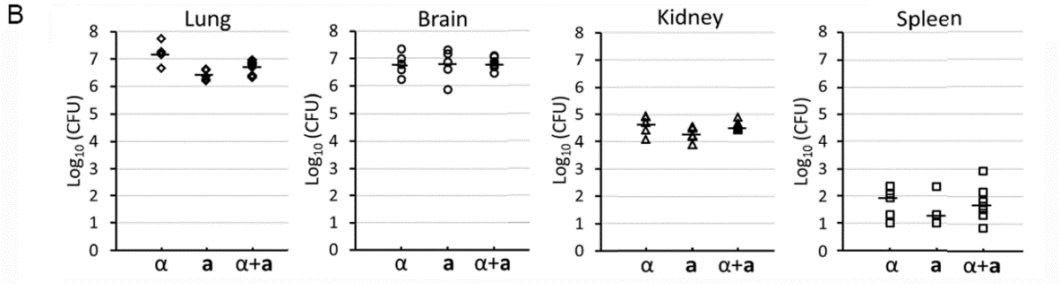

Figure 10 The mating type distribution during a-α co-infection in the inhalation infection model of cryptococcosis

(A) Animals were challenged with the mixture of **a**-α fungal cells ($1x10^6$/animal) by inhalation. At the time of termination, lungs, brains, kidneys, and spleens from eight animals per group were dissected and homogenized. The mating type of randomly picked *Cryptococcus* cells recovered from each organ was determined. (B) Animals were challenged with $1x10^6$ fungal cells (α, **a**, or the **a**-α mixture) intranasally. At the time of termination, lungs, brains, kidneys, and spleens from five animals per group were dissected and homogenized. Serial dilutions of the homogenized tissue were plated and colony forming units (CFUs) were used to determine the organ fungal burden. The short lines indicate the median. The fungal burden of these groups was statistically different in the lungs ($p = 0.001$). No statistically significant difference was found among the groups in the brain ($p = 0.973$), the kidney ($p = 0.110$), or the spleen ($p = 0.575$).

2.3.5. The a-α co-infection in the intravenous infection model of murine cryptococcosis

We further decided to examine the outcome of **a**-α co-infection in the intravenous infection model whereby the pulmonary infection is bypassed. As shown in Fig. 9B, the **a**-α co-infection exhibited similar dynamics in causing animal fatality as the infection by either the **a** or the α strain alone in this intravenous infection model. Here we tested the mating type of fungal cells recovered from brains, kidneys, and spleens of seven mice infected by the **a**-α mixture (21 organs in total). As shown in Fig. 11A, there were slightly more α cells than **a** cells in the brains in all seven mice examined. A similar slightly higher representation of α was also uniformly observed in other two organs in all seven mice. The median α : **a** ratio was 6 : 4 in the brain, 6 : 4 in the kidney, and 5.5 : 4.5 in the spleen. It is not clear why the minor advantages in amplification of α cells during co-infection in this intravenous model did not cause any apparent differences in terms of virulence among the α, **a**, or the α+**a** infections (Fig. 9B). We speculate that rapid progression of the disease caused by these intravenous infections (death within 6 days after infection) could potentially render such modest advantages not important for the animal survival. Consistent with this speculation, the fungal burdens in all organs examined at 5 days post inoculation were all high (typically ~ 10^6 CFU/organ in the brain, kidney, and spleen) and there were no statistically significant differences among the α, **a**, or the **a**-α mixture group in this intravenous model used in this study (Fig. 11B). Neither of the mating type alleles appeared to confer any apparent advantage in neurotropism during individual infection or co-infection under the tested conditions (Fig. 11B).

A

	Brain			Kidney			Spleen		
	α	**a**	n	α	**a**	n	α	**a**	n
Mouse #1	60.0%	40.0%	95	63.5%	36.5%	96	55.2%	44.8%	96
Mouse #2	65.4%	34.6%	78	55.2%	44.8%	96	57.8%	42.2%	64
Mouse #3	52.4%	47.6%	63	54.7%	45.3%	95	52.1%	47.9%	96
Mouse #4	68.8%	31.2%	96	59.4%	40.6%	96	54.7%	45.3%	64
Mouse #5	53.7%	46.3%	95	63.5%	36.5%	96	53.1%	46.9%	96
Mouse #6	64.9%	35.1%	94	67.7%	32.3%	96	62.1%	37.9%	95
Mouse #7	60.0%	40.0%	95	60.9%	39.1%	64	45.2%	54.8%	93
Median	60.0%	40.0%		60.9%	39.1%		54.7%	45.3%	
Initial inoculation				α	**a**	n			
				50.6%	49.4%	7385			

B

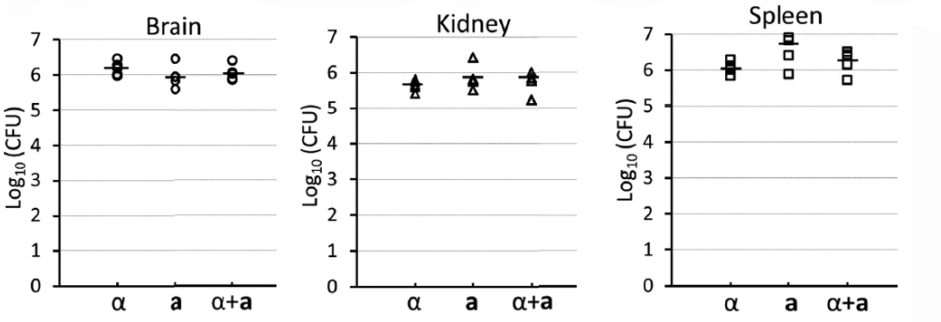

Figure 11 The mating type distribution during a-α co-infection in the intravenous infection model of cryptococcosis

(A) Animals were challenged with the mixture of **a**-α fungal cells ($1x10^6$) intravenously. At the time of termination, brains, kidneys, and spleens from seven animals per group were dissected and homogenized. The mating type of randomly picked *Cryptococcus* cells recovered from each organ was determined. (B) Animals were challenged with $1x10^6$ fungal cells (α, **a**, or the **a**-α mixture) intravenously. At DPI 5 and also the time of termination, brains, kidneys, and spleens from five animals per group were harvested. Serial dilutions of the homogenized tissue were plated and colony forming units (CFUs) were used to determine the organ fungal burden. The short lines indicate the median. No statistically significant difference was found among the groups in the brain ($p = 0.370$), the kidney ($p = 0.410$), or the spleen ($p = 0.070$).

2.3.6. Znf2 is a common factor that governs morphogenesis and mediates fungal ability to cause diseases in the varieties of *Cryptococcus neoformans*

As XL280 can easily undergo the yeast- filament morphological transition on its own under appropriate culture conditions, XL280 could be particularly useful in facilitating the research into the factors that control morphogenesis and virulence in *Cryptococcus*. As discussed in the first chapter, the morphotype-associated pathogenicity has been observed in *C. neoformans* (23, 66, 81, 162).

We then decided to examine a known factor that controls morphogenesis to assess its impact on virulence in the XL280 background. We chose to investigate the zinc finger transcription factor Znf2, as it was previously demonstrated to govern the yeast to filament transition in *C. neoformans* (66, 81). In addition, this regulator governs the formation of complex colony morphology (biofilm) through its control of the expression of multiple cell surface proteins, including the adhesion protein Cfl1 (81).

To examine the role of Znf2 in the morphotype transition in the XL280 background, we inoculated yeast cells of the wild-type strain, the *znf2*Δ mutant, and the *ZNF2*^{oe} strain (P_{GPD1}-*ZNF2* in the *znf2*Δ mutant background) on YPD, YNB, and V8 media and examined their self-filamentation. As expected, the wild type strain did not filament on the rich YPD medium, produced rudimentary filaments on the YNB medium, and generated robust filamentation on the V8 juice media (Fig. 12A). The deletion of *ZNF2* abolished the ability of XL280 to produce any filaments under all conditions, while the overexpression of *ZNF2* conferred more robust filamentation on both YNB and V8 media and enabled XL280 to produce some filaments in the otherwise

suppressive conditions of the YPD medium (Fig. 12A). Thus, Znf2 directs self-filamentation in the XL280 background. It has been shown previously that filamentation during bisexual mating between *znf2*Δ mutant with a wild-type partner is significantly reduced due to a dose effect, and mating hypha production is completely abolished in crosses involving both *znf2*Δ mutant partners in the JEC21α/JEC20**a** or the KN99α/KN99**a** background (66). A similar phenotype was also observed when *ZNF2* was disrupted in XL280 (Fig. 12C). Disruption of *ZNF2* in both partners in the XL280 background also completely eliminated mating hyphae production (data not shown). Taken together, Znf2 is required for filamentation derived from either monokaryotic fruiting (self-filamentation) or from **a**-α bisexual matings. In addition to its fundamental role in filamentation, Znf2 also controls biofilm formation in XL280 as indicated by the increasingly complex colony morphology with increased *ZNF2* expression (the *znf2*Δ mutant < wild type < the $ZNF2^{oe}$ strain) (Fig. 12B). This phenotype is consistent with previous observations made in the serotype A H99 background (81).

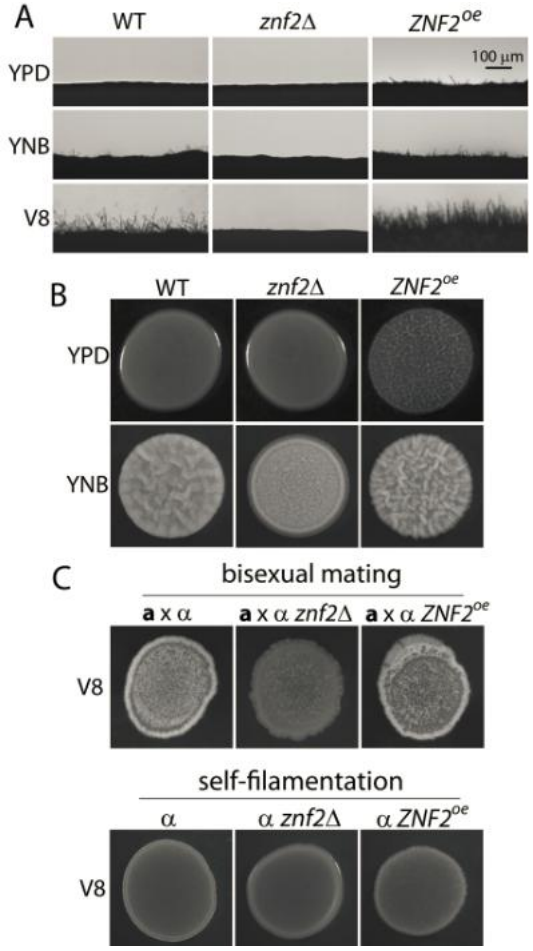

Figure 12 Znf2 controls filamentation and the formation of complex colony morphology in XL280 background

(A) The wild type, the *znf2*Δ mutant, and the *ZNF2*^{oe} strain with the inoculum were cultured on complete YPD medium, minimum YNB medium, and V8 juice medium at 22°C in the dark for 2 days. Photographs of the colony edge were shown to display filamentation (fluffy edge) or yeast cells (smooth edge). (B) The wild type, the *znf2*Δ mutant, and the *ZNF2*^{oe} strain with the inoculum were cultured on YPD and YNB media at 22°C in the dark for 4 days. The wrinkled colony indicates the complex colony morphology. (C) The non-filamentous strain JEC20**a** was mated with the wild type, the *znf2*Δ mutant, and the *ZNF2*^{oe} α strains on V8 juice agar medium. The mating mixtures were cultured at 22°C in the dark for 9 days before the photographs were taken. The white fluffy phenotype reflects aerial hyphal production in the mating colony. The culture of the wild type, the *znf2*Δ mutant, and the *ZNF2*^{oe} α strains without a mating partner is shown below for comparison.

Previously we showed that the expression level of Znf2 is inversely linked to the ability of strain H99 to cause fatal diseases in the inhalation model of murine cryptococcosis. That is, the *ZNF2*^{oe} strain in H99 background was completely avirulent while the *znf2*Δ mutant was slightly more virulent than the wild-type H99 strain (66, 81). Here we tested wild type, the *znf2*Δ mutant, and the *ZNF2*^{oe} strain in the XL280 background in the inhalation model of murine cryptococcosis to assess the role of this regulator in virulence. As shown in Fig. 13A, the overexpression of *ZNF2* resulted in a significant attenuation in virulence. However, the reduction in virulence of the *ZNF2*^{oe} strain is not as dramatic in XL280 compared to that in H99 (66, 81). We could not detect any statistically significant difference between the wild type and the *znf2*Δ mutant. This result is not unexpected given that the *znf2*Δ mutant is only slightly more virulent than the wild type in the H99 background and the effect of Znf2 mutations on virulence in XL280 might be less drastic.

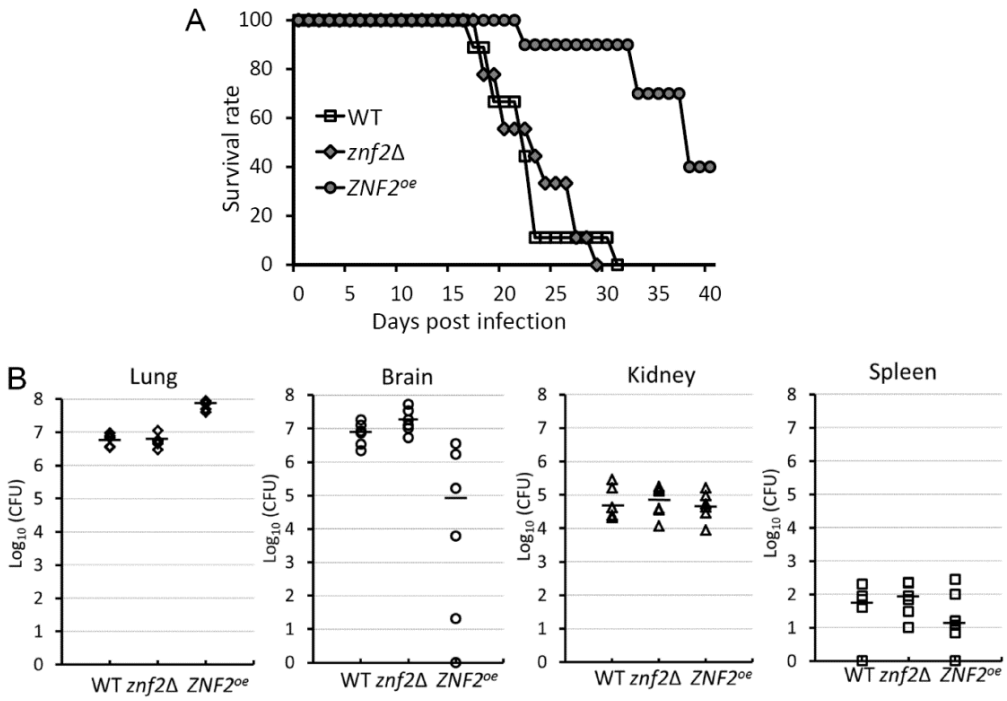

Figure 13 Znf2 mediates the fungal ability to cause fatal diseases in the murine inhalation model of cryptococcosis

(A) Mice were inoculated with $1x10^6$ fungal cells intranasally and the survival was monitored for 40 days. There was no statistically significant difference between the wild type and the *znf2*Δ mutant. The *p* value was 0.07 for WT/*znf2*Δ, and <0.001 for WT/*ZNF2*^{oe} and *ZNF2*^{oe}/*znf2*Δ. (B) Mice were inoculated with $1x10^6$ fungal cells intranasally. At the time of termination, lungs, brains, kidneys, and spleens from six animals per group were dissected and homogenized. Serial dilutions of the homogenized tissue were plated and colony forming units were used to determine the organ fungal burden. The short lines indicate the median. No colonies were recovered from a few dissected organs even with all the suspended tissue plated. Because the Y-axis is log10 of the CFU, "n/a", not applicable, was used to show them as zero on the bottom of the Y-axis. The fungal burdens among the wild type, the *znf2*Δ mutant, and the *ZNF2*^{oe} strain were statistically different in the lungs ($p < 0.001$) and the brain ($p = 0.004$). There was no statistically significant difference in the kidney ($p = 0.874$) or in the spleen ($p = 0.442$).

The *ZNF2*^{oe} strain in the H99 background is avirulent and it did not disseminate to the brain tissue at the early stage of infection in the inhalation infection model of murine cryptococcosis. However, it was not clear if the absence of brain fungal burden was an indirect effect due to the low fungal burden in the lungs or it reflects defective extrapulmonary dissemination of the *ZNF2*^{oe} strain to the brain. Here we examined the fungal burden of the lungs, brains, kidneys, and spleens of the mice infected by the wild-type strain, the *znf2*Δ mutant, and the *ZNF2*^{oe} strain in the XL280 background at the time of their termination. As shown in Fig. 13B, the fungal burden in the lungs was high in mice infected by all the strains, with the *ZNF2*^{oe} strain more than 10 fold higher than the wild-type strain or the *znf2*Δ mutant. By contrast, the presence of the *ZNF2*^{oe} strain in the brain was about 100 fold lower with larger variations (median ~10^5 CFU/organ) than the wild type while the *znf2*Δ mutant showed a slightly higher fungal burden in the brain (>10^7 CFU/organ) (Fig. 13B). The lower burden of the *ZNF2*^{oe} strain in the brain was unlikely a result of poor dissemination from the lungs, as there was no difference observed among all the strains in the kidney and the spleen (Fig. 13B). The results suggest that Znf2 might have a role in interfering with extrapulmonary dissemination to the brain specifically. Further investigation is needed to examine the role of Znf2 and its downstream factors in mediating cryptococcal neurotropism during infection.

2.4. Discussion

XL280 was derived from a clinical isolate NIH12 that can also undergo robust monokaryotic fruiting. The related congenic pairs constructed previously were purposely made in genetic backgrounds that do not self-filament or do so poorly. Among these congenic pairs, the pair JEC21α/JEC20**a** has been used most widely. However, all the serotype D congenic strains, including JEC21α/JEC20**a**, display low levels of virulence in mouse models. Investigating fungal virulence in these backgrounds requires high inocula and often intravenous inoculation (151). Here we found that the animal survival curves produced by XL280 and its congenic pair strains with an inoculum of $1x10^6$ in both the inhalation and the intravenous infection models are similar to what we and others observe for the serotype A strain H99 with an inoculum of $1x10^5$ (7). Although there is no direct comparison to other serotype D strains, XL280 congenic pair strains are likely much more virulent than their related serotype D strains in murine models (6, 65, 153, 154). Based on the pedigree of these serotype D congenic pairs (Fig. 2), JEC21α/JEC20**a**, KN3501α/**a**, and XL280α/**a** in theory should all harbor approximately 50% of the overall genetic background derived from each of the NIH12 and NIH433 genomes. The differences between these pairs in terms of morphogenesis and virulence likely derive from allelic combinations generated by recombination events during meiosis.

We noticed a different pattern of fungal proliferation in various organs in the inhalation model and the intravenous model of murine cryptococcosis at time of animal termination. The high fungal burden observed in the lungs in the inhalation model is

expected, so is the preferential proliferation in the brain over other organs (e.g. kidney or spleen) in this model given the well-known neurotropism of cryptococcal infections (Fig. 10B). In sharp contrast, the fungal presence in all organs examined was uniformly high in the intravenous infection model and there was no apparent tissue tropism (Fig. 11B). These observations indicate that the neurotropism of cryptococcal infections is apparent upon extra-pulmonary dissemination, but not with direct infusion of fungal cells into the blood. Further supporting evidence of the difference of these two models comes from the study of the mating type distribution in various organs during **a**-α co-infection. When mixed **a** and α cells were introduced into animals intravenously, there was non-discriminating slightly higher representation of α in all organs and in all animals examined, likely reflecting slightly better proliferation of the α cells *in vivo*. By contrast, although α uniformly dominated the lungs in all animals when mixed **a** and α cells were introduced into animals through the respiratory tract, **a** and α showed equal predominance in the kidney and the spleen, whereas **a** might even have a slightly better chance than α in dominating the brain. Thus, extrapulmonary dissemination appears to be a critical step in determining cryptococcal tissue tropism.

It is possible that for *Cryptococcus* cells to disseminate successfully from lungs, specific alterations in their cells, such as cell morphology (size and shape) and cell surface composition, might have to happen (76, 77, 81, 163). These alterations might render a higher affinity of these *Cryptococcus* cells to the brain. For instance, it is known that capsule structure differs at different stages of infection and in different organs, and capsule and cell size change during organ invasion (45, 54, 57). It is

conceivable then that certain changes associated with pulmonary extrusion may better assist cryptococcal invasion of the brain. Alternatively, *Cryptococcus* can disseminate through a Trojan horse mechanism and its neurotropism could be derived indirectly from the affinity between the host cells hijacked by *Cryptococcus* and the brain. For instance, monocytes have been shown to assist in cryptococcal dissemination and brain invasion (46). The identification of cryptococcal factors and host factors that affect cryptococcal neurotropism could help in testing these hypotheses.

XL280 congenic pair strains might be adept in regulating cell size in response to host factors. We noticed, for example, that their cell sizes increased when cells were incubated in serum at 37°C under 5% CO_2 (Fig. 8). It is known that cell size regulation is important for cryptococcal virulence (76, 77, 163) and it is not clear if this or other traits of XL280 contribute to its heightened virulence compared to other related serotype D strains. We also noticed that the XL280-infected mice more often showed apparent neurological disorders when they became moribund, while the H99-infected mice more often displayed severe pulmonary stress. In accordance with this observation, the fungal burden in lungs is typically one order higher than that in the brain in H99-infected mice (156, 164). In contrast, the fungal burden in the brain is at the same order as that in the lungs in XL280-infected mice (Fig. 10B and Fig. 11B). For comparison, the *Cryptococcus gattii* reference strain R265 predominantly amplifies in the lungs and very little in the brain (157, 164). Further investigation into the molecular mechanisms underlying the strain or serotype-specific differences in neurotropism is warranted. It is also interesting to note that overexpression of *ZNF2* in XL280 led to drastically lower

fungal burden in the brain even though it was present at higher numbers in the lungs and comparable levels in the kidney and spleen as the wild type (Fig. 13B). This reduced brain fungal burden of *ZNF2* overexpression stain is consistent with previously observed in a virulence analysis with *ZNF2* overexpression stain in H99 background (81). Thus, Znf2 may play a role in interfering with cryptococcal dissemination specifically to the brain after pulmonary extrusion. Given that Znf2 is a transcription factor and its regulon is highly enriched with cell surface proteins (81), it would be interesting to examine surface molecules altered by Znf2 and to investigate their roles in cryptococcal tissue tropism in the future.

In conclusion, the congenic α/**a** strains constructed in the genetic background of the highly filamentous strain XL280 are highly virulent, making them a preferred system for both cryptococcal morphogenesis and virulence studies and enabling the uses of this species complex to understand the genetic basis for dimorphic transitions in pathogenic fungi.

CHAPTER III

THE ANTIBIOTIC POLYMYXIN B EXERTS POTENT ANTIFUNGAL ACTIVITY WITH AZOLES[*]

3.1.Introduction

Polymyxin B is composed of a cationic cyclic polypeptide and a long hydrophobic lipid tail. It was initially discovered in 1940s and approved by FDA for treating gram-negative infections (165). Due to the nephrotoxicity and neurotoxicity, its parenteral use was gradually stopped since 1970s (166, 167). However, recent studies have suggested a much milder toxicity associated with polymyxin B (168). Currently polymyxin B is applied clinically for the treatment on multidrug-resistant Gram-negative infections (169, 170).

This cationic molecule perturbs the stability of the outer membrane of gram-negative bacteria via a neutralizing effect on the negative-charged lipopolysaccharide (LPS) (171). The insertion of polymyxin B into the membrane increases the permeability of the bacteria and further results in the cell lysis (171). In parallel, *Cryptococcus* possesses a unique polysaccharide capsule layer which is highly negative-charged on the cell surface (172). The cryptococcal cells may also succumb to

[*] This material has been published in this or similar form in *International Journal of Antimicrobial Agents* and *Journal of Antimicrobial Chemotherapy*, and is used here with permission of Elsevier B.V. on behalf of the International Society of Chemotherapy and Oxford University Press on behalf of the British Society for Antimicrobial Chemotherapy, respectively.
Zhai B and Lin X (2013) Evaluation of the anticryptococcal activity of the antibiotic polymyxin B in vitro and in vivo. *Int J Antimicrob Agents* 41(3):250-254.
Zhai B[*], Zhou H[*], Yang L, Zhang J, Jung K, Giam CZ, Xiang X, and Lin X. (2010) Polymyxin B, in combination with fluconazole, exerts a potent fungicidal effect. *J Antimicrob Chemother* 65(5):931-938.

polymyxin B as a result of a similar electrostatic interaction. This speculation is supported by this study in that among the pathogenic fungi tested, *Cryptococcus* is particularly sensitive to polymyxin B. In addition, the antifungal activity of other cationic peptide antibiotics, such as colistin and omiganan, has been reported (173, 174). Since polymyxin B is not able to penetrate the blood brain barrier, we hypothesized that to apply polymyxin B together with other antifungals, such as fluconazole, to control the systemic fungal infections.

The serum concentrations of polymyxin B in clinic are about 6.25~50 mg/L (175), which are below the *in vitro* inhibitory concentrations against most fungal pathogens but fall within the range of those of *Cryptococcus* isolates. We then decided to evaluate the *in vivo* efficacy of polymyxin B in two murine models of cryptococcosis. Naturally, hosts inhale cryptococcal cells from the environment. The fungal cells are either cleared in the lungs or they establish latent infections (16). When the immune system of the host is compromised (e.g. HIV infection), cryptococcal cells can activate, disseminate from lungs, and eventually cause the fatal systemic cryptococcosis (16). In the inhalation model, the animals are inoculated intranasally with *Cryptococcus* cells, which is analogous to the natural route of infection. These animals develop primarily pulmonary infections. In the intravenous model, the animals are infected intravenously with fungal cells to represent disseminated cryptococcosis. Although the poor penetration of polymyxin B to the central nervous system may limit its effect on brain infections, our data on the tissue fungal burden of the lung and the kidney suggest a modest efficacy of this compound against systemic cryptococcal infections.

3.2. Material and methods

3.2.1. Strains and media

The strains used in this chapter and in the next chapter are listed in Table 2. All yeast strains were maintained on Yeast Peptone Dextrose (YPD) medium. For the initial drug screening experiments, the *Aspergillus nidulans* strain R21 was grown on YAG medium (0.5% yeast extract, 2% agar and 2% glucose). Time course assays were performed using PBS buffer or RPMI 1640 medium buffered with MOPS (morpholinepropanesulfonic acid).

Table 2 Strain information

Strains	Species	Reference
H99	*Cryptococcus neoformans*	(7)
C45	*Cryptococcus neoformans*	(155)
A7-35-23	*Cryptococcus neoformans*	(155)
C23	*Cryptococcus neoformans*	(155)
Bt31	*Cryptococcus neoformans*	(176)
Bt81	*Cryptococcus neoformans*	(176)
92BC2-45	*Cryptococcus neoformans*	(177)
92BC1-52	*Cryptococcus neoformans*	(177)
98BC1-86	*Cryptococcus neoformans*	(177)
A2-102-5	*Cryptococcus neoformans*	(155)
123.96	*Cryptococcus neoformans*	(178)
Bt50	*Cryptococcus neoformans*	(176)
163.99	*Cryptococcus neoformans*	(178)
UA 1993	*Cryptococcus neoformans*	(153)
JEC21	*Cryptococcus neoformans*	(5)
3-10	*Cryptococcus neoformans*	(155)

Table 2 Continued

Strains	Species	Reference
3-17	*Cryptococcus neoformans*	(155)
93BC2-52	*Cryptococcus neoformans*	(177)
99BC1-40	*Cryptococcus neoformans*	(177)
UA 491	*Cryptococcus neoformans*	(153)
XL1495	*Cryptococcus neoformans*	(154)
UM4	*Cryptococcus neoformans*	(179)
92C	*Cryptococcus neoformans*	(179)
VPCI 87	*Cryptococcus gattii*	from Duke University Medical Center
BY4742	*Saccharomyces cerevisiae*	(180)
SC5314	*Candida albicans*	from Duke University Medical Center
PAT2ISO3	*Candida glabrata*	from Duke University Medical Center
DUMC132.91	*Candida krusei*	from Duke University Medical Center
MMRL1594	*Candida parapsilosis*	from Duke University Medical Center
MMRL2017	*Candida tropicalis*	from Duke University Medical Center
2-367	*Candida lusitaniae*	from Duke University Medical Center
FGSC2489	*Neurospora crassa*	from Fungal Genetics Stock Center

3.2.2. Compounds and animals

For *in vitro* studies, Polymyxin B sulfate was dissolved in water at a stock concentration of 20 mg/ml; fluconazole was dissolved in water at a stock concentration of 2mg/ml; and both of the two drugs were further diluted with PBS buffer or RPMI media to the indicated working concentrations. For animal studies, polymyxin B was dissolved in 0.9% saline at a stock concentration of 20 mg/ml and diluted with 0.9% saline for injection. Fluconazole was dissolved in 0.9% saline at 4 mg/ml. Female A/J mice (6 to 8 weeks old) were purchased from Charles River (Wilmington, MA).

3.2.3. Screening of the clinical compound library

The Johns Hopkins Clinical Compound Library (JHCCL version 1.0), a collection of 1514 FDA approved (1082) and Foreign Approved (432) Drugs (181), were screened for an inhibitory effect on *A. nidulans* colony growth. The library was assembled in a 96-well plate format with 25 µl aliquots of 10 mM stocks of drug in either water or DMSO. An aliquot of 2 µl from each well was spotted onto YAG plate and approximately $1x10^5$ spores of *Aspergillus nidulans* strain R21were point-inoculated onto the spots of original drug application. The cells were incubated at 37°C for two days. Drugs that either significantly or completely inhibited *A. nidulans* colony development were selected. Selected drugs at 2 µM were tested again for inhibitory effect on *A. nidulans* in liquid medium. *A. nidulans* spores (approximately 10^5) were inoculated into 500 µl of drug-containing liquid medium and incubated at 37°C for overnight in the 8-chambered Lab-Tek Borosilicate Coverglass System. Eleven compounds that significantly inhibited colony growth of *A. nidulans* strain R21 at this concentration were identified.

3.2.4. Disk diffusion halo assay for antifungal activity

Briefly, yeast cells at cell density of approximately $5x10^6$ were spread onto RPMI 1640 agar medium with L-glutamine and without sodium bicarbonate. The plates were allowed to solidify and dry. Whatman paper disks (7mm) containing water, fluconazole, polymyxin B, and their combination at various concentrations were dried and placed on the solidified agar surface. The cells were incubated for 24 to 48 hours at 37°C in 5% CO_2 to mimic the host environment.

3.2.5. Microdilution assays for antifungal activity

Microdilution assay was performed according to the CLSI standard except that the cells were incubated at 37°C in 5% CO_2 to mimic the host environment. Briefly, yeast cells at final concentration of approximately 1×10^3 per ml (or *Aspergillus* spores at final concentration of approximately 5×10^4 per ml) were inoculated in the RPMI 1640 liquid medium with serial (2×) dilutions of each drug being tested. The concentrations used in for polymyxin B and fluconazole were indicated in the text. Wells that contained no drugs or no yeast inoculation were included as positive and negative controls. The MIC_{100} of polymyxin B or the combination was defined as the lowest drug concentration that resulted in a 100% decrease in absorbance compared with that of the control in drug free medium. MIC_{90} of fluconazole was defined as the lowest drug concentration that resulted in a 90% decrease in absorbance compared with that of the control in drug free medium. MICs were read after incubation without agitation for 24 hours for *Candida* strains and 48 hours for the *Aspergillus*, *Rhizopus***,** or *Cryptococcus* isolates. Fungicidal effect was examined by counting CFU of the suspension from each well after plating it onto YPD medium and incubated for 24 (for *Candida* strains) to 48 hours (for *Cryptococcus* strains). MFC stands for minimal fungicidal concentration and was defined as at least 99% of cells were killed compared to the original inoculum. Synergistic or additive fungicidal effect between fluconazole and polymyxin B for each strain was calculated based on fractional fungicidal concentration index. FFC = $[F]/MFC_F + [P]/MFC_P$, where MFC_F and MFC_P are the MFCs of fluconazole and polymyxin B, respectively, and [F] and [P] are the concentrations at which fluconazole

and polymyxin B, in combination, are fungicidal. FFCs lower than 0.5 indicate synergistic interactions, FFCs between 0.5-1.0 indicate additive interactions, and FFCs between1.0-2.0 indicate indifferent interactions, and FFCs greater than 2.0 indicate antagonistic interactions (182).

3.2.6. Generation of fluconazole resistant $H99F^R$

C. neoformans H99 reference strain was cultured in YNB liquid medium with fluconazole at an inhibitory but sublethal concentration of 2.4 μg/ml. The culture was maintained at 37°C with shaking. An aliquot of the culture was transferred to fresh YNB medium with fluconazole every other day and continued for 16 weeks.

3.2.7. The effect of the polysaccharide capsule on the drug efficacy

Time course assays were employed to evaluate the effect of polysaccharide capsule on the drug efficacy. To induce the capsule production, H99 cells were cultured on RPMI agar media at 37ºC in 5% CO_2. To suppress the capsule production, H99 cells were cultured on YPD agar with addition of 1M NaCl at 30ºC in ambient air. After three days of incubation, the cells grown under each condition were collected, washed, and suspended in PBS buffer to obtain a cell density between 1500 to 2000 cells/ml. The cell suspension was treated with polymyxin B (8 mg/L). The no drug treatment was used as the positive control. At different time points (0, 1, 2, 4, 6, 8 hours post inoculation), aliquots of cell suspensions were spread onto drug-free solid YPD medium to determine the number of viable cells by measuring the colony forming units (CFUs).

3.2.8. *In vivo* murine models of cryptococcosis

The animal models of systemic cryptococcosis were induced by two infectious routes: intravenous infection and intranasal infection. In each infection model, the mice were assigned into 4 treatment groups: control (0.9% saline), fluconazole, polymyxin B, and the drug combination. Five animals per group were used for the fungal burden assay and ten animals per group were used for the survival study. All the drugs were administrated intraperitoneally. For the intravenous infection, each mouse was challenged with 1.0×10^4 H99 cells at Day 0. The drug treatment with fluconazole (10 mg/kg/day), polymyxin B (2.5 mg/kg/day), or the drug combination started on Day 1 and lasted for 5 consecutive days. The mice were given drugs once every 24 hours. The mice were then sacrificed on Day 6 and their organs were harvested to be used for the determination of the tissue fungal burden. For the intranasal infection, animals were first sedated with Ketamine and Xylazine, and then 1.0×10^5 H99 cells suspended in 50 µl of saline were slowly inoculated into the left nostril of sedated animals. In the survival study, the drug treatment with fluconazole (16 mg/kg/day), polymyxin B (2.5 mg/kg/day), or the drug combination was initiated at Day 2 and lasted for 5 consecutive days. In the fungal burden study, the drug treatment with fluconazole (4 mg/kg/day), polymyxin B (2.5 mg/kg/day), or the drug combination was initiated at Day 10 and lasted for 3 consecutive days. The mice were sacrificed one day (24 hours) after the last dose of treatment and their lungs were harvested. The kidneys or lungs were homogenized in 2 ml of cold PBS buffer using an IKA* Ultra-Turrax T18 homogenizer with the same setting for each type of organ. The cell suspensions were serial diluted

(10x), plated onto YPD agar, and incubated at 30°C for additional 2 days such that the colonies became visible in order to calculate CFUs. Animals were weighed daily and monitored twice a day for disease progression and potential severe side effects, including weight loss, gait changes, labored breaths, or fur ruffling. The animal experiments were performed according to the recommendations in the Guide for the Care and Use of Laboratory Animals of the National Institutes of Health. The protocol was approved by the Texas A&M University Institutional Animal Care and Use Committee (IACUC, Animal protocol permit number: 2011-22).

3.2.9. Statistical analysis

The one-way ANOVA tests in the fungal burden studies were performed using Graphpad Prism 5 program. The *p* values lower than 0.05 were considered significant.

3.3. Results

3.3.1. Drug screen suggested the anti-*Aspergillus nidulans* activity of polymyxin B

The Johns Hopkins Clinical Compound Library (181), composed of 1514 approved drugs was screened for anti-*A. nidulans* activity. *A. nidulans* is a model filamentous fungus used widely in mycology research. Twenty three drugs were found to either significantly or completely inhibit the colony growth of the *A. nidulans* strain R21 when 2 μl of the drugs from 10 mM stock were directly spotted onto each point inoculum containing approximately $1x10^5$ spores (Fig. 14A). Eleven compounds that significantly inhibited spore germination in liquid medium at a concentration of 2 μM were listed in Table 3 (Fig. 14B and C). Not surprisingly, the majority of them were

known antifungals belonging to the azole family. One antibiotic (polymyxin B sulfate) and three antiseptic compounds were also identified. Because of our interest in compounds that have the potential to treat systemic fungal infections, only polymyxin B was chosen for further studies. The effect of polymyxin B on *A. nidulans* is fungicidal. Both spores and pre-germinated germ tubes inhibited by polymyxin B failed to re-grow after transfer to fresh drug free medium (Fig. 14B-D).

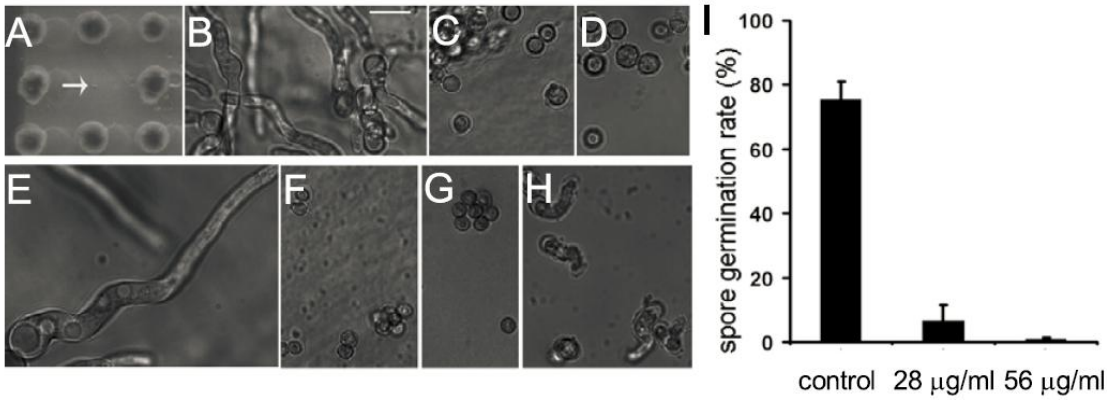

Figure 14 Polymyxin B inhibits the growth of *A. nidulans* (A-D) and *A. fumigatus* (E-H)
(**A**) A portion of the drug-screening plate showing that 2 μl of 1 mM Polymyxin B sulfate, when applied to the spot of the plate (arrow), completely inhibited the growth of *A. nidulans* colony. (**B**) Wild type *A. nidulans* in drug free medium. Bar, 5 μm. (**C**) Polymyxin B at 2 μM (2.8 μg/ml) inhibited germination of *A. nidulans*. (**D**) *A. nidulans* conidia treated with 2 μM polymyxin B did not germinate when transferred to drug free medium. (**E**) *A. fumigatus* spores in drug free medium. (**F**) Polymyxin B of 20 μM (28 μg/ml) inhibited germination of the majority of *A. fumigatus* spores. (**G**) *A. fumigatus* conidia treated with 2 μM polymyxin B did not germinate when transferred to drug free medium. (**H**) Pre-germinated germ tubes of *A. fumigatus* did not grow in the presence of polymyxin B at 20 μM. (**I**) Quantitative measurements of the effectiveness of polymyxin B at 20 μM (28 μg/ml) or 40 μM (56 μg/ml) in inhibiting the germination of *A. fumigatus* spores. Spores of *A. fumigatus* strain B5233 were incubated at 37^{o}C for 9.5 hours. 150 cells were counted for each treatment. The average and standard deviation based on three independent repeats are shown in the graph.

Table 3 Drugs that significantly inhibited *A. nidulans* spore germination at 2 μM

Name	Drug Type	Usage
Clotrimazole	Antifungal	Topical
Econazole	Antifungal	Topical
Oxiconazole nitrate	Antifungal	Topical
Voriconazole	Antifungal	Systemic
Butoconazole nitrate	Antifungal	Topical
Miconazole	Antifungal	Topical
Tioconazole	Antifungal	Topical
Polymyxin B sulfate	Antibiotic	Topical and systemic
Brilliant green	Antiseptic	Topical
Cetylpyridinium bromide monohydrate	Antiseptic	Topical
Methylbenzethonium chloride	Antiseptic	Topical

3.3.2. Polymyxin B alone is fungicidal at relatively high concentrations

We further tested the susceptibility to polymyxin B of the pathogenic filamentous fungi *A. fumigatus* and *Rhizopus oryzae*, and pathogenic yeasts including *Cryptococcus neoformans*, *Candida albicans*, *Candida glabrata*, *Candida krusei*, and *Candida parapsilosis* was examined using the standard microdilution assay. Microscopic examination revealed that more than 80% *A. fumigatus* (B5233) spores did not germinate in the presence of polymyxin B at 28 μg/ml compared to no drug treatment control (Fig. 14I). Those spores also failed to grow even after the drug removal, consistent with the fungicidal effect of the drug (Fig. 14F-G). Growth of pregerminated germ tubes also failed to grow in the presence of polymyxin B (Fig. 14H). However, some spores present in the population were resistant and were able to form hyphae in the presence of the drug

after an overnight incubation. Thus, as expected, both B5233 and Af293 isolates showed strong resistance to polymyxin B in the disk diffusion assay (data not shown) and the microdilution assay (MIC_{100} >1 mg/ml) based on visual examination. In contrast, the *R. oryzae* strain 99-880 is more sensitive, with a MIC_{100} 32 μg/ml. The pathogenic yeast strains tested also showed varied sensitivity to polymyxin B, with MIC_{100} ranging from 8 to 256 ug/ml (Table 4, columns 1-2). This range is consistent with MICs reported in the literatures (183-185). Given that bacterial strains with MICs greater than 8 μg/ml are considered resistant (186), the relatively high MICs observed in these fungal species preclude the clinical use of polymyxin B as a monothereapy.

3.3.3. In combination with fluconazole, polymyxin B at lower concentrations is fungicidal for all yeast strains tested

Polymyxins act against Gram-negative bacteria by binding lipopolysaccharide (LPS) and anionic phospholipids in bacterial membrane, disrupting membrane integrity (171, 187, 188). It is possible that polymyxin B binds fungal membrane in an analogous manner, but with lower efficiency because eukaryotic membrane has low membrane potentials, high levels of sterols, and higher contents of neutral lipid (171, 189, 190). The azole antifungals target the lanosterol 14α-demethylase Erg11 in the fungal ergosterol biosynthesis pathway (191). It results in a reduced ergosterol level and altered membrane property (116, 192, 193). We reason that polymyxin B and azole antifungals may have synergistic interactions against fungi. To test this hypothesis, the susceptibility of *C. neoformans*, *C. albicans*, *C. glabrata*, *C. krusei*, and *C. parapsilosis* strains to fluconazole, polymyxin B, and a combination of these two compounds was

analyzed by disk diffusion halo assay. As shown in Fig. 15B, the strains demonstrated varied sensitivity to fluconazole with the *C. krusei* strain DUMC132.91 and the *C. parapsilosis* strain MMRL1594 highly resistant. Polymyxin B alone at 20 μg per disk had no or minimal fungicidal activity against the strains tested (Fig. 15B). Interestingly, when fluconazole was combined with polymyxin B, the halo surrounding the disk was significantly more clear (Fig. 15B), an indication of potential fungicidal activity.

Table 4 Polymyxin B and fluconazole exhibit a synergistic fungicidal effect

Yeast Strains	**MIC_{100} PMB****	**MFC* PMB**	**MIC_{90} FLC****	**MFC FLC**	**MFC PMB - FLC**	**FFC index**
Cryptococcus neoformans H99α	8	8	1	8	1 - 2	0.266
Candida albicans SC5314	128	>256	0.2	64	6 - 8	0.125
Candida glabrata PAT2ISO3	256	256	8	>64	25 - 15	0.236
Candida krusei DUMC132.91	32	32	64	64	8 - 10	0.160
Candida parapsilosis MMRL1594	128	256	>64	>64	10 - 10	0.078
Saccharomyces cerevisiae BY4741	32	64	4	16	2 - 4	0.252
Filamentous Fungal Strains	**MIC_{100} PMB**	**MFC* PMB**	**MIC_{90} ICZ****	**MFC ICZ**	**MFC PMB - ICZ**	**FFC index**
Aspergillus fumigatus Af293	>1000	>1000	0.4	12.8	12 - 1.6	0.137
Rhizopus oryzae 99-880	32	32	0.4	1.6	4 - 0.4	0.375

*: MFC is defined as the lowest concentration at which over 99% of the original inoculums cells were killed. When fluconazole is used alone, MFC is not achieved sometimes in the dose range tested and is indicated by ">".

**: PMB: polymyxin B (susceptible breakpoint for bacteria is 2 or 4 μg/ml); FLC: fluconazole (susceptible breakpoint for yeasts is 8 μg/ml); ICZ: itraconazole (susceptible breakpoint for moulds is 1.0 μg/ml).

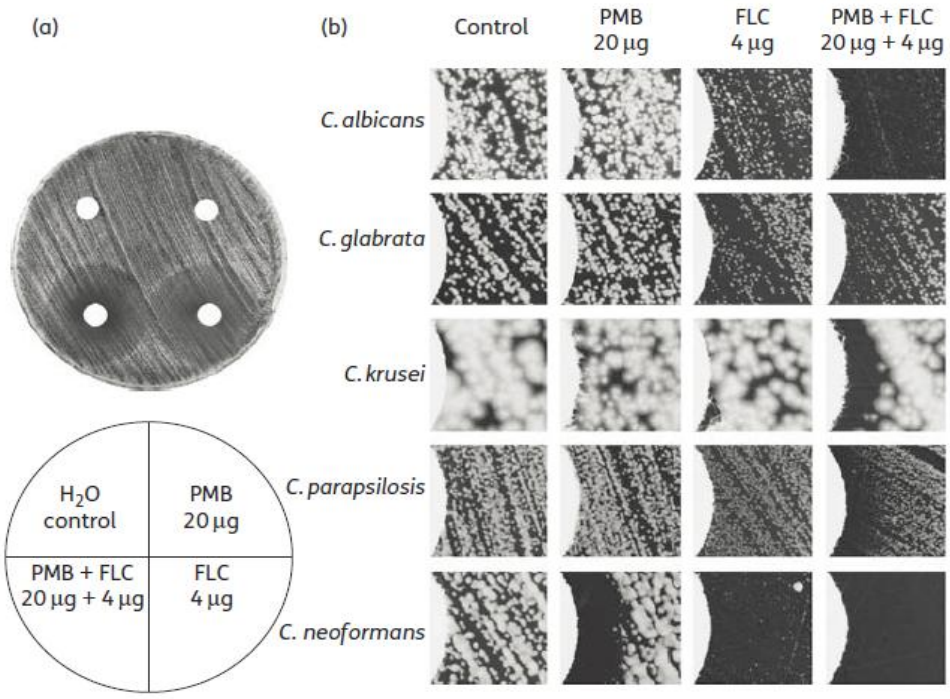

Figure 15 Synergistic interaction between fluconazole and polymyxin B against *Candida* and *Cryptococcus*

Disks containing water, polymyxin B, fluconazole, and the drug combination were dried and placed on top of a lawn of yeast cells derived from the strains indicated. Cells were incubated for 24 hours (*Candida* species) or 48 hours (*Cryptococcus*). Inhibition of fungal growth in regions surrounding the disk produces a halo. A completely clear halo indicates fungicidal activity. (**A**) Disk diffusion halo assays of the *C. albicans* strain SC5314 demonstrate a clear halo when the disk used contained fluconazole and polymyxin B combination. (**B**) Microscopic observations reveal significant clearing of the zone of inhibition (halo) when fluconazole and polymyxin B were used in combination. The left corner of each image shows the edge of the disk. PMB stands for polymyxin B and FLC stands for fluconazole.

Because the disk diffusion method was not quantitative in determining the susceptibility to polymyxin B due to the relatively large size of this molecule (30), the synergy of the drug combination was further examined using the microdilution assay. Cells from the microdilution assay after incubation with polymyxin B alone, fluconazole

alone, or the combination at various concentrations were also plated on drug-free medium for colony forming units (CFUs) to determine the minimal fungicidal concentration (MFC). As shown in Table 4, the strains showed varied sensitivity to polymyxin B and fluconazole, and there is no apparent correlation between the sensitivity towards polymyxin B and the sensitivity towards fluconazole. Consistent with results from the disk diffusion assays, the *C. krusei* strain DUMC132.91 and the *C. parapsilosis* strain MMRL1594 are highly resistant to fluconazole (the susceptibility breakpoint for fluconazole is 8 μg/ml according the CLSI standard). The MFC of polymyxin B is similar to the MIC_{100} (column 2 and 3), supporting its fungicidal property. Conversely, MFC of fluconazole can be much higher than the MIC_{90} (column 4 and 5) and complete cell killing is often not achievable. This is in accord with its classification as a fungistatic drug. A synergistic fungicidal interaction between polymyxin B and fluconazole was observed against all fungal strains tested (last two columns). Similar synergistic interactions against the *C. neoformans* H99 strain were also observed for polymyxin B and itraconazole (another azole antifungal), and polymyxin B and amphotericin B combinations (data not shown).

The susceptibility of the filamentous fungal (mould) pathogens *A. fumigatus* strain Af293 and *R. oryzae* strain 99-880 towards polymyxin B alone, itraconazole alone, and the drug combination was also examined using the microdilution assay. Itraconazole rather than fluconazole is often used in clinic to treat mould infections. As shown at the bottom of Table 4, a synergistic interaction between itraconazole and polymyxin B was also observed.

3.3.4. The combination of polymyxin B and fluconazole at clinically relevant concentrations is effective against *Cryptococcus* strains with varied fluconazole resistance

The *C. neoformans* strain H99 is more sensitive to polymyxin B than the *Candida* strains tested (Table 4). To examine whether the sensitivity to polymyxin B and the high sensitivity to polymyxin B and fluconazole combination is specific to the H99 strain or is general for *Cryptococcus*, additional clinical and environmental *C. neoformans* isolates that are genetically distinct were examined (16, 31, 155, 176) (Table 4). These strains belong to the three major *C. neoformans* molecular types VNI, VNII, or VNB and are of either **a** or α mating type (Table 5). Despite the variations in sensitivity towards polymyxin or fluconazole, the combination of polymyxin B at 2 μg/ml and fluconazole at 8 μg/ml was able to achieve greater than 99% cell killing for all strains tested except two strains Bt81 and A2-102-5 where 93-96% killing was achieved. Because the concentrations of either fluconazole (≤8 μg/ml) or polymyxin B (≤2 μg/ml) used are within the susceptible breakpoint for each agent according to the CLSI standards, the drug combination has the potential to be effective *in vivo*.

As long-term fluconazole therapy is necessary for AIDS patients with cryptococcal meningitis, the emergence of azole resistance is becoming a grave concern. Here we have shown that natural *Cryptococcus* isolates with variable resistance to fluconazole (MIC_{90} ranging from 1-32 μg/ml) are all susceptible to the drug combination. We also obtained a relatively fluconazole-resistant strain $H99F^R$ by culturing H99 in the presence of sublethal fluconazole for 16 weeks. The strain $H99F^R$

showed a sixteen fold increase in MIC_{90} to fluconazole (Table 5) and significantly increased resistance to itraconazole (data not shown). Again, a synergistic interaction against $H99F^R$ was observed between polymyxin B and fluconazole, and the combination of polymyxin B at 2 μg/ml and fluconazole at 8 μg/ml was again effective (Table 5). Taken together, the results suggest that that this combination also is likely to be effective against infections caused by azole resistant *Cryptococcus* isolates.

Table 5 In combination with fluconazole, polymyxin B at low concentrations effective against different *Cryptococcus neoformans* isolates

Strains	Genotype*	Source*	Virulence*	MIC_{100} PMB	MFC PMB	MIC_{90} FLC	MFC FLC	MFC PMB-FLC
H99	VNI (A1)	C	High	8	8	1	4	1 - 2
C45	VNII	C	High	20	24	2	6	2 - 8
A7-35-23	VNII	E	Low	16	20	4	>64	2 - 8
C23	VNI (A1)	C	High	8	20	8	64	2 - 8
Bt65	VNB (A15)	C	—	12	12	8	12	2 - 8
Bt31	VNB (A4)	C	—	8	8	12	32	2 - 8
Bt81	VNB (A15)	C	—	24	32	12	>64	2 - 8 #
Bt85	VNB (A21)	C	—	8	8	12	>64	2 - 8
A2-102-5	VNI (A2)	E	Low	10	10	16	32	2 - 8 #
Bt70	VNB (A19)	C	—	8	8	16	>64	2 - 8
$H99F^R$	VNI (A1)	L	—	5	6	16	48	2 - 8
Bt50	VNB (A4)	C	—	6	8	32	>64	2 - 8

The highest concentration of fluconazole tested was 64 μg/ml.
*: VNI, VNII, and VNB indicate *C. neoformans* three molecular types. A capital "A" followed by a number indicates further genotypic classification based on Amplified fragment length polymorphism (AFLP) genetic typing pattern. C: clinical; E: environmental; L: laboratory. The symbol "—"indicates no information available.
#: the combination at the indicated concentrations achieved 93-96% rather than >99% killing.

3.3.5. Polymyxin B is fungicidal against both proliferative and non-proliferative cryptococcal cells *in vitro*

To examine whether polymyxin B is fungicidal against both proliferative and non-proliferative cryptococcal cells, we performed a comparative time course assay of cell viability of H99 and XL280 strains *in vitro* treated with polymyxin B, fluconazole, or the drug combination. We cultured the fungal cells in RPMI medium or suspended in PBS buffer to represent rapidly proliferative or quiescent cells, respectively. As shown in Fig. 16, the survival curves of H99 and XL280 to the drug treatment displayed similar patterns. In RPMI medium, the fungal cells with all of the drug treatments were cleared within the experimental period (Fig. 16A and B). The number of viable H99 cells started to decrease within 6 hours in the presence of polymyxin B compared to the no-drug control. Similarly, viable XL280 cells started to decrease within 4 hours after being treated with polymyxin B. The drug combination showed strongest effect on H99 cells, indicating a synergistic interaction of the two drugs; whereas polymyxin B displayed a more dominant role in the drug combination in clearing XL280 cells. Similarly, the fungal cells of both strains in PBS buffer were completely cleared by polymyxin B (Fig. 16C and D). These results indicate that polymyxin B is fungicidal and is potent against *Cryptococcus* cells irrespective of the cell growth status. In contrast, fluconazole was effective in clearing rapidly proliferative cells incubated in the RPMI medium (Fig. 16A and B); but it did not show any effect on clearance of non-proliferative fungal cells in the PBS buffer by itself (Fig. 16C and D). Fluconazole also failed to enhance the potency of polymyxin B against cryptococcal cells in the PBS

buffer. These results indicate that polymyxin B is fungicidal and is more potent than fluconazole against quiescent fungal cells.

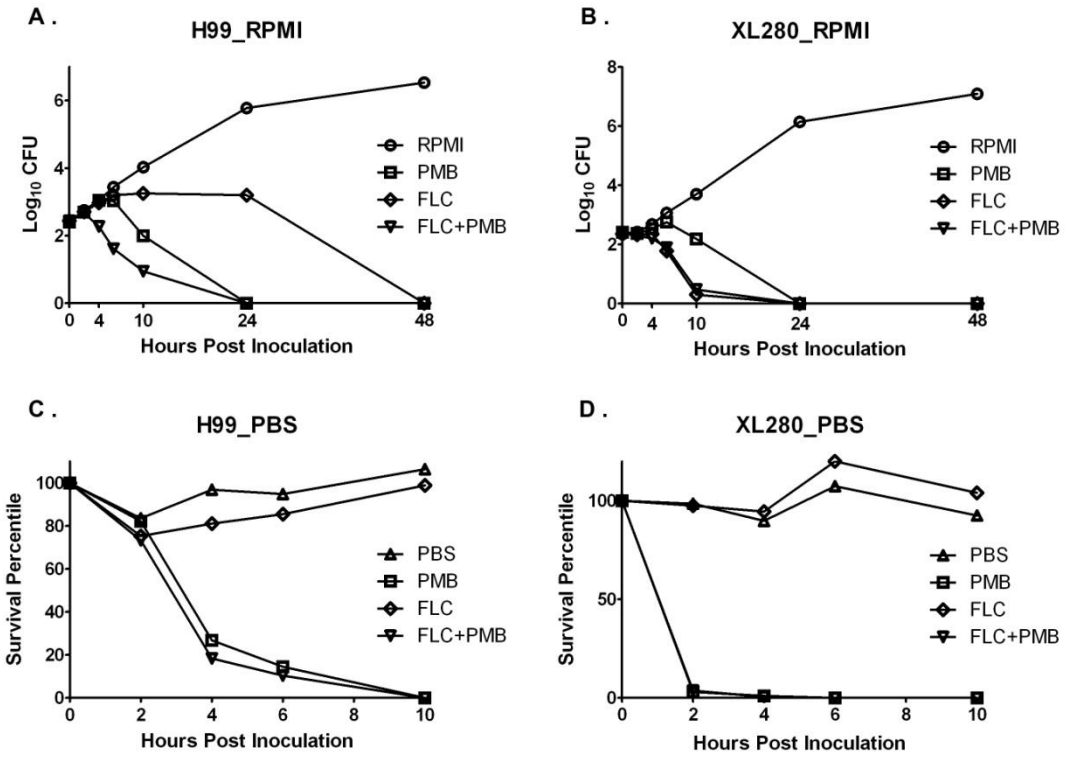

Figure 16 Polymyxin B is fungicidal against proliferative and quiescent *Cryptococcus* cells of the serotype A strain H99 and the serotype D strain XL280
H99 cells were inoculated into RPMI media (A) or PBS buffer (C) and cultured without any drug (control) or in the presence of fluconazole (FLC; 8 mg/L), polymyxin B (PMB; 16 mg/L), or a combination of these two drugs. XL280 cells were inoculated into RPMI media (B) or PBS buffer (D) and cultured without any drug (control) or in the presence of fluconazole (FLC; 6 mg/L), polymyxin B (PMB; 10 mg/L), or a combination of these two drugs. At the indicated time points, aliquots of cell suspensions were transferred and plated onto drug-free agar medium. CFUs were measured after 2 more days of incubation.

3.3.6. The polysaccharide capsule of *Cryptococcus* facilitates the fungicidal activity of polymyxin B

Given that isolates of *Cryptococcus* are much more susceptible to polymyxin B compared with isolates of *Candida* and *Aspergillus spps*., we hypothesize that differences in the cell surface composition may contribute to the difference in their susceptibility to polymyxin B. The polysaccharide capsule is a prominent and unique structure present in *Cryptococcus* that is negatively charged (172). Therefore, we suspect that the presence of the capsule may contribute to the hypersensitivity of this fungus to polymyxin B. To test this hypothesis, we firstly compared the inhibitory concentration of polymyxin B against the acapsular *cap59*Δ mutant (53) with the wild-type H99. The *cap59*Δ mutant is more resistant to polymyxin B compared to H99, with a 20% higher MIC_{100} (MIC_{100} of *cap59*Δ is 10 mg/L and the MIC_{100} of the wild-type H99 is 8 mg/L). This suggests that the lack of capsule confers the cryptococcal resistance against the stress caused by polymyxin B.

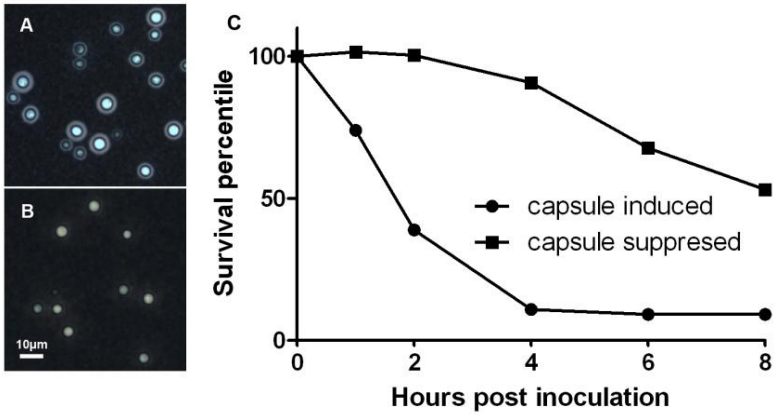

Figure 17 The capsule enhances the susceptibility of *Cryptococcus* to polymyxin B
The cells were examined by India ink staining. The capsule excludes Indian ink and appears as a halo surrounding the yeast cell. The size of the halo reflects the size of the capsule. (A) Capsule induced. (B) Capsule suppressed. Fungal cells previously grown at each condition were suspended in PBS buffer with addition of polymyxin B at the concentration of 8 mg/L. At the indicated time points, aliquots of cell suspensions were transferred and plated onto drug-free agar medium to determine CFUs after 2 more days of incubation.

As the mutation in the *cap59*Δ strain could result in other physiological changes in the fungal cells that may account for the drug resistance(194), we decided to test the effect of capsule on *Cryptococcus* sensitivity to polymyxin B by examining the drug sensitivity of wild-type H99 cells with different size of capsules. We cultured the wildtype H99 cells under a capsule-inducing condition that is relevant to the host physiological condition (mammalian cell culture media with neutral pH, 37ºC, 5%CO_2), and under a capsule-suppressing condition (YPD media with addition of a high concentration of salt). The difference in capsule size of the H99 cells cultured under these two conditions was apparent after 3 days of incubation by India ink staining (Fig.

17A and B). The cells grown at these conditions were then collected individually, washed, and suspended in PBS buffer. The susceptibility of these cells to polymyxin B (8 mg/L) was measured by a time-course cell viability assay. We chose to maintain the cells in the non-proliferative status in the PBS buffer during the assay to avoid potential complication of changes in capsule size during cell proliferation if RPMI media were used. The survival rates of these fungal cells treated with polymyxin B were examined at different time points. As shown in Fig. 17C, over 50% of the fungal cells with large capsule were cleared by polymyxin B within 2 hours; while it took more than 8 hours to reach a similar clearance level of the cells with no visible capsule. Taken together, these results indicate that the capsule of *Cryptococcus* renders this fungus more susceptible to polymyxin B.

3.3.7. Polymyxin B modestly reduces the kidney fungal burden in the intravenous infection models of systemic cryptococcosis

In the *in vivo* study, we adopted a murine model of systemic cryptococcosis where animals were infected intravenously. Our pilot experiments showed that the organ fungal burden displayed relatively low variations among individual animals in this model. Previous studies on polymyxin B had defined a safe dose of 2.5 mg/kg/day or below (195); therefore we set all the polymyxin B treatments at this dose in our animal experiments. As shown in Fig. 18, polymyxin B modestly reduced the tissue fungal burden in kidney, although the reduction is not statistically significant (p value = 0.058). Surprisingly, the drug combination did not show any synergistic effect. We also performed the animal survival study using this model, but no significant difference was

observed among the groups (data not shown). The rapid progression of the disease in this model might prevent us from observing any apparent effect of the drug treatments on animal survival as the animals succumbed to the cryptococcal infection within 7 days after inoculation even with the fluconazole therapy.

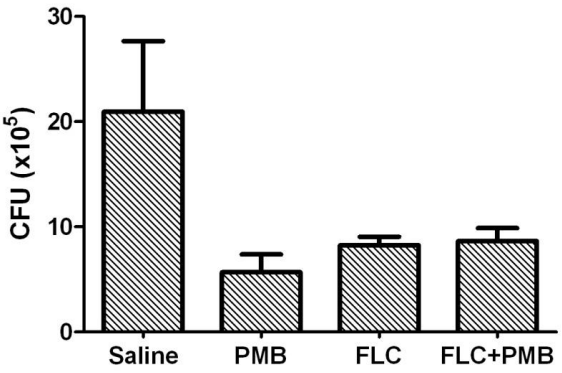

Figure 18 Polymyxin B modestly reduces the fungal burden of kidney in a murine model of disseminated cryptococcosis
Mice were challenged with H99 cells intravenously and treated with saline, polymyxin B (2.5 mg/kg/day), fluconazole (10 mg/kg/day), or the drug combination for 5 consecutive days and then sacrificed. The fungal burden of the kidney was determined by calculating CFUs. Polymyxin B alone was able to modestly reduce the fungal burden (*p* value = 0.058). However, there is no significant difference among the three drug treatment groups.

3.3.8. Polymyxin B slightly prolongs the survival period of animals, reduces the fungal burden in the lungs, and works synergistically with fluconazole in an intranasal infection model

We further tested the effect of these treatments in the murine inhalation model of cryptococcosis where the infect route reflects the natural route of cryptococcal infection.

We increased the dose of fluconazole from 10 mg/kg/day to 16 mg/kg/day to achieve a better protective result. As shown in Fig. 19A, the treatment with polymyxin B or fluconazole modestly prolonged the survival of infected mice. However, the drug combination did not show any apparent advantage in prolonging animal survival comparing to the treatments with single drug alone.

We reasoned that the high dose of fluconazole, although by itself is more effective, may mask the potential synergistic effect between fluconazole and polymyxin B *in vivo*. The modest differences in animal survival among these groups may also prevent us seeing the potential synergy between the drugs. Therefore, we reduced the dose of fluconazole to 4 mg/kg/day in the intranasal infection model and examined the lung fungal burden instead. Lungs are the primary infectious site in this model. As shown in Fig. 19B, the 3-day treatment with polymyxin B alone significantly reduced the lung fungal burden (p value < 0.05). The fluconazole group did not show any protective effect, as expected with such low dose used. However, the drug combination displayed a strong inhibitory effect on the fungal proliferation (p value < 0.001), indicating the synergy between fluconazole and polymyxin B. Taken together, our data suggest that polymyxin B is effective *in vivo* against cryptococcal infections.

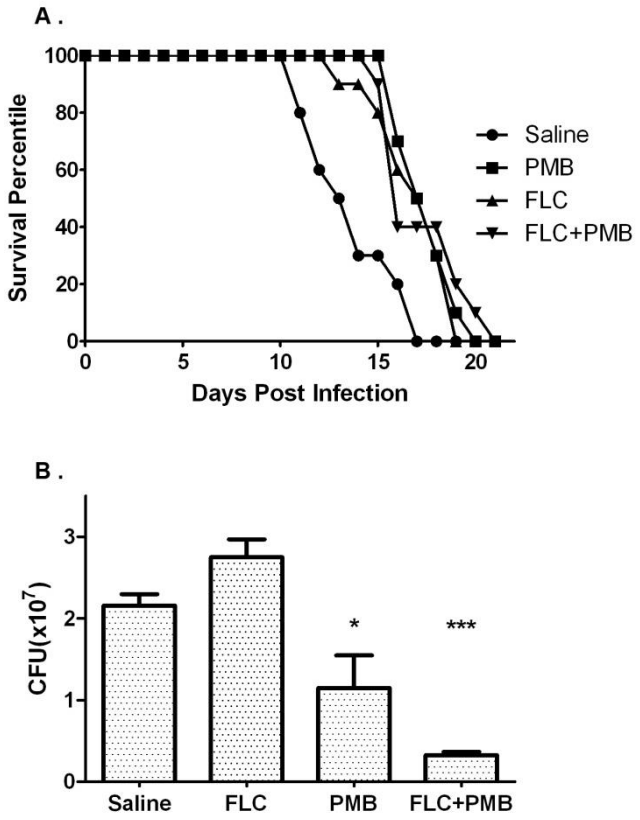

Figure 19 Polymyxin B is effective in reducing lung fungal burden and modestly prolongs animal survival in a murine model of pulmonary cryptococcosis
Mice were challenged with H99 cells intranasally. (A) The treatment started at Day 2 and last for 5 consecutive days. The survival of animals in each group was examined. (B) The lung of infected mice were dissected and homogenized after 3 days of drug treatment. Polymyxin B alone is able to reduce the fungal burden in lung (p value < 0.05) and the drug combination displays the best protection (p value < 0.001).

3.4. Discussion

Here we showed that through a screen of the clinical approved compound library, polymyxin B was identified to possess antifungal activity. Moreover, the combination of polymyxin B and fluconazole at low concentrations are fungicidal against a variety of pathogenic fungal species and also relatively fluconazole resistant strains. We found

that polymyxin B is particularly potent against *Cryptococcus*. Therefore we further examined the efficacy of polymyxin B against *Cryptococcus* both *in vitro* and *in vivo*. Our results indicate that this combination could potentially be used to treat fungal infections, particularly cryptococcal infections, and to reduce the risk of the development of resistance to the popular azole antifungals.

The antifungal property of the polymyxins and other cationic peptides antibiotics has been proposed by several groups recently (173, 174). These studies suggested that the mechanisms of the antifungal property of these drugs are analogous to their antibacterial effect, that is, disruption of the integrity of membranes (cytoplasmic and/or vacuolar). Due to the huge differences between the composition and structure of the eukaryotic and bacterial membrane (e.g. the presence or the absence of sterols in the membrane, the prevalence of negatively charged lipids etc.), fungi are in general more resistant to polymyxin B and other cationic antibiotics compared to Gram-negative bacteria. However, *Cryptococcus* is more susceptible to polymyxin B than other tested fungal pathogens. The evidence presented here suggests that the polysaccharide capsule of *Cryptococcus* may contribute to this hypersensitivity. This unique negatively charged layer may enrich the effective concentration of cationic molecules in the microenvironment of the cell surface and render the *Cryptococcus* cells more susceptible to polymyxin B.

Compared to the *in vitro* potency of polymyxin B, the *in vivo* efficacy of this drug against *Cryptococcus* is modest in our animal models. One possible reason is the difference between the *in vitro* and the *in vivo* conditions. The non-specific binding of

polymyxin B to proteins in serum or host tissues may decrease the effective concentration of the drug against *Cryptococcus in vivo*. This is supported by previous studies showing that polymyxins lost approximately 50% of their activity in the presence of serum (195, 196). Additionally, the animal models used in this study may diminish the observable effect of polymyxin B *in vivo*. The A/J mouse is highly susceptible to cryptococcal infections, and the H99 strain is one of the most virulent clinical isolates (197). The rapid progression of cryptococcosis in the models used here may underestimate the drug effect. A better effect of polymyxin B might be expected on a more robust animal model, such as rat or rabbit, or when the animals are infected by a less virulent cryptococcal strain. However, the fact that polymyxin B displayed a modest efficacy *in vivo* against *Cryptococcus*, especially in the clearance of tissue fungal burden, in the models used in this study suggests the potential of polymyxin B as an option for the treatment of cryptococcosis. Furthermore, polymyxin B could be used in topical and eye treatment to combat local fungal infections, where much higher doses of polymyxin B are often used to treat bacterial infections.

CHAPTER IV

THE ANTIDEPRESSANT SERTRALINE PROVIDES A PROMISING THERAPEUTIC OPTION FOR NEUROTROPIC CRYPTOCOCCAL INFECTIONS[*]

4.1.Introduction

Sertraline belongs to the selective serotonin reuptake inhibitors; it is also the most frequently prescribed antidepressant. Potential antifungal activity of this antidepressant was first observed in a clinical setting: three patients with premenstrual dysphoric disorder (PMDD) and recurrent vulvovaginal candidiasis (VVC) were treated with sertraline for their PMDD. Their clinical symptoms of VVC disappeared during the sertraline therapy but recurred after treatment was stopped (198). Follow-up *in vitro* studies demonstrated that sertraline is fungicidal against *Aspergillus* and *Candida* with minimum inhibitory concentrations (MIC) ranging from 7 to >256 μg/ml (198, 199). Because the MICs of sertraline against these *Aspergillus* and *Candida* strains are much higher than the achievable serum concentrations of sertraline (55 to 250 ng/ml) under standard therapeutic regimens (200), the potential clinical value of sertraline in treating systemic infections caused by these fungi was considered low (201).

The data presented in this study demonstrate that sertraline is particularly potent against *Cryptococcus*, with its fungicidal concentrations falling below 10μg/ml. Furthermore, previous pharmacokinetics studies of sertraline in rats and dogs indicate

[*] This material has been published in this or similar form in *Antimicrobial Agents and Chemotherapy* and is used here with permission of American Society for Microbiology.
Zhai B, Wu C, Wang L, Sachs MS, and Lin X (2012) The antidepressant sertraline provides a promising therapeutic option for neurotropic cryptococcal infections. *Antimicrob Agents Chemother* 56(7):3758-3766.

that sertraline concentrations in cerebrospinal fluid, brain, and some other organs are 20- to 40- fold higher than its serum concentration (202). Such levels could meet or exceed the MICs of sertraline against *Cryptococcus* isolates. In addition, abundant clinical data support the safety of long-term use of this antidepressant (203-205). Given its psychotropic nature and its potent fungicidal activity against *Cryptococcus*, we hypothesized that sertraline could be uniquely suitable in treating systemic cryptococcosis.

The mechanism of action of sertraline on the mammalian nervous system has been well characterized: it blocks the 5-hydroxytryptamine (5-HT) transporter and inhibits the reuptake of 5-HT into the presynaptic cell (206). However, there is no conserved homolog of the 5-HT transporter in fungi. Thus the underlying mechanisms responsible for the antifungal activity of sertraline remain mysterious. One report attributed the antifungal activity of sertraline to a non-specific cytotoxicity due to its lipophilicity (201). However, findings of two recent studies suggested membrane organization and vesicle-mediated transport as its antifungal targets (150, 207). Sertraline was also shown to possess antitumor activity (208-210). The antitumor activity was attributed to the inhibition of the initiation of protein synthesis through its effects on mTOR pathway (209). It is not clear if translation is also a target of sertraline in fungal cells as homologs of certain relevant factors important for translational regulation in mammals do not exist in fungi. In addition to antifungal and antitumor activities, sertraline has been shown to exert antiviral activity (211), antibacterial activity (212, 213), anti-parasite activity (214), and spermicidal activity (215). The anti-

proliferative activity of sertraline against evolutionarily diverse organisms implicates its interference with some fundamental processes. Based on our genetic screen and *in vitro* translation assays using fungal cell extracts, we demonstrate here that sertraline indeed inhibits protein synthesis in fungi. Thus, together with previous studies, our results indicate that the broad anti-proliferative activity of sertraline might be attributable to its interference with translation.

4.2.Materials and methods

4.2.1. Strains and media

The strains used in this study are listed in Table 2. All yeast strains were maintained on Yeast Peptone Dextrose (YPD) medium. Drug disk diffusion assay or microdilution assay were performed using RPMI 1640 medium buffered with MOPS according to the standard protocol of CLSI.

4.2.2. Compounds and animals

Sertraline hydrochloride was dissolved in DMSO at a stock concentration of 20 mg/ml. The drug was diluted with water or with appropriate media to the indicated working concentrations in the *in vitro* studies. For animal studies, sertraline was dissolved in 0.9 volume of water first and then 0.1 volume of 10x PBS stock solution was added. Fluconazole was dissolved at a stock concentration of 2mg/ml in water, and was diluted by water or appropriate media in the *in vitro* studies. Fluconazole was dissolved in 1x PBS buffer at 3mg/ml for the animal studies. Female A/J mice of 10-12

weeks old were purchased from Charles River (Wilmington, MA). Drug solutions for animal studies were prepared freshly before daily injection.

4.2.3. *In vitro* study of antifungal activity

The drug disk diffusion assay was performed as described in Chapter III. The microdilution assay was performed according to the CLSI standard except that cells were incubated at 37°C to mimic host conditions. The initial inocula of fungal cells ranged from 1500 to 2000 cells/ml. Drugs were added by calculating the desired dose as indicated. The minimum inhibitory concentrations (MICs) were defined by comparing the growth of the treated samples after 48 hours of incubation for *Cryptococcus* strains or 24 hours of incubation for *Candida* strains versus the no drug control *via* measuring the absorbance at 600nm. The minimum fungicidal concentrations (MFCs) were defined as at least 99% of cells were killed compared to the original inocula. The number of viable cells was determined by plating the suspension on drug free solid media and then measuring colony forming units (CFUs).

The interaction between sertraline (SRT) and fluconazole (FLC) was quantified by the fractional fungicidal concentration index (FFCI) = $[FLC]/MFC_{FLC}$ + $[SRT]/MFC_{SRT}$, where MFC_{FLC} and MFC_{SRT} were the concentration of fluconazole and sertraline used alone, respectively, and [FLC] and [SRT] were the concentrations at which fluconazole and sertraline, in combination, killed at least 99% of cells compared to the original inocula. When MFC was not achieved (> was used in these cases), the concentration 2 × that of the highest concentration tested was used for the FFC index calculation. For the interaction of sertraline and fluconazole on *Candida* strains, the

status of cell proliferation were measured by the absorbance at 600nm and quantitatively displayed with color.

4.2.4. *In vivo* model of systemic cryptococcosis

Mice were assigned into 4 groups: control (PBS), fluconazole, sertraline, and the drug combination. All treatments, including the PBS control, were given intraperitoneally. The mice of the sertraline and the drug combination groups were treated with sertraline at the dose of 15 mg/kg/day for 7 days before *Cryptococcus* infection. All the mice were challenged with $1.0x10^4$ H99 cells intravenously. The sertraline treatment continued. The fluconazole treatment at the dose of 15 mg/kg/day and the drug combination group was initiated after 24 hours of infection. All the drug treatment continued for three consecutive days after infection and the mice were sacrificed. Brains, kidneys, and spleens of mice were harvested and homogenized. Suspensions were serial diluted (10x), plated onto YPD agar, and incubated for another two days for the colonies to become visible in order to calculate CFU. Animals were weighed daily and monitored twice a day for disease progression and potential severe side effects, including weight loss, gait changes, labored breaths, or fur ruffling. The animal experiments were carried out in strict accordance with the recommendations in the Guide for the Care and Use of Laboratory Animals of the National Institutes of Health. The protocol was approved by the Texas A&M University Institutional Animal Care and Use Committee (IACUC, Animal protocol permit number: 2011-22).

4.2.5. Gene ontology analysis on the fungal target of sertraline

The genome deletion mutant collection in 96-well plates were replicated onto RPMI agar medium, or RPMI agar medium with addition of 4 μg/ml or 6 μg/ml of sertraline, for the selection of sensitive and resistant strains, respectively. After 2 days of incubation, about 300 strains with visually detectable differences in colony growth were selected (either more sensitive or more resistant). These selected strains were streaked out for individual colonies and tested through two additional rounds to exclude issues of contamination during replication or storage. In total, 89 resistant mutants and 33 sensitive mutants were selected.

4.2.6. Cell-free translation analysis

Cryptococcus H99 cells from an overnight culture were inoculated into 2-liter YPD medium to the optical density of 0.05 (OD. 600). The culture was incubated at 30°C with shaking for approximately 10 more hours to reach the optical density of 2. At this stage, the cells were collected, washed, and resuspended for the preparation of yeast cell-free extract. The resuspended cells were dripped directly into liquid nitrogen by using a sterile Pasteur pipette to form small ice beads. Frozen cell beads were transferred into pre-chilled grinding vials of a SPEX SamplePrep 6850 Freezer/Mill and powdered in the liquid nitrogen-filled tub using a setting consisting of 10 minutes of pre-cooling followed by three 2-min grind cycles with 1-min re-cooling between each cycle. The powdered cells were transferred to pre-chilled 50-mL polycarbonate centrifuge tubes, allowed to thaw on ice, and then centrifuged at 4°C for 15 min at 16,000 rpm in an SS34 rotor. The supernatant was carefully collected with a sterile Pasteur pipette,

avoiding both the pellet and the fatty upper layer, and placed in a fresh 15 ml conical tube that was maintained on ice. Small molecules were removed from the extract by chromatography through Sephadex G-25 superfine columns (216).

Capped, polyadenylated RNA encoding the firefly luciferase was synthesized using T7 RNA polymerase from a pPQ101(216). Uncapped RNA transcripts were also synthesized using the same procedure by omitting cap analog. The yield of RNA was quantified using ImageQuantTL software by comparison to standard markers with known masses using ethidium bromide-stained agarose gels. Gel images were acquired with a GE Typhoon Trio phosphorimager.

The *in vitro* translation reaction mixtures (10 µl, programmed with 60 ng of template RNA) were incubated at 26°C for 40 min. The reactions programmed in *Cryptococcus* extract contained 110 mM KOAc, 35 mM HEPES-KOH (pH 7.6), 2.6 mM $Mg(OAc)_2$, and 10 µM of each amino acid. Translation reactions were stopped by adding passive lysis buffer (Promega) to final 1× concentration. Firefly luciferase activity was determined using the Luciferase Assay System (Promega), and measured with a Perkin Elmer Victor^{3}V multilabel counter. Where 5 µCi of [^{35}S]Met (MP Biomedical, > 1000 Ci/mmol) was used to label the translation products, the translation reaction mixtures contained 10 µM of each amino acid except methionine. Translation reactions were stopped by adding SDS-PAGE loading buffer (Invitrogen) to final 1x concentration. [^{35}S]Met-labeled translation products were analyzed on SDS-PAGE gels and visualized using a GE Typhoon Trio phosphorimager.

4.3. Results

4.3.1. Sertraline is fungicidal against various *Cryptococcus* isolates *in vitro*

During the drug screen described in the previous chapter, we found that sertraline exhibited a modest inhibitory effect on *Aspergillus nidulans*. We investigated the activity of this antidepressant against *Cryptococcus* given the brain involvement of cryptococcal infections and the psychotropic property of this drug. Sertraline displayed high potency against H99, a clinical and reference *Cryptococcus* strain. The MIC_{90} against H99 is approximately 6μg/ml (Table 6), which is much lower than the reported MICs against many other fungal strains of *Candida* or *Aspergillus* species (198, 199).

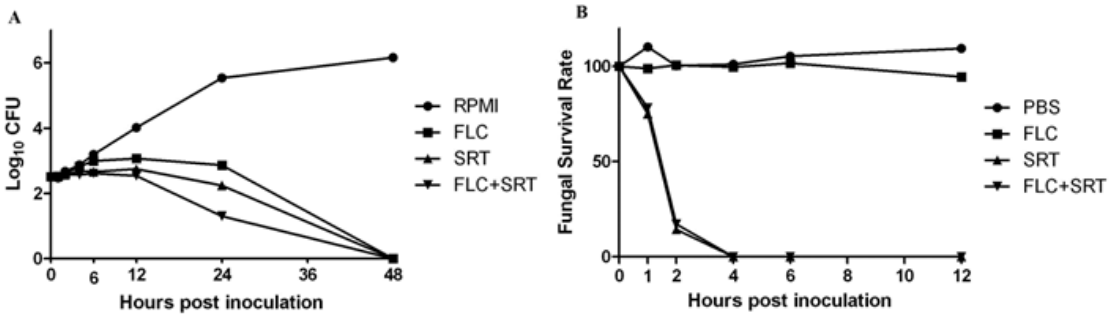

Figure 20 Sertraline is fungicidal against both proliferative and quiescent *Cryptococcus* cells
(A): H99 cells were inoculated into RPMI media and cultured without any drug (control), or in the presence of fluconazole (FLC, 8 μg/ml), sertraline (SRT, 10μg/ml), or a combination of these two drugs. At the indicated time points, aliquots of cell suspensions were transferred and plated onto drug-free agar medium to determine CFU after two more days of incubation. Fungal cells proliferated rapidly in the absence of any drugs, but they were gradually cleared with any of the drug treatments. (B): H99 cells were inoculated into PBS buffer and cultured without any drug (control), or in the presence of fluconazole (8 μg/ml), sertraline (8 μg/ml), or a combination of these two drugs. At the indicated time points, aliquots of cell suspensions were transferred and plated on drug-free medium to determine CFU after two more days of incubation. Fungal cells in PBS maintained the viability during the tested period.

To determine whether sertraline is fungistatic or fungicidal, we performed a comparative time-course assay of cell viability in the presence of sertraline and the commonly used fungistatic drug fluconazole. We cultured *Cryptococcus* H99 cells in RPMI medium or in PBS buffer to represent rapidly proliferative or quiescent cells, respectively. These cells were treated with no drug, sertraline alone, fluconazole alone, or with a combination of sertraline and fluconazole. At different time points, aliquots of cell suspensions were spread onto drug-free solid medium to determine the number of viable cells by measuring the colony forming units (CFU). In RPMI medium, the number of viable cryptococcal cells started to decrease as early as 2 hours in the presence of sertraline compared to the no drug control; and there were no viable fungal cells in the presence of sertraline after 48 hours of incubation (Fig. 20A). Sertraline was modestly more effective than fluconazole under this condition (Fig. 20A). The drug combination showed the highest efficiency in clearing the yeast cells (Fig. 20A).

Similarly, *Cryptococcus* cells in PBS buffer were rapidly cleared by sertraline (within 4 hours after inoculation), indicating that sertraline is fungicidal and is potent against H99 cells regardless whether cells are growing or not (Fig. 20B). In sharp contrast, fluconazole showed no effect on the viability of the fungal cells in PBS buffer (Fig. 20B). The lack of killing effect of fluconazole on quiescent fungal cells is consistent with the classification of fluconazole as a fungistatic drug: that is, it is effective in inhibiting fungal cell proliferation, but ineffective in destroying cells that are not actively growing. The fungicidal effect of sertraline is not specific to *Cryptococcus*, as sertraline also kills *S. cerevisiae* BY4742 cells regardless whether they were in RPMI

medium growing or in PBS buffer quiescent (Fig. 21). These results indicate that sertraline is able to kill fungal cells independent of whether they are proliferating.

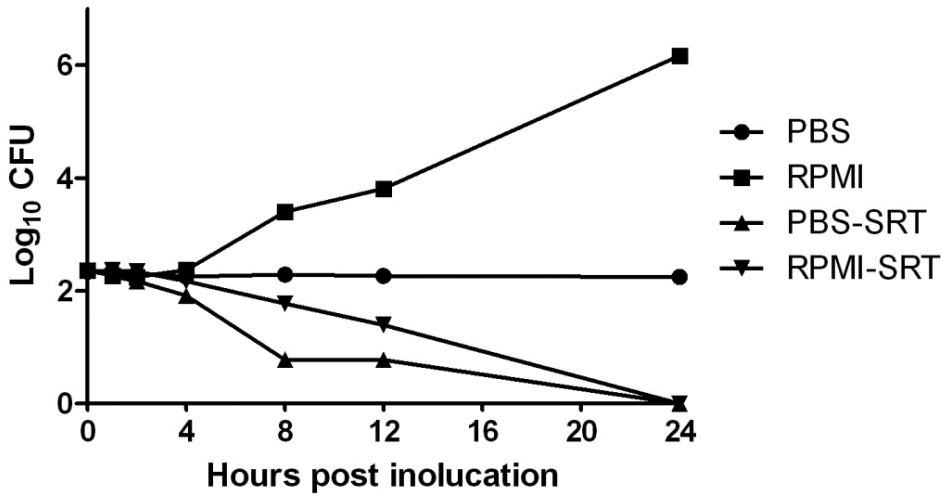

Figure 21 Sertraline time-course study with *S. cerevisiae*
Saccharomyces cerevisiae BY4742 cells were inoculated into RPMI media or PBS buffer with or without the addition of sertraline at the final concentration of 6μg/ml. At the indicated time points, aliquots of cell suspensions were plated onto drug-free medium to determine CFU. Sertraline cleared both proliferative and quiescent *S. cerevisiae* cells.

Table 6 Sertraline, alone or with fluconazole, is potent against diverse *Cryptococcus* isolates

Strains	Serotype (source)	Geographic Origins	MIC_{90} SRT	MFC SRT	MIC_{90} FLC	MFC FLC	MFC SRT – FLC	FFCI
H99	A (C)	North America	6	10	1	8	2 – 2	0.45
C45	A (C)	North America	2	6	2	6	1 – 2	0.50
A7-35-23	A (E)	North America	3	10	4	>64	4 – 4	0.43
C23	A (C)	North America	5	8	8	64	2 – 8	0.38
Bt31	A (C)	Africa	4	8	12	32	4 – 8	0.63
Bt81	A (C)	Africa	5	8	12	>64	2 – 16	0.38
92BC2-45	A (C)	Europe	6	10	4	>64	6 – 32	0.85
92BC1-52	A (C)	Europe	3	8	3	64	2 – 4	0.31
98BC1-86	A (C)	Europe	5	8	2	32	2 – 16	0.75
A2-102-5	A (E)	North America	5	8	16	32	4 – 8	0.75
123.96	A (C)	North America	4	8	8	>64	4 – 16	0.63
Bt50	A (C)	Africa	6	10	16	>64	4 – 32	0.65
163.99	A (C)	North America	4	6	6	>64	2 – 32	0.58
UA 1993	A (C)	Europe	5	8	2	6	2 – 2	0.54
JEC21	D (L)	North America	2	6	1	4	1 – 2	0.83
3-10	D (E)	North America	3	10	4	>64	2 – 8	0.26
3-17	D (E)	North America	4	8	2	64	2 – 4	0.31
93BC2-52	D (C)	Europe	3	8	4	32	1 – 8	0.38
99BC1-40	D (C)	Europe	4	8	3	32	2 – 4	0.38
UA 491	D (C)	Europe	4	8	2	8	2 – 2	0.50
XL1495	AD hybrid (L)	North America	4	8	3	8	2 - 4	0.75
UM4	AD hybrid (N)	Europe	4	10	6	>64	4 – 16	0.53
92C	AD hybrid (N)	Europe	4	10	4	>64	6 – 32	0.85
VPCI 87	*C. gattii* (E)	North America	4	10	6	64	2 – 8	0.33

(C): clinical strain; (E): environmental strain; (L): laboratory strain; (N): not clear.
MIC_{90} (μg/ml): drug concentration that resulted in a 90% decrease in absorbance.
MFC (μg/ml): minimal fungicidal concentration, the lowest concentration at which at least 99% of cells were killed compared to the original inoculums. When fluconazole is used alone, MFC is indicated by ">"when is not achieved in the dose range tested.
FFCI: fractional fungicidal concentration index. FFCIs < 0.5: synergistic, FFCIs between 0.5-1.0: additive, FFCIs between 1.0-2.0: indifferent, FFCIs > 2.0: antagonistic.

To examine whether the susceptibility to sertraline is specific to the H99 strain or is a general trait of *Cryptococcus*, we further tested 23 genetically and phenotypically distinct *Cryptococcus* strains, including 13 serotype A (this serotype accounts for 95% of the clinical representation of cryptococcosis cases), 6 serotype D (serotype D represents fewer than 5% of clinical cases of cryptococcosis), 3 AD hybrid, and 1 *C. gattii* strain (Table 6). These strains are clinical or environmental isolates originated from North America, Europe, or Africa. The MICs of sertraline were determined by the microdilution assay according to the CLSI standard. Compared to the wide range of inhibitory concentrations of fluconazole (from 1 to >64 μg/ml), all of these strains are very sensitive to sertraline, with a surprisingly narrow spectrum of inhibitory concentrations (≤10 μg/ml) (Table 6). Notably, there is no correlation between the level of susceptibility to fluconazole and to sertraline among these strains, indicating that there is no cross-resistance between sertraline and fluconazole. Thus, it is unlikely that these two drugs share common mechanisms of action. These results imply the general susceptibility of *Cryptococcus* to sertraline irrespective of their susceptibility level to fluconazole.

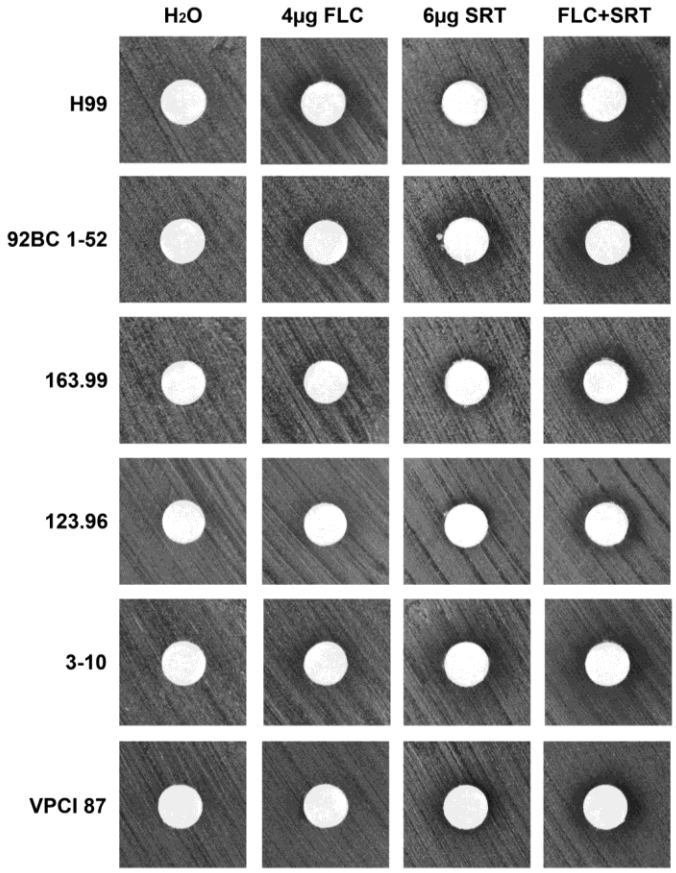

Figure 22 The synergy between sertraline and fluconazole in the disc diffusion assay against *Cryptococcus* isolates
Disks containing water, fluconazole, sertraline, or the drug combination were air dried and then placed on top of a lawn of yeast cells derived from the strains indicated. Cells were incubated at 37°C for 48 hours. Inhibition of fungal growth in regions surrounding the disk produced a halo and the drug efficacy was determined by the size and the clearance of the halo. The drug combination demonstrated a better efficacy against all tested strains compared to single drugs alone.

4.3.2. Sertraline interacts synergistically or additively with fluconazole against *Cryptococcus in vitro*

As fluconazole is the most commonly used antifungal in cryptococcosis treatment, drugs that can act additively or synergistically with fluconazole are more

likely to be used clinically. In the time-course assay described above, we observed that the combination of sertraline and fluconazole accelerated the clearance of proliferative *Cryptococcus* cells (Fig. 20A). To determine the interaction between sertraline and fluconazole against *Cryptococcus*, we compared the susceptibility of the 24 isolates to a combination of these drugs with their susceptibility to each drug alone using the disk diffusion halo assay. For all the strains tested, halos formed near disks containing the drug combination were larger and clearer than those formed near disks containing either fluconazole or sertraline alone (Fig. 22). The results indicate possible synergistic or additive interactions between sertraline and fluconazole against *Cryptococcus*.

We next quantified the interaction between sertraline and fluconazole against *Cryptococcus* by using a microdilution assay to determine the fractional fungicidal concentration index (FFCI). Sertraline increases the antifungal activity of fluconazole against all the tested *Cryptococcus* strains, demonstrating a synergistic (FFCI < 0.5) or additive (FFCI between 0.5-1.0) (182) effect between the two drugs (Table 6). This is consistent with the results obtained by the disk-diffusion method. Considering the divergence of genetic background of the tested strains, these observations suggest the possibility that the combination of sertraline and fluconazole could be more effectively clearing different *Cryptococcus* isolates in mammalian cryptococcosis.

4.3.3. Sertraline alone or in combination with fluconazole displays antifungal activity in a murine model of systemic cryptococcosis

As described earlier, sertraline exerts anti-*Cryptococcus* activity alone or in combination with fluconazole *in vitro*. To determine the efficacy of sertraline or its

combination with fluconazole *in vivo*, we adopted a murine model of systemic cryptococcosis. We chose the intravenous model of cryptococcosis here because our pilot experiments showed that organ fungal burden displayed relatively low variations among individual animals. To examine the drug efficacy in this model, we assigned mice into four groups: the control (PBS) group, fluconazole treatment group, sertraline treatment group, and the group receiving a drug combination. Given that it takes at least 5~7 days for sertraline to reach a steady state in the mouse brain (217), mice of the sertraline group and the drug combination group were given a 7-day pretreatment of sertraline prior to the infection by the *Cryptococcus* reference strain H99. Based on previous studies, the serum level of sertraline in these animals was likely to be too low (55 to 250 ng/ml (200)) to exert any growth inhibitory effect on the fungal cells initially inoculated into the blood stream. Fluconazole treatment was initiated at one day post infection (DPI 1) in both the fluconazole alone treatment group and the drug combination treatment group. Such treatment was continued for three consecutive days. The animals were sacrificed at DPI 4; their brain, kidney, and spleen were homogenized and the fungal burdens of these organs were determined by measuring CFU. As shown in Fig. 23, the treatment with sertraline alone reduced the fungal burden in the brain (P value < 0.05), with its efficacy comparable with that of fluconazole. Sertraline also reduced fungal burden in kidney, while fluconazole showed no apparent effect. Sertraline appeared to have a modest effect on fungal burden in spleen but such effect was not statistically significant. The difference in the drug efficacy on the three organs examined may reflect variations of drug concentrations at these organs. Importantly, the

treatment with the combination of sertraline and fluconazole displayed the most potent efficacy in reducing fungal burden of all three organs examined (Fig. 23). Therefore, the data demonstrate that sertraline alone is efficacious against cryptococcosis and the combination of sertraline with fluconazole is a more effective treatment than either drug alone due to their strong synergy *in vivo*.

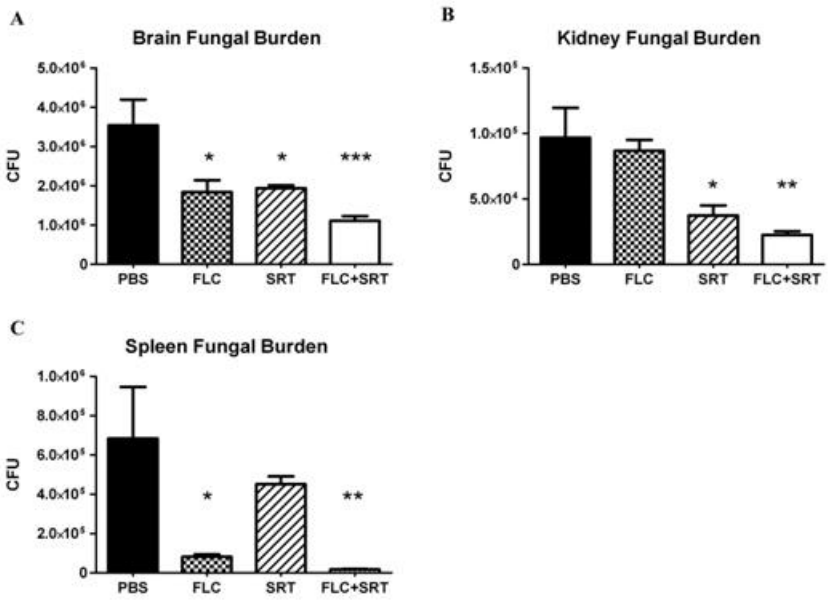

Figure 23 Sertraline reduces the fungal burden alone or in combination with fluconazole *in vivo*
Brains (A), kidneys (B) and spleens (C) of mice from different treatment groups were dissected and homogenized. The suspensions were diluted serially and the fungal burden was determined by calculating CFU. Sertraline alone significantly reduced the brain and the kidney fungal burden while the drug combination reduced the fungal burden significantly in all three organs. *: P value < 0.05; **: P value < 0.01; ***: P value < 0.001. In brain, the drug combination displays higher potency comparing to either fluconazole or sertraline alone (both P values < 0.05). The efficacy of the drug combination is also superior to that of fluconazole alone in kidney (P value < 0.001), or that of sertraline alone in spleen (P value < 0.001).

4.3.4. Sertraline antagonizes the growth inhibitory effect of fluconazole against many *Candida* strains

To examine if the potency of sertraline alone or in combination with fluconazole can be extended to *Candida* species, we tested the MICs of sertraline against six strains that represent six different *Candida spp.*: *C. albicans* SC5314, *C. glabrata* PAT2ISO3, *C. krusei* DUMC132.91, *C. parapsilosis* MMRL1594, *C. tropicalis* MMRL2017, and *C. lusitaniae* 2-367. The MIC_{90}s ranged from 12 to 24 μg/ml (Table 7), which are considerably higher than the MICs against *Cryptococcus* but are consistent with previous studies (198). These MIC values are higher than the achievable blood or even organ levels of sertraline.

Table 7 Sertraline is less potent against *Candida* strains

Strains	**MIC_{90}**	**MIC_{100}**
Candida albicans SC5314	32	48
Candida glabrata PAT2ISO3	12	16
Candida krusei DUMC132.91	12	16
Candida parapsilosis MMRL1594	24	24
Candida tropicalis MMRL2017	24	32
Candida lusitaniae 2-367	8	24

MIC_{100}: the lowest drug concentration that resulted in a 100% decrease in absorbance.
Unit: μg/ml

In striking contrast to the results obtained with *Cryptococcus*, sertraline exerted a significant antagonistic impact on the inhibitory effect of fluconazole against the majority of the tested *Candida* stains *in vitro* (Fig. 24). For example, one-day incubation with fluconazole alone was able to effectively inhibit the growth of *C. tropicalis* MMRL2017 strain at a concentration of 1.0μg/ml. However, with the addition of sertraline (1.0~6.0 μg/ml), fungal growth in the presence of fluconazole not only recovered but actually became more robust. The spectrum of the concentrations at which sertraline exerts antagonistic effect with fluconazole, unfortunately falls in the clinically relevant range. Similar antagonistic interactions between sertraline and fluconazole were also observed among three other *Candida* strains: *C. albicans* SC5314, *C. glabrata* PAT2ISO3, and *C. parapsilosis* MMRL1594 (Fig. 24). Sertraline did not decrease the inhibitory effect of fluconazole on *C. lusitaniae* 2-367 or on *C. krusei* DUMC132 (Fig. 24). Although synergistic or additive interactions between sertraline and fluconazole were reported in some *Candida* strains (150), antagonistic interactions between fluconazole and sertraline are commonly observed among *Candida* and *Aspergillus* strains (this study and (218)).

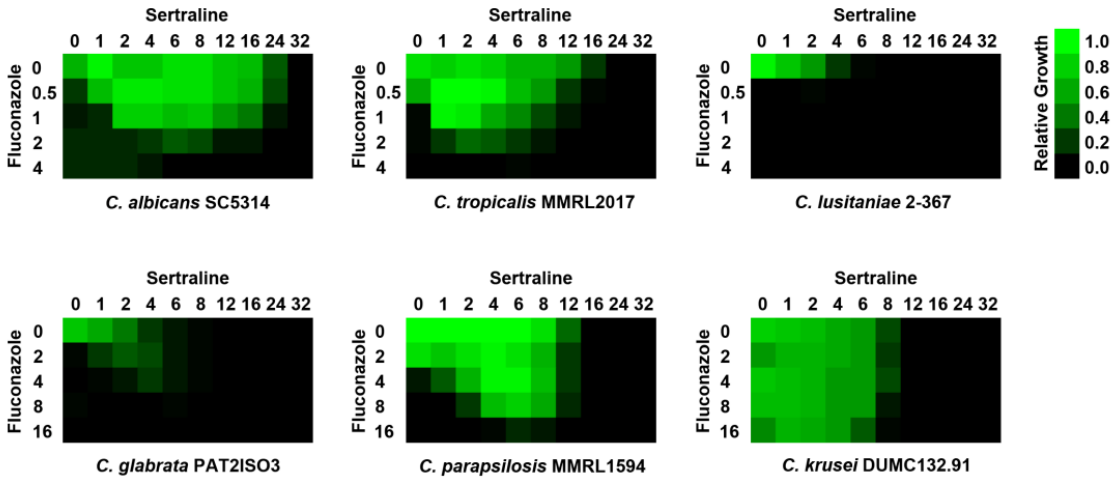

Figure 24 Antagonistic effects between sertraline and fluconazole among *Candida* strains
Six *Candida* strains, *C. albicans* SC5314, *C. glabrata* PAT2ISO3, *C. krusei* DUMC132.91, *C. parapsilosis* MMRL1594, *C. tropicalis* MMRL2017, and *C. lusitaniae* 2-367 were incubated in RPMI media with indicated drug treatment. Gradient by columns: sertraline (μg/ml); gradient by rows: fluconazole (μg/ml). The scale of the fluconazole concentrations was determined based on the results from Chapter III. Growth was measured by absorbance at 600 nm after 24 hours of incubation. Green indicates fungal growth and black indicates the lack of fungal growth.

4.3.5. Sertraline interferes with translation in fungal cells

The broad anti-proliferative activity of sertraline against many organisms indicates that the mechanism underlying its fungicidal activity may involve some fundamental cellular processes. To identify the potential fungal molecules and processes affected by sertraline, we screened the whole genome deletion collection of *S. cerevisiae* for sertraline-sensitive or sertraline-resistant mutants. This mutant collection set is composed of a non-essential gene deletion set in a haploid background and an essential gene deletion in a heterozygous diploid background (180). After one round of initial

screen and two rounds of additional screen to confirm the selected phenotype, 88 resistant and 36 sensitive strains were identified. Gene ontology analyses indicate that these genes are enriched for those with roles in intracellular vesicle transport and membrane organization (Fig. 25), which is consistent with the findings of two recent studies of sertraline on yeast (150, 207).

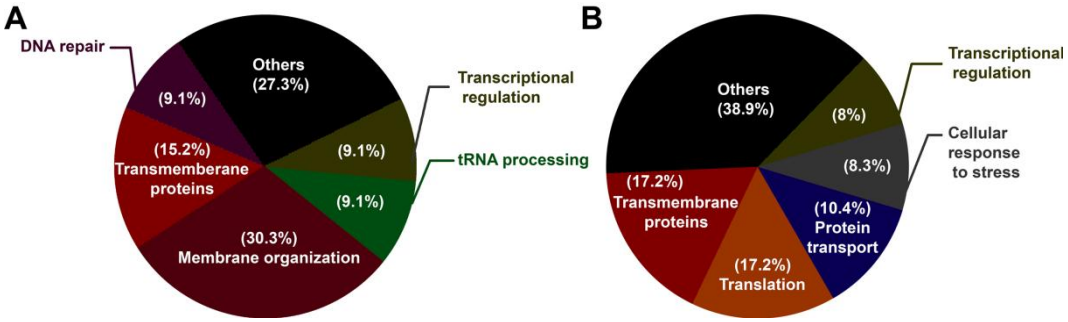

Figure 25 Gene ontology analysis of the *S. cerevisiae* genes involved in sertraline tolerance or susceptibility
Gene ontology (GO) terms for annotated *S. cerevisiae* genes involved in sertraline resistance (A) or susceptibility (B) were extracted from the GO database and sorted into the immediate subcategories for molecular functions and biological processes.

Interestingly, genes related to protein synthesis are highly enriched in the resistant group; and the most sensitive mutant selected from our screen was Δ*tif3*, a strain in which an important translation initiation factor Tif3 was disrupted. Since previous studies in mammalian cells have indicated that sertraline inhibits translation initiation (209), these data indicated that it was possible that sertraline also disrupts translation in fungi.

4.3.6. Sertraline inhibits translation in a *Cryptococcus* cell-free system

To determine the effect of sertraline on translation in *Cryptococcus*, we performed *in vitro* translation assays. In these assays, the luciferase mRNA was used as the template and the translation machinery was provided by the cell extract obtained from *C. neoformans* strain H99. As expected, translation in these *Cryptococcus* cell extracts was synergistically dependent on the mRNA 5' terminal cap and 3' terminal poly(A) tail, as with *Saccharomyces* cell extract (Fig. 26A) and *Neurospora crass* cell extract (216, 219). This result verified that *Cryptococcus in vitro* translation system faithfully recapitulated the dependence of cap and poly(A) for translation.

The effects of sertraline on translation of cap and poly(A) luciferase mRNA was assessed by two means: 1) the enzymatic activity of the luciferase produced by the *in vitro* translation, and 2) the level of [^{35}S] methionine incorporation into the luciferase polypeptide produced. We found that sertraline inhibited the translation efficiency in a dose-dependent manner using both detection methods (Fig. 26B and C). Luciferase enzyme activity dropped 50% compared to the control when the concentration of sertraline was increased to 0.1 mM (30.6 μg/ml). No enzyme activity above background was detected in the presence of sertraline at 0.4 mM (122.4 μg/ml). The decrease in luciferase enzyme activity in the presence of sertraline was not due to direct interference of sertraline on the enzymatic activity of the synthesized luciferase, since addition of sertraline into the cell extract after translation was completed did not alter enzyme activity based on this measurement (Fig. 26B). The [^{35}S] methionine incorporation assay showed that sertraline affected the yield of luciferase polypeptide synthesized in this cell

extract (Fig. 26C). Protein synthesis was also affected by sertraline in fungal extracts derived from the yeast *S. cerevisiae* and the filamentous fungus *N. crassa*, although higher concentrations of sertraline were required to achieve a similar level of inhibition (Fig. 27). In contrast, fluconazole, which is known to target the enzyme Erg11 in the ergosterol biosynthetic pathway, did not show any inhibitory effect on protein synthesis in a similar concentration range in such assays (Fig. 28). These data obtained in cell-free translation systems using fungal extracts show that sertraline interferes with fungal protein synthesis.

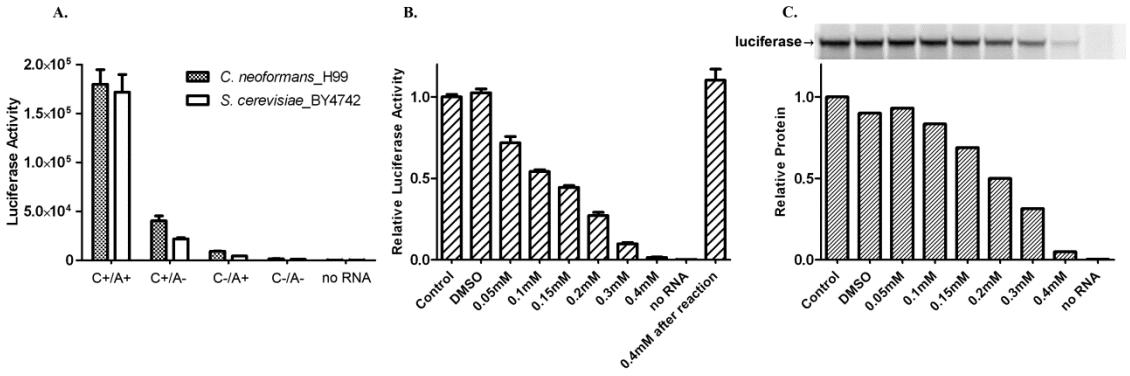

Figure 26 Sertraline inhibits translation in a *Cryptococcus* cell-free system
Cell-free translation system was prepared as described in Materials & Methods. (A): The translation of luciferase in both *Cryptococcus* and *Saccharomyces* cell free extracts is dependent on the mRNA 5' terminal cap, designated as C, and on the 3' terminal poly(A) tail, designated as A. The cap and poly(A) synergistically stimulate RNA translation in both cell free systems. (B) and (C): Water, the solvent (DMSO), or sertraline in stock solution was added into reactions to reach the indicated concentrations. Luciferase protein synthesis by the cell-free translation system was measured based on the relative light units arising from the enzymatic activity of luciferase (B), or the level of [^{35}S] methionine incorporated into the synthesized luciferase polypeptide (C). Both measurements showed that sertraline inhibited translation in a dose-dependent manner.

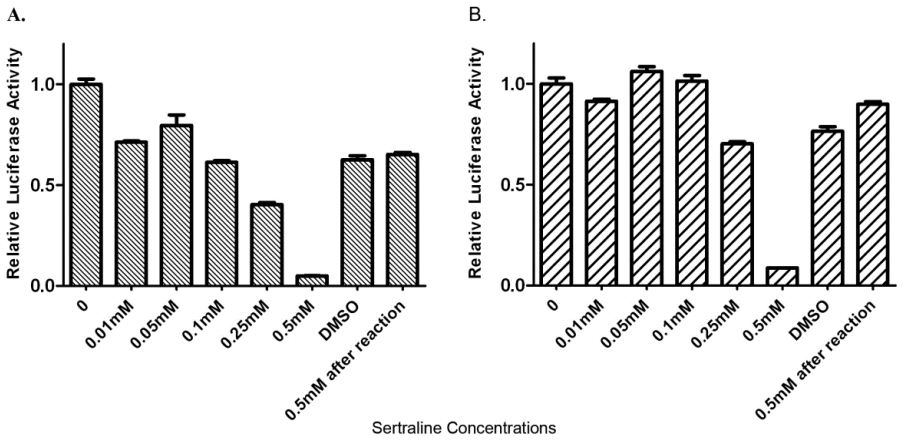

Figure 27 Sertraline inhibits translation with the cell extract of *S. cerevisiae* or *Neurospora crassa*

Luciferase protein synthesis by the cell-free translation system was measured based on the relative light units generated due to the enzymatic activity of luciferase. The cell extracts of *S. cerevisiae* (A) or *N. crassa* (B) were inhibited by sertraline in a dose-dependent manner. The *in vitro* translation processes in both systems dropped sharply when the sertraline concentration was increased to 0.5mM.

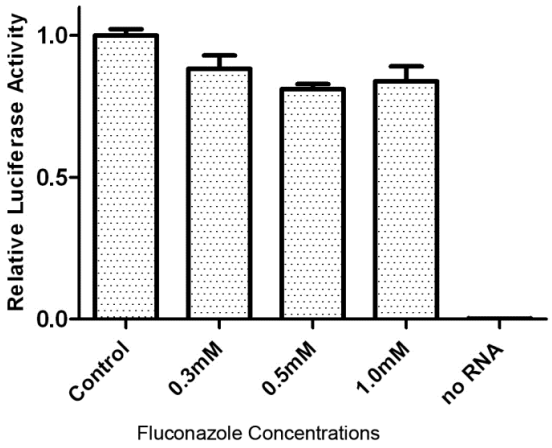

Figure 28 Fluconazole shows no apparent inhibition on protein synthesis in the *in vitro* translation assay

The *in vitro* translation of luciferase in *Cryptococcus* cell extract was accomplished in the presence of fluconazole at indicated concentrations. No dramatic decrease of luciferase activity was observed even when the concentration of fluconazole reached 1mM.

4.4. Discussion

4.4.1. Sertraline offers a promising option for the therapy of cryptococcal meningitis

Here we provide evidence for the potent anti-cryptococcal activity of the antidepressant sertraline both *in vitro* and *in vivo*. Given the difficulties in developing antifungal drugs *de novo*, recent studies have explored existing clinical compounds for potential use as antifungals (220). Existing pharmaceutical and safety information concerning the use of these drugs in animals or in humans could greatly accelerate the investigation into their clinical use as antifungals. Consistent with the safety profile of sertraline for long-term use in patients, we did not observe any severe side-effects due to sertraline administration during the treatment process in the animal studies presented here. Previous studies also showed the safety of sertraline administration in mice with a similar daily dose but for a much longer period of time (214).

The discovery that sertraline has anti-cryptococcal activity offers the potential for an additional choice for treating cryptococcosis. Our tests of 24 diverse *Cryptococcus* strains indicate a uniformly high sensitivity of this fungus to sertraline relative to other fungal species tested. Compared to fluconazole, sertraline showed a much narrower range of inhibitory concentrations against these diverse *Cryptococcus* isolates (Table 6), suggesting a lower probability of naturally occurring resistance to sertraline in existing *Cryptococcus* populations. The fungicidal nature of sertraline and its synergy with fluconazole against *Cryptococcus* as previously observed *in vitro* and *in vivo* in an insect model (150) and this study shown in a mammalian model, could potentially shorten the duration of anti-cryptococcal therapy, and reduce the risk of emerging drug-resistance.

During latent infection or during fluconazole treatment, *Cryptococcus* cells are likely dormant or grow slowly. Given that even dormant cells need transcription and translation (221), and that sertraline is capable of killing fungal cells under quiescent conditions, it is reasonable to speculate that sertraline might be useful to clear latent cryptococcal infections or to kill residual fungal cells unharmed by the fluconazole treatment. This could be tested by further investigation.

It is worth mentioning that we did not observe any difference in survival in any of the treatment groups (including the fluconazole treated groups). This is consistent with the observation in Chapter III. The A/J mouse used in this study is very susceptible to *Cryptococcus* infections and H99 is one of the most virulent clinical isolates of *Cryptococcus* (197). We tried different inocula of the fungal cells ($1x10^3$, $1x10^4$, and $1x10^5$ cells/mouse) in this intravenous infection model and found that a 10-fold decrease in inoculum prolonged survival for an additional 1- 2 days, and that infected mice all succumbed to the diseases within 8 days. We speculate that better protection against cryptococcosis by sertraline or the drug combination might be observed in other animal models or in humans, or if cryptococcosis is caused by less virulent strains. Optimization of drug doses, the route and frequency of drug administration, and the duration of treatment warrant further investigation in order to assess the treatment outcomes.

One of the most valuable aspects of sertraline as a potential anti-cryptococcal drug is its superior ability to accumulate in CNS relative to other antifungals. This is particularly critical in the treatment of cryptococcosis given that *Cryptococcus*

preferentially proliferates in the brain. Consistent with our expectations, the *in vivo* study presented here supports the ability of sertraline in reducing brain fungal burden, either alone or in combination with fluconazole.

Although sertraline demonstrates comparable efficacy against cryptococcosis as fluconazole based on the data presented here, the potential application of this drug to treat mycoses caused by fungal pathogens such as *Candida* or *Aspergillus* requires further investigation. The commonly observed antagonistic interaction between sertraline and fluconazole against *Candida* and *Aspergillus* strains is particularly concerning (this study and (218)). It is possible that specific chemical modification of sertraline could increase its efficacy against these other fungi and abolish its antagonistic interaction with fluconazole. Such modifications would increase its value in the battle against systemic mycoses.

4.4.2. The antifungal mechanism of sertraline

Sertraline displays extremely broad anti-proliferative activity against evolutionarily diverse organisms (117, 198, 199, 209, 211, 212, 215). Recent studies indicate the influence of sertraline on membrane stability or vesicle transport in fungi (150, 207). The results of our *S. cerevisiae* mutant screens are consistent with these discoveries. Our mutant screens and the *in vitro* translation assays also indicated protein synthesis as another process interfered by sertraline. Our finding regarding the inhibitory effect of sertraline on translation is consistent with a recent study on translation in tumor cells (209), even though the implicated mammalian factors in the mTOR pathway identified in that study, such as PDCD4 or REDD1, do not have obvious homologs in

fungi. Inhibition of translation could possibly cause changes in other processes, as molecules involved in protein trafficking and membrane proteins are also significantly enriched in our screen (Fig. 25). Sertraline's impact on translation might more acutely affect protein synthesis from specific transcripts in *Cryptococcus* important for growth such that it does not need to completely inhibit protein synthesis for its strong anti-cryptococcal activity. Thus, while sertraline inhibits mammalian protein synthesis, it may be that qualitative, not quantitative, differences in sertraline's effects on fungal protein synthesis are crucial for sertraline's anti-proliferative activity.

The possibility of emergence of fungal resistance to sertraline seems low based on the following observations. First, we noted during our genetic screen that *S. cerevisiae* gene deletion mutants selected for sertraline resistance showed only up to 50% increase in MIC compared to the wildtype. Second, our repeated attempts of UV mutagenesis of *S. cerevisiae* and *C. neoformans* failed to yield any sertraline-resistant strains with MICs greater than 14μg/ml. Third, all natural *Cryptococcus* strains tested uniformly showed high sensitivity to sertraline. Such observations are drastically different from what is known for azole drugs, as more than 10-100 fold difference in fluconazole susceptibility can be easily observed in both clinical and laboratory settings. This feature, although making it rather challenging to pinpoint the underlying fungicidal mechanisms of sertraline, could be advantageous for its clinical application, as the possibility of encountering sertraline-resistant *Cryptococcus* isolates and the risk of developing fungal resistance during therapy would be low.

CHAPTER V

CONCLUSIONS AND FUTURE DIRECTIONS

5.1. Summary of research

The purpose of this research is to understand the pathogenesis of *Cryptococcus* and to explore novel antifungal drugs.

5.1.1. Construct and characterize the congenic strains of the filamentous form of *Cryptococcus neoformans*

We used a series of backcrosses to generate a pair of congenic α and **a** strains in the highly self-filamentous XL280 background. We characterized the behaviors of the strains *in vitro* and in two mouse models of cryptococcosis. Our data showed that the congenic strains are phenotypically similar under various conditions *in vitro*. They are also nearly equivalent in virulence, as observed from the animal survival curve, fungal burden in organs, and the competitive growth during co-infection. One obvious exception was better self-filamentation observed in the α strain. Enhanced filamentation of the α strain is consistent with previous research showing that the mating type locus is a quantitative trait locus controlling self-filamentation and the α allele promotes filamentation (68). Therefore, the difference in the mating type allele does not directly contribute to the difference in virulence in XL280 background.

Meanwhile, we tested the function of a known master regulator of morphogenesis, Znf2, in the XL280 background. We found that Znf2 plays predicted roles in filamentation and biofilm formation. It also negatively regulated virulence as

we expected. The overexpression of Znf2 reduces the CNS penetration of cryptococcal cells, consistent with what we have observed in H99 background. Our lab previously showed that Znf2 regulates a set of cell surface and secretory proteins, and studies on other fungal pathogens had demonstrated that the cell surface proteins are critical during the fungal invasion of brain (72, 222). Therefore we speculate that the neurotropic activity of *Cryptococcus* is influenced by the altered expression level of Znf2 via the changing of cell surface composition or structure.

As XL280 has been used in a variety of studies to investigate morphogenesis, sporulation, and cryptococcal interaction with various hosts since its generation on 2006 (27, 30, 66, 68, 81, 160, 161), the congenic pair strains generated from this current study, in combination with its recently sequenced genome (158), will enable XL280 to be a useful model for future analysis of morphogenesis and virulence in *C. neoformans*.

5.1.2. Repositioning of polymyxin B and sertraline as novel antifungals

The benefits of research on existing clinical compounds that exert antifungal activity are attracting more attention in recent years. The existing information concerning the pharmaceutical and safety of these drugs implicates a much shorter period of investigation before their potential clinical use as antifungals. Through a screen of the Johns Hopkins Clinical Compound Library, we found that the antibiotic polymyxin B and the antidepressant sertraline possess antifungal activity.

Polymyxin B alone is toxic to a variety of pathogenic fungi at relatively high inhibitory concentrations. However, it is particularly potent against *Cryptococcus*. Here we showed that the combination of polymyxin B and fluconazole (or itraconazole) at

low concentrations are fungicidal with a broad spectrum, including fluconazole-resistant strains. We then confirmed this synergy between polymyxin B and fluconazole in a murine model of systemic cryptococcosis. Further analysis suggested that the capsule of *Cryptococcus* renders the fungal cells hypersensitive towards polymyxin B. This is in contrast to its usual protective role in various stress conditions. However, polymyxin B frequently binds with proteins in serum and organs in a non-specific manner. It also lacks the ability of CNS penetration. In these cases, the efficacy of this drug against brain fungal infections may be modest. Therefore polymyxin B could be more promising for treating infections other than brain, or for topical use.

A more encouraging discovery is the potent anti-cryptococcal activity of sertraline. Sertraline displays a much narrower range of inhibitory concentrations comparing with fluconazole. It also interacts with fluconazole synergistically or additively against divergent *Cryptococcus* isolates. These data suggested that 1) there is a low probability that *Cryptococcus* isolates are intrinsically resistant to sertraline; 2) the outcome of a combinational therapy with sertraline and fluconazole is likely to be synergistic. More importantly, sertraline alone is fungicidal and is able to accumulate in CNS. These are the two key features desirable for the ideal anti-cryptococcal drug. The *in vivo* data further confirmed that the antifungal activity of sertraline is comparable with fluconazole in reducing fungal burden in the brain. Sertraline also interacts synergistically with fluconazole in all the tested organs. Our study is the first to demonstrate the anti-cryptococcal activity of sertraline, specifically in the central nervous system. This discovery provides the key evidence that supports the clinical trial

of adjunctive sertraline for the treatment of HIV-associated cryptococcal meningitis (ClinicalTrials.gov Identifier: NCT01802385). This is an essential step bridging laboratory findings and clinical application of the discovery.

Several recent studies including ours have suggested that sertraline is a compound with pleiotropic effects in eukaryotic cells. We found that sertraline inhibits protein synthesis, which is supported by the GO analysis of the screen results of *Saccharomyces* genome deletion set against sertraline and the *in vitro* translation assay. The GO analysis and a recent study on *Saccharomyces* also have suggested the potential influence of sertraline on membrane stability or vesicle transport in fungi. The pleiotropic effects of sertraline may account for the extremely low incidence of resistance among various *Cryptococcus* isolates.

5.2. Future directions

5.2.1. Dissection of the relationship of fungal virulence and morphotype transition in *Cryptococcus*

The yeast-hyphal transition is particularly critical in fungal virulence of many pathogenic fungi during the host-pathogen interaction (70, 73, 74). We have observed a protective immune response in the host during the infection with a *ZNF2* overexpression strain in the H99 background. We would like to further characterize the factor(s) in *Cryptococcus* that mediate(s) this protection. The research will have three directions: 1) the ongoing research suggests that Znf2 regulates the hyphal formation mainly via two parallel downstream factors, Cfl1 and Pum1. We plan to further test the fungal virulence

influenced by the overexpression of *ZNF2* in the absence of Cfl1 and Pum1. This could help us to determine whether the attenuated virulence is related to the hyphal form of *Cryptococcus per se*. 2) The regulon of Znf2 contains factors that affect the cell wall composition. Therefore we plan to examine the cell wall composition of the *ZNF2* overexpression strain. We also plan to characterize the factor(s) that is (are) responsible for this cell wall remodeling and the consequent impact on virulence. 3) We have collected the serum from the animals that had developed protective immune response as a result of *ZNF2* overexpression strain infection. By proteomics assay of the serum, we would potentially find the immunogenic factors in the *ZNF2* overexpression strain.

Another potential impact of Znf2 on fungal virulence is the regulation of cell surface adherence by the altered expression of secretory/surface proteins. These factors may involve in the initial adhesion in lungs and/or the invasion of CNS during cryptococcal infections. Our data have shown a reduction of brain fungal burden of *ZNF2* overexpression strains in different strain backgrounds. We would like to further test the role of these proteins on the CNS penetration.

5.2.2. Characterization of the fungal target of sertraline

The clinical trial of sertraline in treating AIDS-related cryptococcosis is encouraging and it reinforces the value of drug repositioning strategy in antifungal development. Further research on sertraline as an antifungal would be to determine its fungal target. This potentially will provide new drug target(s) for the future investigation and help the development of a new compound with enhanced efficacy and low toxicity.

Although some evidence suggested that sertraline disturbs the membrane stability or vesicle transport in fungi, we favor the hypothesis that sertraline targets the protein synthesis process. As reviewed in Chapter IV, sertraline displays a broad anti-proliferative activity ranging from bacteria to higher eukaryotes (117, 198, 199, 209, 211, 212, 215). The protein synthesis is a fundamental process in organisms at different domains. To further characterize the direct fungal target(s) of sertraline, a recently developed variomic library in the model yeast *Saccharomyces cerevisiae* would be helpful (223). Comparing with the classic genome deletion set with the deletion of the whole ORF in each strain, this variomic library contains an average of ~10,000 variant alleles for each ORF. Therefore, this tool could help specify the drug target at amino acid residue level.

5.2.3. New strategy of antifungal drug development

Natural products and newly synthesized compounds from various screens, as well as the repositioning drugs are the main sources for searching for novel antifungals. Currently, nearly all the screens with different sets of natural products or chemical compounds aim to the essential process of fungal cells and consequently inhibit the fungal growth. Growth inhibition potentially creates strong selective pressures and could drive the emergence of drug resistance (224). An alternative direction of antifungal drug discovery is to target the virulence of fungi (224). For instance, urease, phospholipase B1 or other cell surface proteins are potentially related to the capacity of the CNS penetration of cryptococcal cells. Drug screens against these factors could discover compound(s) that prevent(s) the fungal cell dissemination. This kind of

compounds would be particularly valuable for the prophylaxis of cryptococcal meningitis among people that are susceptible to the infection.

REFERENCES

1. Steinbach WJ & Stevens DA (2003) Review of newer antifungal and immunomodulatory strategies for invasive aspergillosis. *Clin Infect Dis* 37 Suppl 3:S157-187.

2. Filioti J, Spiroglou K, Panteliadis CP, & Roilides E (2007) Invasive candidiasis in pediatric intensive care patients: epidemiology, risk factors, management, and outcome. *Intensive Care Med* 33(7):1272-1283.

3. Longley N, *et al.* (2008) Dose response effect of high-dose fluconazole for HIV-associated cryptococcal meningitis in southwestern Uganda. *Clin Infect Dis* 47(12):1556-1561.

4. Park BJ, *et al.* (2009) Estimation of the current global burden of cryptococcal meningitis among persons living with HIV/AIDS. *AIDS* 23(4):525-530.

5. Kwon-Chung KJ, Edman JC, & Wickes BL (1992) Genetic association of mating types and virulence in *Cryptococcus neoformans*. *Infect Immun* 60(2):602-605.

6. Nielsen K, *et al.* (2005) Interaction between genetic background and the mating-type locus in *Cryptococcus neoformans* virulence potential. *Genetics* 171(3):975-983.

7. Nielsen K, *et al.* (2003) Sexual cycle of *Cryptococcus neoformans* var. grubii and virulence of congenic a and alpha isolates. *Infect Immun* 71(9):4831-4841.

8. Loftus BJ, *et al.* (2005) The genome of the basidiomycetous yeast and human pathogen *Cryptococcus neoformans*. *Science* 307(5713):1321-1324.

9. Liu OW, *et al.* (2008) Systematic genetic analysis of virulence in the human fungal pathogen *Cryptococcus neoformans*. *Cell* 135(1):174-188.

10. Heitman J & American Society for Microbiology. (2011) *Cryptococcus : from human pathogen to model yeast* (ASM Press, Washington, DC) pp xvii, 620 p.

11. Pappas PG, *et al.* (2004) Recombinant interferon- gamma 1b as adjunctive therapy for AIDS-related acute cryptococcal meningitis. *J Infect Dis* 189(12):2185-2191.

12. Franzot SP, Salkin IF, & Casadevall A (1999) *Cryptococcus neoformans* var. *grubii*: separate varietal status for *Cryptococcus neoformans* serotype A isolates. *J Clin Microbiol* 37(3):838-840.

13. Belay T, Cherniak R, O'Neill EB, & Kozel TR (1996) Serotyping of *Cryptococcus neoformans* by dot enzyme assay. *J Clin Microbiol* 34(2):466-470.

14. Sorrell TC (2001) *Cryptococcus neoformans* variety *gattii*. *Med Mycol* 39(2):155-168.

15. Fraser JA, *et al.* (2005) Same-sex mating and the origin of the Vancouver Island *Cryptococcus gattii* outbreak. *Nature* 437(7063):1360-1364.

16. Lin X & Heitman J (2006) The biology of the *Cryptococcus neoformans* species complex. *Annu Rev Microbiol* 60:69-105.

17. Viviani MA, *et al.* (2006) Molecular analysis of 311 *Cryptococcus neoformans* isolates from a 30-month ECMM survey of cryptococcosis in Europe. *FEMS Yeast Res* 6(4):614-619.

18. Liaw SJ, Wu HC, & Hsueh PR (2010) Microbiological characteristics of clinical isolates of *Cryptococcus neoformans* in Taiwan: serotypes, mating types, molecular types, virulence factors, and antifungal susceptibility. *Clin Microbiol Infect* 16(6):696-703.

19. Escandon P, Sanchez A, Martinez M, Meyer W, & Castaneda E (2006) Molecular epidemiology of clinical and environmental isolates of the *Cryptococcus neoformans* species complex reveals a high genetic diversity and the presence of the molecular type VGII mating type a in Colombia. *FEMS Yeast Res* 6(4):625-635.

20. Meyer W, *et al.* (1999) Molecular typing of global isolates of *Cryptococcus neoformans* var. *neoformans* by polymerase chain reaction fingerprinting and randomly amplified polymorphic DNA-a pilot study to standardize techniques on which to base a detailed epidemiological survey. *Electrophoresis* 20(8):1790-1799.

21. Hull CM & Heitman J (2002) Genetics of *Cryptococcus neoformans*. *Annu Rev Genet* 36:557-615.

22. Xue C, Tada Y, Dong X, & Heitman J (2007) The human fungal pathogen *Cryptococcus* can complete its sexual cycle during a pathogenic association with plants. *Cell Host & Microbe* 1(4):263-273.

23. Lin X (2009) *Cryptococcus neoformans*: morphogenesis, infection, and evolution *Infect Genet Evol* 9(4):401-416.

24. Wang L & Lin X (2011) Mechanisms of unisexual mating in *Cryptococcus neoformans*. *Fungal Genet Biol* 48(7):651-660.

25. Idnurm A (2010) A tetrad analysis of the basidiomycete fungus *Cryptococcus neoformans*. *Genetics* 185(1):153-163.

26. Botts MR, Giles SS, Gates MA, Kozel TR, & Hull CM (2009) Isolation and characterization of *Cryptococcus neoformans* spores reveal a critical role for capsule biosynthesis genes in spore biogenesis. *Eukaryot Cell* 8(4):595-605.

27. Velagapudi R, Hsueh YP, Geunes-Boyer S, Wright JR, & Heitman J (2009) Spores as infectious propagules of *Cryptococcus neoformans*. *Infect Immun* 77(10):4345-4355.

28. Shadomy HJ & Utz JP (1966) Preliminary studies on a hyphaforming mutant of *Cryptococcus neoformans*. *Mycologia* 58(3):383-390.

29. Wickes BL, Mayorga ME, Edman U, & Edman JC (1996) Dimorphism and haploid fruiting in *Cryptococcus neoformans:* association with the alpha-mating type. *Proc Natl Acad Sci U S A* 93(14):7327-7331.

30. Lin X, Hull CM, & Heitman J (2005) Sexual reproduction between partners of the same mating type in *Cryptococcus neoformans*. *Nature* 434(7036):1017-1021.

31. Litvintseva AP, *et al.* (2003) Evidence of sexual recombination among *Cryptococcus neoformans* serotype A isolates in sub-Saharan Africa. *Eukaryot Cell* 2(6):1162-1168.

32. Halliday CL & Carter DA (2003) Clonal reproduction and limited dispersal in an environmental population of *Cryptococcus neoformans* var *gattii* isolates from Australia. *J Clin Microbiol* 41(2):703-711.

33. Cogliati M, Esposto MC, Tortorano AM, & Viviani MA (2006) *Cryptococcus neoformans* population includes hybrid strains homozygous at mating-type locus. *FEMS Yeast Res* 6(4):608-613.

34. Saul N, Krockenberger M, & Carter D (2008) Evidence of recombination in mixed-mating-type and alpha-only populations of *Cryptococcus gattii* sourced from single eucalyptus tree hollows. *Eukaryot Cell* 7(4):727-734.

35. Lin X, *et al.* (2009) Diploids in the *Cryptococcus neoformans* serotype A population homozygous for the alpha mating type originate via unisexual mating. *PLoS Pathog* 5(1):e1000283.

36. Derengowski Lda S, *et al.* (2013) The transcriptional response of *Cryptococcus neoformans* to ingestion by Acanthamoeba castellanii and macrophages provides insights into the evolutionary adaptation to the mammalian host. *Eukaryot Cell* 12(5):761-774.

37. Idnurm A, *et al.* (2005) Deciphering the model pathogenic fungus *Cryptococcus neoformans*. *Nature reviews. Microbiology* 3(10):753-764.

38. Goldman DL, *et al.* (2001) Serologic evidence for *Cryptococcus neoformans* infection in early childhood. *Pediatrics* 107(5):E66.

39. Xue C, *et al.* (2010) Role of an expanded inositol transporter repertoire in *Cryptococcus neoformans* sexual reproduction and virulence. *mBio* 1(1).

40. Del Poeta M & Casadevall A (2012) Ten challenges on *Cryptococcus* and cryptococcosis. *Mycopathologia* 173(5-6):303-310.

41. Olszewski MA, *et al.* (2004) Urease expression by *Cryptococcus neoformans* promotes microvascular sequestration, thereby enhancing central nervous system invasion. *Am J Pathol* 164(5):1761-1771.

42. Maruvada R, *et al.* (2012) *Cryptococcus neoformans* phospholipase B1 activates host cell Rac1 for traversal across the blood-brain barrier. *Cell Microbiol* 14(10):1544-1553.

43. Liu TB, *et al.* (2013) Brain inositol is a novel stimulator for promoting *Cryptococcus* penetration of the blood-brain barrier. *PLoS Pathog* 9(4):e1003247.

44. Shi M, *et al.* (2010) Real-time imaging of trapping and urease-dependent transmigration of *Cryptococcus neoformans* in mouse brain. *J Clin Invest* 120(5):1683-1693.

45. Chretien F, *et al.* (2002) Pathogenesis of cerebral *Cryptococcus neoformans* infection after fungemia. *J Infect Dis* 186(4):522-530.

46. Charlier C, *et al.* (2009) Evidence of a role for monocytes in dissemination and brain invasion by *Cryptococcus* neoformans. *Infect Immun* 77(1):120-127.

47. Sabiiti W, *et al.* (2014) Efficient phagocytosis and laccase activity affect the outcome of HIV-associated cryptococcosis. *J Clin Invest* 124(5):2000-2008.

48. Chrisman CJ, Albuquerque P, Guimaraes AJ, Nieves E, & Casadevall A (2011) Phospholipids trigger *Cryptococcus neoformans* capsular enlargement during interactions with amoebae and macrophages. *PLoS Pathog* 7(5):e1002047.

49. Garcia-Rodas R, Casadevall A, Rodriguez-Tudela JL, Cuenca-Estrella M, & Zaragoza O (2011) *Cryptococcus neoformans* capsular enlargement and cellular gigantism during *Galleria mellonella* infection. *PloS One* 6(9):e24485.

50. Steenbergen JN, Shuman HA, & Casadevall A (2001) *Cryptococcus neoformans* interactions with amoebae suggest an explanation for its virulence and intracellular pathogenic strategy in macrophages. *Proc Natl Acad Sci U S A* 98(26):15245-15250.

51. Chang YC, Penoyer LA, & Kwon-Chung KJ (1996) The second capsule gene of *cryptococcus neoformans*, CAP64, is essential for virulence. *Infect Immun* 64(6):1977-1983.

52. James PG, Cherniak R, Jones RG, Stortz CA, & Reiss E (1990) Cell-wall glucans of *Cryptococcus neoformans* Cap 67. *Carbohydr Res* 198(1):23-38.

53. Chang YC & Kwon-Chung KJ (1994) Complementation of a capsule-deficient mutation of *Cryptococcus neoformans* restores its virulence. *Mol Cel Biol* 14(7):4912-4919.

54. Garcia-Hermoso D, Dromer F, & Janbon G (2004) *Cryptococcus neoformans* capsule structure evolution *in vitro* and during murine infection. *Infect Immun* 72(6):3359-3365.

55. Zaragoza O, *et al.* (2008) Capsule enlargement in *Cryptococcus neoformans* confers resistance to oxidative stress suggesting a mechanism for intracellular survival. *Cell Microbiol* 10(10):2043-2057.

56. Vecchiarelli A, *et al.* (1996) Purified capsular polysaccharide of *Cryptococcus neoformans* induces interleukin-10 secretion by human monocytes. *Infect Immun* 64(7):2846-2849.

57. Charlier C, *et al.* (2005) Capsule structure changes associated with *Cryptococcus neoformans* crossing of the blood-brain barrier. *Am J Pathol* 166(2):421-432.

58. Eisenman HC & Casadevall A (2012) Synthesis and assembly of fungal melanin. *Appl Microbiol Biotechnol* 93(3):931-940.

59. Wang Y, Aisen P, & Casadevall A (1995) *Cryptococcus neoformans* melanin and virulence: mechanism of action. *Infect Immun* 63(8):3131-3136.

60. Mednick AJ, Nosanchuk JD, & Casadevall A (2005) Melanization of *Cryptococcus neoformans* affects lung inflammatory responses during cryptococcal infection. *Infect Immun* 73(4):2012-2019.

61. Salas SD, Bennett JE, Kwon-Chung KJ, Perfect JR, & Williamson PR (1996) Effect of the laccase gene CNLAC1, on virulence of *Cryptococcus neoformans*. *J Exp Med* 184(2):377-386.

62. Ikeda R, Sugita T, Jacobson ES, & Shinoda T (2003) Effects of melanin upon susceptibility of *Cryptococcus* to antifungals. *Microbiol Immunol* 47(4):271-277.

63. Fraser JA, *et al.* (2004) Convergent evolution of chromosomal sex-determining regions in the animal and fungal kingdoms. *PLoS Biol* 2(12):e384.

64. Wang P, *et al.* (2002) Mating-type-specific and nonspecific PAK kinases play shared and divergent roles in *Cryptococcus neoformans*. *Eukaryot Cell* 1(2):257-272.

65. Davidson RC, Nichols CB, Cox GM, Perfect JR, & Heitman J (2003) A MAP kinase cascade composed of cell type specific and non-specific elements controls mating and differentiation of the fungal pathogen *Cryptococcus neoformans*. *Mol Microbiol* 49(2):469-485.

66. Lin X, Jackson JC, Feretzaki M, Xue C, & Heitman J (2010) Transcription factors Mat2 and Znf2 operate cellular circuits orchestrating opposite- and same-sex mating in *Cryptococcus neoformans*. *PLoS Genet* 6(5):e1000953.

67. Fan W, Kraus PR, Boily MJ, & Heitman J (2005) *Cryptococcus neoformans* gene expression during murine macrophage infection. *Eukaryot Cell* 4(8):1420-1433.

68. Lin X, Huang JC, Mitchell TG, & Heitman J (2006) Virulence attributes and hyphal growth of *C. neoformans* are quantitative traits and the *MAT*alpha allele enhances filamentation. *PLoS Genet* 2(11):e187.

69. Beyhan S, Gutierrez M, Voorhies M, & Sil A (2013) A temperature-responsive network links cell shape and virulence traits in a primary fungal pathogen. *PLoS Biol* 11(7):e1001614.

70. Kane J (1984) Conversion of *Blastomyces dermatitidis* to the yeast form at 37 degrees C and 26 degrees C. *J Clin Microbiol* 20(3):594-596.

71. Whiteway M & Bachewich C (2007) Morphogenesis in *Candida albicans*. *Annu Rev Microbiol* 61:529-553.

72. Liu Y & Filler SG (2011) *Candida albicans* Als3, a multifunctional adhesin and invasin. *Eukaryot Cell* 10(2):168-173.

73. Jacobsen ID*, et al.* (2012) *Candida albicans* dimorphism as a therapeutic target. *Expert Rev Anti Infect Ther* 10(1):85-93.

74. Rappleye CA & Goldman WE (2006) Defining virulence genes in the dimorphic fungi. *Annu Rev Microbiol* 60:281-303.

75. Love GL, Boyd GD, & Greer DL (1985) Large *Cryptococcus neoformans* isolated from brain abscess. *J Clin Microbiol* 22(6):1068-1070.

76. Okagaki LH*, et al.* (2010) Cryptococcal cell morphology affects host cell interactions and pathogenicity. *PLoS Pathog* 6(6):e1000953.

77. Zaragoza O*, et al.* (2010) Fungal cell gigantism during mammalian infection. *PLoS Pathog* 6(6):e1000945.

78. Freed ER, Duma RJ, Shadomy HJ, & Utz JP (1971) Meningoencephalitis due to hyphae-forming *Cryptococcus neoformans*. *Am J Clin Pathol* 55(1):30-33.

79. Lurie HI & Shadomy HJ (1971) Morphological variations of a hypha-forming strain of *Cryptococcus neoformans* (Coward strain) in tissues of mice. *Sabouraudia* 9(1):10-14.

80. Williamson JD, Silverman JF, Mallak CT, & Christie JD (1996) Atypical cytomorphologic appearance of *Cryptococcus neoformans:* a report of five cases. *Acta cytologica* 40(2):363-370.

81. Wang L, Zhai B, & Lin X (2012) The link between morphotype transition and virulence in *Cryptococcus neoformans*. *PLoS Pathog* 8(6):e1002765.

82. Neilson JB, Ivey MH, & Bulmer GS (1978) *Cryptococcus neoformans:* pseudohyphal forms surviving culture with *Acanthamoeba polyphaga*. *Infect Immun* 20(1):262-266.

83. Fromtling RA, Blackstock R, Hall NK, & Bulmer GS (1979) Immunization of mice with an avirulent pseudohyphal form of *Cryptococcus neoformans*. *Mycopathologia* 68(3):179-181.

84. Neilson JB, Fromtling RA, & Bulmer GS (1981) Pseudohyphal forms of *Cryptococcus neoformans:* decreased survival in vivo. *Mycopathologia* 73(1):57-59.

85. Shadomy HJ & Lurie HI (1971) Histopathological observations in experimental cryptococcosis caused by a hypha-producing strain of *Cryptococcus neoformans* (Coward strain) in mice. *Sabouraudia* 9(1):6-9.

86. Zimmer BL, Hempel HO, & Goodman NL (1983) Pathogenicity of the hyphae of *Filobasidiella neoformans*. *Mycopathologia* 81(2):107-110.

87. Fromtling RA, Blackstock R, Hall NK, & Bulmer GS (1979) Kinetics of lymphocyte transformation in mice immunized with viable avirulent forms of *Cryptococcus neoformans*. *Infect Immun* 24(2):449-453.

88. Wang L, Tian X, Gyawali R, & Lin X (2013) Fungal adhesion protein guides community behaviors and autoinduction in a paracrine manner. *Proc Natl Acad Sci U S A* 110(28):11571-11576.

89. Antachopoulos C & Walsh TJ (2012) Immunotherapy of *Cryptococcus infections*. *Clin Microbiol Infect* 18(2):126-133.

90. Casadevall A, Feldmesser M, & Pirofski LA (2002) Induced humoral immunity and vaccination against major human fungal pathogens. *Curr Opin Microbiol* 5(4):386-391.

91. Casadevall A & Pirofski LA (2006) A reappraisal of humoral immunity based on mechanisms of antibody-mediated protection against intracellular pathogens. *Adv Immunol* 91:1-44.

92. Larsen RA*, et al.* (2005) Phase I evaluation of the safety and pharmacokinetics of murine-derived anticryptococcal antibody 18B7 in subjects with treated cryptococcal meningitis. *Antimicrob Agents Chemother* 49(3):952-958.

93. Dadachova E, Nakouzi A, Bryan RA, & Casadevall A (2003) Ionizing radiation delivered by specific antibody is therapeutic against a fungal infection. *Proc Natl Acad Sci U S A* 100(19):10942-10947.

94. Dadachova E*, et al.* (2004) Evaluation of acute hematologic and long-term pulmonary toxicities of radioimmunotherapy of *Cryptococcus neoformans* infection in murine models. *Antimicrob Agents Chemother* 48(3):1004-1006.

95. Saag MS*, et al.* (2000) Practice guidelines for the management of cryptococcal disease. Infectious Diseases Society of America. *Clin Infect Dis* 30(4):710-718.

96. Laniado-Laborin R & Cabrales-Vargas MN (2009) Amphotericin B: side effects and toxicity. *Rev Iberoam Micol* 26(4):223-227.

97. Ellis D (2002) Amphotericin B: spectrum and resistance. *J Antimicrob Chemother* 49 Suppl 1:7-10.

98. Baginski M & Czub J (2009) Amphotericin B and its new derivatives - mode of action. *Curr Drug Metab* 10(5):459-469.

99. Deray G (2002) Amphotericin B nephrotoxicity. *J Antimicrob Chemother* 49 Suppl 1:37-41.

100. Craddock C, *et al.* (2010) Best practice guidelines for the management of adverse events associated with amphotericin B lipid complex. *Expert Opin Drug Saf* 9(1):139-147.

101. Arthur RR, Drew RH, & Perfect JR (2004) Novel modes of antifungal drug administration. *Expert Opin Invest Drug* 13(8):903-932.

102. Robinson PA, *et al.* (1999) Early mycological treatment failure in AIDS-associated cryptococcal meningitis. *Clin Infect Dis* 28(1):82-92.

103. Powderly WG (1996) Recent advances in the management of cryptococcal meningitis in patients with AIDS. *Clin Infect Dis* 22 Suppl 2:S119-123.

104. Vanden Bossche H (1985) Biochemical targets for antifungal azole derivatives: hypothesis on the mode of action. *Curr Top Med Mycol* 1:313-351.

105. Vanden Bossche H, Willemsens G, & Marichal P (1987) Anti-*Candida* drugs--the biochemical basis for their activity. *Crit Rev Microbiol* 15(1):57-72.

106. Pappas PG, *et al.* (2001) Cryptococcosis in human immunodeficiency virus-negative patients in the era of effective azole therapy. *Clin Infect Dis* 33(5):690-699.

107. van der Horst CM, *et al.* (1997) Treatment of cryptococcal meningitis associated with the acquired immunodeficiency syndrome. National Institute of Allergy and Infectious Diseases Mycoses Study Group and AIDS Clinical Trials Group. *N Engl J Med* 337(1):15-21.

108. Lutsar I, Roffey S, & Troke P (2003) Voriconazole concentrations in the cerebrospinal fluid and brain tissue of guinea pigs and immunocompromised patients. *Clin Infect Dis* 37(5):728-732.

109. Nau R, Sorgel F, & Eiffert H (2010) Penetration of drugs through the blood-cerebrospinal fluid/blood-brain barrier for treatment of central nervous system infections. *Clin Microbiol Rev* 23(4):858-883.

110. Paugam A, *et al.* (1994) Increased fluconazole resistance of *Cryptococcus neoformans* isolated from a patient with AIDS and recurrent meningitis. *Clin Infect Dis* 19(5):975-976.

111. Birley HD, *et al.* (1995) Azole drug resistance as a cause of clinical relapse in AIDS patients with cryptococcal meningitis. *International journal of STD & AIDS* 6(5):353-355.

112. Berg J, Clancy CJ, & Nguyen MH (1998) The hidden danger of primary fluconazole prophylaxis for patients with AIDS. *Clin Infect Dis* 26(1):186-187.

113. Armengou A, Porcar C, Mascaro J, & Garcia-Bragado F (1996) Possible development of resistance to fluconazole during suppressive therapy for AIDS-associated cryptococcal meningitis. *Clin Infect Dis* 23(6):1337-1338.

114. Cheong JW & McCormack J (2013) Fluconazole resistance in cryptococcal disease: emerging or intrinsic? *Med Mycol* 51(3):261-269.

115. Cowen LE, Anderson JB, & Kohn LM (2002) Evolution of drug resistance in *Candida albicans*. *Annu Rev Microbiol* 56:139-165.

116. Lupetti A, Danesi R, Campa M, Del Tacca M, & Kelly S (2002) Molecular basis of resistance to azole antifungals. *Trend Mol Med* 8(2):76-81.

117. Marichal P, *et al.* (1999) Contribution of mutations in the cytochrome P450 14alpha-demethylase (Erg11p, Cyp51p) to azole resistance in *Candida albicans*. *Microbiol* 145 (Pt 10):2701-2713.

118. Sanglard D, Ischer F, Monod M, & Bille J (1997) Cloning of *Candida albicans* genes conferring resistance to azole antifungal agents: characterization of CDR2, a new multidrug ABC transporter gene. *Microbiol* 143 (Pt 2):405-416.

119. Sanglard D, *et al.* (1995) Mechanisms of resistance to azole antifungal agents in *Candida albicans* isolates from AIDS patients involve specific multidrug transporters. *Antimicrob Agents Chemother* 39(11):2378-2386.

120. Kuhn DM, George T, Chandra J, Mukherjee PK, & Ghannoum MA (2002) Antifungal susceptibility of *Candida* biofilms: unique efficacy of amphotericin B lipid formulations and echinocandins. *Antimicrob Agents Chemother* 46(6):1773-1780.

121. Blankenship JR & Mitchell AP (2006) How to build a biofilm: a fungal perspective. *Curr Opin Microbiol* 9(6):588-594.

122. Sionov E, Chang YC, Garraffo HM, & Kwon-Chung KJ (2009) Heteroresistance to fluconazole in *Cryptococcus neoformans* is intrinsic and associated with virulence. *Antimicrob Agents Chemother* 53(7):2804-2815.

123. Sionov E, Chang YC, & Kwon-Chung KJ (2013) Azole heteroresistance in *Cryptococcus neoformans*: emergence of resistant clones with chromosomal disomy in the mouse brain during fluconazole treatment. *Antimicrob Agents Chemother* 57(10):5127-5130.

124. Sionov E, Lee H, Chang YC, & Kwon-Chung KJ (2010) *Cryptococcus neoformans* overcomes stress of azole drugs by formation of disomy in specific multiple chromosomes. *PLoS Pathog* 6(4):e1000848.

125. Andes D (2013) Optimizing antifungal choice and administration. *Curr Med Res Opin* 29 Suppl 4:13-18.

126. Sucher AJ, Chahine EB, & Balcer HE (2009) Echinocandins: the newest class of antifungals. *Annals Pharmacother* 43(10):1647-1657.

127. Krishnarao TV & Galgiani JN (1997) Comparison of the in vitro activities of the echinocandin LY303366, the pneumocandin MK-0991, and fluconazole against *Candida* species and *Cryptococcus neoformans*. *Antimicrob Agents Chemother* 41(9):1957-1960.

128. Malhotra P, Shah SS, Kaplan M, & McGowan JP (2005) Cryptococcal fungemia in a neutropenic patient with AIDS while receiving caspofungin. *J Infect* 51(3):e181-183.

129. Maligie MA & Selitrennikoff CP (2005) *Cryptococcus neoformans* resistance to echinocandins: (1,3)beta-glucan synthase activity is sensitive to echinocandins. *Antimicrob Agents Chemother* 49(7):2851-2856.

130. Thompson JR, *et al.* (1999) A glucan synthase FKS1 homolog in *cryptococcus neoformans* is single copy and encodes an essential function. *J bacteriol* 181(2):444-453.

131. Gallis HA, Drew RH, & Pickard WW (1990) Amphotericin B: 30 years of clinical experience. *Rev Infect Dis* 12(2):308-329.

132. Vermes A, Guchelaar HJ, & Dankert J (2000) Flucytosine: a review of its pharmacology, clinical indications, pharmacokinetics, toxicity and drug interactions. *J Antimicrob Chemother* 46(2):171-179.

133. Bachmann SP, *et al.* (2003) Antifungal combinations against *Candida albicans* biofilms *in vitro*. *Antimicrob Agents Chemother* 47(11):3657-3659.

134. Sarkar S, Uppuluri P, Pierce CG, & Lopez-Ribot JL (2014) In vitro study of sequential fluconazole and caspofungin treatment against *Candida albicans* biofilms. *Antimicrob Agents Chemother* 58(2):1183-1186.

135. Mitsuyama J, *et al.* (2008) In vitro and in vivo antifungal activities of T-2307, a novel arylamidine. *Antimicrob Agents Chemother* 52(4):1318-1324.

136. Yamada E, Nishikawa H, Nomura N, & Mitsuyama J (2010) T-2307 shows efficacy in a murine model of *Candida glabrata* infection despite in vitro trailing growth phenomena. *Antimicrob Agents Chemother* 54(9):3630-3634.

137. Nishikawa H, *et al.* (2010) Uptake of T-2307, a novel arylamidine, in *Candida albicans*. *J Antimicrob Chemother* 65(8):1681-1687.

138. Shibata T, *et al.* (2012) T-2307 causes collapse of mitochondrial membrane potential in yeast. *Antimicrob Agents Chemother* 56(11):5892-5897.

139. Hata K, *et al.* (2011) Efficacy of oral E1210, a new broad-spectrum antifungal with a novel mechanism of action, in murine models of candidiasis, aspergillosis, and fusariosis. *Antimicrob Agents Chemother* 55(10):4543-4551.

140. Miyazaki M, *et al.* (2011) In vitro activity of E1210, a novel antifungal, against clinically important yeasts and molds. *Antimicrob Agents Chemother* 55(10):4652-4658.

141. Lu SE, *et al.* (2009) Occidiofungin, a unique antifungal glycopeptide produced by a strain of *Burkholderia contaminans*. *Biochemistry* 48(35):8312-8321.

142. Tan W, *et al.* (2012) Nonclinical toxicological evaluation of occidiofungin, a unique glycolipopeptide antifungal. *Int J Toxicol* 31(4):326-336.

143. Emrick D, *et al.* (2013) The antifungal occidiofungin triggers an apoptotic mechanism of cell death in yeast. *J Nat Prod* 76(5):829-838.

144. Butts A & Krysan DJ (2012) Antifungal drug discovery: something old and something new. *PLoS Pathog* 8(9):e1002870.

145. Rudin CM, *et al.* (2013) Phase 2 study of pemetrexed and itraconazole as second-line therapy for metastatic nonsquamous non-small-cell lung cancer. *J Thorac Oncol* 8(5):619-623.

146. Weiss VC, West DP, & Mueller CE (1981) Topical minoxidil in alopecia areata. *J Am Acad Dermatol* 5(2):224-226.

147. Del Poeta M, Cruz MC, Cardenas ME, Perfect JR, & Heitman J (2000) Synergistic antifungal activities of bafilomycin A(1), fluconazole, and the pneumocandin MK-0991/caspofungin acetate (L-743,873) with calcineurin inhibitors FK506 and L-685,818 against *Cryptococcus neoformans*. *Antimicrob Agents Chemother* 44(3):739-746.

148. Dolan K, *et al.* (2009) Antifungal activity of tamoxifen: in vitro and in vivo activities and mechanistic characterization. *Antimicrob Agents Chemother* 53(8):3337-3346.

149. Breger J, *et al.* (2007) Antifungal chemical compounds identified using a C. elegans pathogenicity assay. *PLoS Pathog* 3(2):e18.

150. Spitzer M, *et al.* (2011) Cross-species discovery of syncretic drug combinations that potentiate the antifungal fluconazole. *Mol Syst Biol* 7:499.

151. Heitman J, Allen B, Alspaugh JA, & Kwon-Chung KJ (1999) On the origins of congenic MATalpha and MATa strains of the pathogenic yeast *Cryptococcus neoformans*. *Fungal Genet Biol* 28(1):1-5.

152. Lin X, *et al.* (2007) alpha AD alpha hybrids of *Cryptococcus neoformans*: evidence of same-sex mating in nature and hybrid fitness. *PLoS Genet* 3(10):1975-1990.

153. Barchiesi F, *et al.* (2005) Comparative analysis of pathogenicity of *Cryptococcus neoformans* serotypes A, D and AD in murine cryptococcosis. *J Infect* 51(1):10-16.

154. Lin X, Nielsen K, Patel S, & Heitman J (2008) Impact of mating type, serotype, and ploidy on the virulence of *Cryptococcus neoformans*. *Infect Immun* 76(7):2923-2938.

155. Litvintseva AP & Mitchell TG (2009) Most environmental isolates of *Cryptococcus neoformans* var. *grubii* (serotype A) are not lethal for mice. *Infect Immun* 77(8):3188-3195.

156. Nielsen K, *et al.* (2005) *Cryptococcus neoformans* {alpha} strains preferentially disseminate to the central nervous system during coinfection. *Infect Immun* 73(8):4922-4933.

157. Zhu P, Zhai B, Lin X, & Idnurm A (2013) Congenic strains for genetic analysis of virulence traits in *Cryptococcus gattii*. *Infect Immun* 81(7):2616-2625.

158. Ni M, *et al.* (2013) Unisexual and heterosexual meiotic reproduction generate aneuploidy and phenotypic diversity de novo in the yeast *Cryptococcus neoformans*. *PLoS Biol* 11(9):e1001653.

159. Marra RE, *et al.* (2004) A genetic linkage map of *Cryptococcus neoformans* variety *neoformans* serotype D (*Filobasidiella neoformans*). *Genet* 167(2):619-631.

160. Hsueh YP, Xue C, & Heitman J (2009) A constitutively active GPCR governs morphogenic transitions in *Cryptococcus neoformans*. *EMBO J* 28(9):1220-1233.

161. Lee SC & Heitman J (2012) Function of *Cryptococcus neoformans* KAR7 (SEC66) in karyogamy during unisexual and opposite-sex mating. *Eukaryot Cell* 11(6):783-794.

162. Magditch DA, Liu TB, Xue C, & Idnurm A (2012) DNA mutations mediate microevolution between host-adapted forms of the pathogenic fungus *Cryptococcus neoformans*. *PLoS Pathog* 8(10):e1002936.

163. Crabtree JN, *et al.* (2012) Titan cell production enhances the virulence of *Cryptococcus neoformans*. *Infect Immun* 80(11):3776-3785.

164. Ngamskulrungroj P, Chang Y, Sionov E, & Kwon-Chung KJ (2012) The primary target organ of *Cryptococcus gattii* is different from that of *Cryptococcus neoformans* in a murine model. *mBio* 3(3).

165. Molina J, Cordero E, & Pachon J (2009) New information about the polymyxin/colistin class of antibiotics. *Exp Opin Pharmacother* 10(17):2811-2828.

166. Brown JM, Dorman DC, & Roy LP (1970) Acute renal failure due to overdosage of colistin. *Med J Aust* 2(20):923-924.

167. Koch-Weser J, *et al.* (1970) Adverse effects of sodium colistimethate. Manifestations and specific reaction rates during 317 courses of therapy. *Ann Intern Med* 72(6):857-868.

168. Falagas ME & Kasiakou SK (2006) Toxicity of polymyxins: a systematic review of the evidence from old and recent studies. *Crit care* 10(1):R27.

169. Zavascki AP, Goldani LZ, Li J, & Nation RL (2007) Polymyxin B for the treatment of multidrug-resistant pathogens: a critical review. *J Antimicrob Chemother* 60(6):1206-1215.

170. Evans ME, Feola DJ, & Rapp RP (1999) Polymyxin B sulfate and colistin: old antibiotics for emerging multiresistant gram-negative bacteria. *Ann Pharmacother* 33(9):960-967.

171. Hancock RE & Chapple DS (1999) Peptide antibiotics. *Antimicrob Agents Chemother* 43(6):1317-1323.

172. Nosanchuk JD & Casadevall A (1997) Cellular charge of *Cryptococcus neoformans:* contributions from the capsular polysaccharide, melanin, and monoclonal antibody binding. *Infect Immun* 65(5):1836-1841.

173. Fritsche TR, Rhomberg PR, Sader HS, & Jones RN (2008) Antimicrobial activity of omiganan pentahydrochloride against contemporary fungal pathogens responsible for catheter-associated infections. *Antimicrob Agents Chemother* 52(3):1187-1189.

174. Ben-Ami R, Lewis RE, Tarrand J, Leventakos K, & Kontoyiannis DP (2010) Antifungal activity of colistin against mucorales species in vitro and in a murine model of *Rhizopus oryzae* pulmonary infection. *Antimicrob Agents Chemother* 54(1):484-490.

175. Sarria JC, Angulo-Pernett F, Kimbrough RC, McVay CS, & Vidal AM (2004) Use of intravenous polymyxin B during continuous venovenous hemodialysis. *Eur J Clin Microbiol Infect Dis* 23(4):340-341.

176. Litvintseva AP, Thakur R, Vilgalys R, & Mitchell TG (2006) Multilocus sequence typing reveals three genetic subpopulations of *Cryptococcus neoformans* var. grubii (serotype A), including a unique population in Botswana. *Genet* 172(4):2223-2238.

177. Neuville S, *et al.* (2003) Primary cutaneous cryptococcosis: a distinct clinical entity. *Clin Infect Dis* 36(3):337-347.

178. Miller JL, *et al.* (2004) In vitro and in vivo efficacies of the new triazole albaconazole against *Cryptococcus neoformans*. *Antimicrob Agents Chemother* 48(2):384-387.

179. Chaturvedi V, *et al.* (2002) Molecular genetic analyses of mating pheromones reveal intervariety mating or hybridization in *Cryptococcus neoformans*. *Infect Immun* 70(9):5225-5235.

180. Winzeler EA, *et al.* (1999) Functional characterization of the *S. cerevisiae* genome by gene deletion and parallel analysis. *Science* 285(5429):901-906.

181. Chong CR, Chen X, Shi L, Liu JO, & Sullivan DJ, Jr. (2006) A clinical drug library screen identifies astemizole as an antimalarial agent. *Nat Chem Biol* 2(8):415-416.

182. Berenbaum MC (1978) A method for testing for synergy with any number of agents. *J Infect Dis* 137(2):122-130.

183. Falla TJ, Karunaratne DN, & Hancock RE (1996) Mode of action of the antimicrobial peptide indolicidin. *J Biol Chem* 271(32):19298-19303.

184. Moneib NA (1995) In-vitro activity of commonly used antifungal agents in the presence of rifampin, polymyxin B and norfloxacin against *Candida albicans*. *J Chemother* 7(6):525-529.

185. Schwartz SN, Medoff G, Kobayashi GS, Kwan CN, & Schlessinger D (1972) Antifungal properties of polymyxin B and its potentiation of tetracycline as an antifungal agent. *Antimicrob Agents Chemother* 2(1):36-40.

186. Kwa A, Kasiakou SK, Tam VH, & Falagas ME (2007) Polymyxin B: similarities to and differences from colistin (polymyxin E). *Exp Rev Anti Infect Ther* 5(5):811-821.

187. Srimal S, Surolia N, Balasubramanian S, & Surolia A (1996) Titration calorimetric studies to elucidate the specificity of the interactions of polymyxin B with lipopolysaccharides and lipid A. *Biochem J* 315 (Pt 2):679-686.

188. Storm DR, Rosenthal KS, & Swanson PE (1977) Polymyxin and related peptide antibiotics. *Ann Rev Biochem* 46:723-763.

189. HsuChen CC & Feingold DS (1973) The mechanism of polymyxin B action and selectivity toward biologic membranes. *Biochemistry* 12(11):2105-2111.

190. Teuber M & Miller IR (1977) Selective binding of polymyxin B to negatively charged lipid monolayers. *Biochim Biophys Acta* 467(3):280-289.

191. Jandrositz A, Turnowsky F, & Hogenauer G (1991) The gene encoding squalene epoxidase from *Saccharomyces cerevisiae*: cloning and characterization. *Gene* 107(1):155-160.

192. Anderson JB (2005) Evolution of antifungal-drug resistance: mechanisms and pathogen fitness. *Nat Rev Microbiol* 3(7):547-556.

193. Odds FC, Brown AJ, & Gow NA (2003) Antifungal agents: mechanisms of action. *Trends Microbiol* 11(6):272-279.

194. Garcia-Rivera J, Chang YC, Kwon-Chung KJ, & Casadevall A (2004) *Cryptococcus neoformans* CAP59 (or Cap59p) is involved in the extracellular trafficking of capsular glucuronoxylomannan. *Eukaryot Cell* 3(2):385-392.

195. Hermsen ED, Sullivan CJ, & Rotschafer JC (2003) Polymyxins: pharmacology, pharmacokinetics, pharmacodynamics, and clinical applications. *Infect Dis Clin North Am* 17(3):545-562.

196. Li J, *et al.* (2003) Use of high-performance liquid chromatography to study the pharmacokinetics of colistin sulfate in rats following intravenous administration. *Antimicrob Agents Chemother* 47(5):1766-1770.

197. Zaragoza O, Alvarez M, Telzak A, Rivera J, & Casadevall A (2007) The relative susceptibility of mouse strains to pulmonary *Cryptococcus neoformans* infection is associated with pleiotropic differences in the immune response. *Infect Immun* 75(6):2729-2739.

198. Lass-Florl C, Dierich MP, Fuchs D, Semenitz E, & Ledochowski M (2001) Antifungal activity against *Candida* species of the selective serotonin-reuptake inhibitor, sertraline. *Clin Infect Dis* 33(12):E135-136.

199. Lass-Florl C, *et al.* (2001) Antifungal properties of selective serotonin reuptake inhibitors against *Aspergillus* species in vitro. *J Antimicrob Chemother* 48(6):775-779.

200. Winek CL, Wahba WW, Winek CL, Jr., & Balzer TW (2001) Drug and chemical blood-level data 2001. *Forensic Sci Int* 122(2-3):107-123.

201. Young TJ, Oliver GP, Pryde D, Perros M, & Parkinson T (2003) Antifungal activity of selective serotonin reuptake inhibitors attributed to non-specific cytotoxicity. *J Antimicrob Chemother* 51(4):1045-1047.

202. Tremaine LM, Welch WM, & Ronfeld RA (1989) Metabolism and disposition of the 5-hydroxytryptamine uptake blocker sertraline in the rat and dog. *Drug Metab Dispos* 17(5):542-550.

203. Cook EH, *et al.* (2001) Long-term sertraline treatment of children and adolescents with obsessive-compulsive disorder. *J Am Acad Child Adolesc Psychiatry* 40(10):1175-1181.

204. Rapaport MH, *et al.* (2001) Sertraline treatment of panic disorder: results of a long-term study. *Acta Psychiatr Scand* 104(4):289-298.

205. Rasmussen S, *et al.* (1997) A 2-year study of sertraline in the treatment of obsessive-compulsive disorder. *Int Clin Psychopharmacol* 12(6):309-316.

206. Aberg-Wistedt A (1989) The antidepressant effects of 5-HT uptake inhibitors. *Br J Psychiatry Suppl* (8):32-40.

207. Rainey MM, Korostyshevsky D, Lee S, & Perlstein EO (2010) The antidepressant sertraline targets intracellular vesiculogenic membranes in yeast. *Genetics* 185(4):1221-1233.

208. Tuynder M, *et al.* (2004) Translationally controlled tumor protein is a target of tumor reversion. *Proc Natl Acad Sci U S A* 101(43):15364-15369.

209. Lin CJ, Robert F, Sukarieh R, Michnick S, & Pelletier J (2010) The antidepressant sertraline inhibits translation initiation by curtailing mammalian target of rapamycin signaling. *Cancer Res* 70(8):3199-3208.

210. MacDonald ML, *et al.* (2006) Identifying off-target effects and hidden phenotypes of drugs in human cells. *Nat Chem Biol* 2(6):329-337.

211. Letendre SL, *et al.* (2007) The role of cohort studies in drug development: clinical evidence of antiviral activity of serotonin reuptake inhibitors and HMG-CoA reductase inhibitors in the central nervous system. *J Neuroimmune Pharmacol* 2(1):120-127.

212. Munoz-Criado S, Munoz-Bellido JL, & Garcia-Rodriguez JA (1996) In vitro activity of nonsteroidal anti-inflammatory agents, phenotiazines, and antidepressants against *Brucella* species. *Eur J Clin Microbiol Infect Dis* 15(5):418-420.

213. Munoz-Bellido JL, Munoz-Criado S, & Garcia-Rodriguez JA (2000) Antimicrobial activity of psychotropic drugs: selective serotonin reuptake inhibitors. *Int J Antimicrob Agents* 14(3):177-180.

214. Peng Q, *et al.* (2008) The antidepressant sertraline improves the phenotype, promotes neurogenesis and increases BDNF levels in the R6/2 Huntington's disease mouse model. *Exp Neurol* 210(1):154-163.

215. Kumar VS, *et al.* (2006) The spermicidal and antitrichomonas activities of SSRI antidepressants. *Bioorg Med Chem Lett* 16(9):2509-2512.

216. Wu C, Amrani N, Jacobson A, & Sachs MS (2007) The use of fungal in vitro systems for studying translational regulation. *Methods Enzymol* 429:203-225.

217. Hiemke C & Hartter S (2000) Pharmacokinetics of selective serotonin reuptake inhibitors. *Pharmacol Ther* 85(1):11-28.

218. Heller I, Leitner S, Dierich MP, & Lass-Florl C (2004) Serotonin (5-HT) enhances the activity of amphotericin B against *Aspergillus fumigatus* in vitro. *Int J Antimicrob Agents* 24(4):401-404.

219. Wang Z & Sachs MS (1997) Arginine-specific regulation mediated by the *Neurospora crassa* arg-2 upstream open reading frame in a homologous, cell-free in vitro translation system. *J Biol Chem* 272(1):255-261.

220. Zhai B & Lin X (2011) Recent progress on antifungal drug development. *Curr Pharm Biotechnol* 12(8):1255-1262.

221. Oliver JD (2010) Recent findings on the viable but nonculturable state in pathogenic bacteria. *FEMS Microbiol Rev* 34(4):415-425.

222. Liu Y, Mittal R, Solis NV, Prasadarao NV, & Filler SG (2011) Mechanisms of *Candida albicans* trafficking to the brain. *PLoS Pathog* 7(10):e1002305.

223. Huang Z, *et al.* (2013) A functional variomics tool for discovering drug-resistance genes and drug targets. *Cell Rep* 3(2):577-585.

224. Pierce CG & Lopez-Ribot JL (2013) Candidiasis drug discovery and development: new approaches targeting virulence for discovering and identifying new drugs. *Expert Opt Drug Discov* 8(9):1117-1126.